

The Pennsylvania State University

The Graduate School

Bioengineering Program

**SURFACE-MEDIATED MOLECULAR EVENTS IN MATERIAL-INDUCED  
BLOOD-PLASMA COAGULATION**

A Thesis in

Bioengineering

by

Kaushik Chatterjee

© 2007 Kaushik Chatterjee

Submitted in Partial Fulfillment  
of the Requirements  
for the Degree of

Doctor of Philosophy

December 2007

The thesis of Kaushik Chatterjee was reviewed and approved\* by the following:

Christopher A. Siedlecki  
Associate Professor of Surgery and Bioengineering  
Thesis Advisor  
Chair of Committee

Erwin A. Vogler  
Professor of Materials Science and Engineering and Bioengineering

William O. Hancock  
Associate Professor of Bioengineering

Alan J. Snyder  
Professor of Surgery and Bioengineering

Ira J. Ropson  
Associate Professor of Biochemistry and Molecular Biology

Herbert H. Lipowsky  
Professor of Bioengineering  
Head of the Department of Bioengineering

\*Signatures are on file in the Graduate School

## ABSTRACT

Coagulation and thrombosis persist as major impediments associated with the use of blood-contacting medical devices. We are investigating the molecular mechanism underlying material-induced blood-plasma coagulation focusing on the role of the surface as a step towards prospective development of improved hemocompatible biomaterials.

A classic observation in hematology is that blood/blood-plasma in contact with clean glass surface clots faster than when in contact with many plastic surfaces. The traditional biochemical theory explaining the underlying molecular mechanism suggests that hydrophilic surfaces, like that of glass, are specific activators of the coagulation cascade because of the negatively-charged groups on the surface. Hydrophobic surfaces are poor procoagulants or essentially “benign” because they lack anionic groups. Further, these negatively-charged surfaces are believed to not only activate blood factor XII (FXII), the key protein in contact activation, but also play a cofactor role in the amplification and propagation reactions that ultimately lead to clot formation.

In sharp contrast to the traditional theory, our investigations indicate a need for a paradigm shift in the proposed sequence of contact activation events to incorporate the role of protein adsorption at the material surfaces. These studies have lead to the central hypothesis for this work proposing that protein adsorption to hydrophobic surfaces attenuates the contact activation reactions so that poorly-adsorbent hydrophilic surfaces appear to be stronger procoagulants relative to hydrophobic surfaces.

Our preliminary studies measuring the plasma coagulation response of activated FXII (FXIIa) on different model surfaces suggested that the material did not play a

cofactor role in the processing of this enzyme dose through the coagulation pathway. Therefore, we focused our efforts on studying the mechanism of initial production of enzyme at the procoagulant surface.

Calculations for the amounts of FXIIa generated at material surfaces in plasma using a mathematical model for measured coagulation responses indicate that the relative contributions of the individual pathways of enzyme generation are similar at both hydrophilic and hydrophobic surfaces, only the amounts of enzyme generated scale with surface energy and area of the activating surface.

Further, from direct measurement of enzyme activation at test surfaces we observed that contact activation reactions are not specific to negatively-charged hydrophilic surfaces. Rather, the molecular interactions are attenuated at hydrophobic surfaces due to protein adsorption so that poorly-adsorbent hydrophilic surfaces exhibit an apparent specificity for contact activation reactions.

Preliminary studies were performed to assay the plasma coagulation response to low-fouling surfaces prepared by either grafting poly(ethylene glycol) chains or using zwitterions. Results indicate that poly(ethylene glycol)-modified surfaces are significantly weaker procoagulants than surfaces containing zwitterions underscoring a need to specifically evaluate the coagulation response despite similarities in observed protein adsorption to both surfaces.

In summary, our studies demonstrate a need to incorporate protein-adsorption competition at procoagulant surfaces into the mechanism of contact activation to account for the observed moderation of FXII activation by blood proteins unrelated to the plasma coagulation cascade.

## TABLE OF CONTENTS

LIST OF FIGURES .....	ix
LIST OF TABLES .....	xiv
ACKNOWLEDGEMENTS .....	xv
Chapter 1 Introduction .....	1
1.1 Problems of coagulation and thrombosis in blood-contacting medical devices .....	1
1.2 Blood hemostasis .....	2
1.2.1 Blood coagulation cascades .....	2
1.2.2 Extrinsic coagulation cascade .....	3
1.2.3 Intrinsic coagulation cascade .....	4
1.2.4 Biochemistry of contact activation .....	6
1.2.5 Role of platelets in hemostasis .....	8
1.3 Principles of protein adsorption .....	9
1.3.1 Langmuir model of protein adsorption .....	10
1.3.2 Gibbs/Guggenheim model of protein adsorption .....	12
1.4 Proposed hypothesis .....	14
1.5 Significance of proposed work .....	16
1.6 Literature citations .....	16
Chapter 2 Procoagulant activity of surface immobilized Hageman factor .....	23
2.1 Introduction .....	23
2.2 Materials and methods .....	27
2.2.1 Plasma and proteins .....	27
2.2.2 Surface preparation of solid procoagulants .....	28
2.2.3 Protein immobilization on solid procoagulants .....	30
2.2.4 In vitro coagulation assay .....	31
2.2.5 Mathematical analysis .....	32
2.3 Results .....	33
2.3.1 Soluble FXIIa titration in PPP .....	33
2.3.2 Procoagulant efficiency of solid procoagulants .....	36
2.3.3 Titration of FXIIa-coated-particles in PPP .....	38
2.3.4 Titration of BSA-coated particles in PPP .....	41
2.3.5 FXIIa titration in $d_{XII}$ PPP .....	43
2.3.6 Titration of BSA-coated solid procoagulants in $d_{XII}$ PPP .....	44
2.4 Discussion .....	45
2.5 Conclusions .....	47
2.6 Literature citations .....	48

Chapter 3 Contributions of contact activation pathways of coagulation factor XII in plasma.....	52
3.1 Introduction .....	52
3.2 Materials and methods.....	56
3.2.1 Plasma and proteins.....	56
3.2.2 Surface preparation of solid procoagulants .....	56
3.2.3 In vitro coagulation assay.....	57
3.2.4 Mathematical analysis .....	58
3.3 Results.....	59
3.3.1 FXIIa titration of $d_{PK}PPP$ and $Rd_{PK}PPP$ .....	59
3.3.2 Surface area titration of solid procoagulants.....	61
3.3.3 Calculation of FXIIa generation.....	63
3.4 Discussion.....	68
3.4.1 Modeling material-induced coagulation.....	69
3.4.2 Calculation of FXIIa generation.....	70
3.5 Conclusions.....	73
3.6 Literature citations .....	73
Chapter 4 Moderation of prekallikrein-factor XII interactions in surface activation of coagulation by protein-adsorption competition.....	76
4.1 Introduction .....	76
4.2 Materials and Methods .....	79
4.2.1 Preparation of model material surfaces .....	79
4.2.2 Proteins and plasma .....	80
4.2.3 Coagulation assay.....	81
4.2.4 Kallikrein generation assay .....	81
4.2.5 Chromogenic assay.....	82
4.2.6 Statistical analyses.....	83
4.3 Results.....	83
4.3.1 Coagulation response to model surfaces .....	83
4.3.2 Kallikrein generation in solutions of PK and FXIIa.....	84
4.3.3 Kallikrein generation in solutions of PK and FXII .....	86
4.3.4 Displacement of adsorbed enzymes at hydrophobic surfaces using BSA .....	88
4.4 Discussion.....	89
4.4.1 Effect of adsorption on interactions of PK and FXII .....	91
4.4.2 Effect of adsorption on interactions of PK and FXIIa.....	92
4.4.3 Competitive displacement of adsorbed enzymes from hydrophobic surfaces.....	93
4.4.4 Role of the material surface in contact activation .....	94
4.5 Conclusions.....	96
4.6 Literature citations .....	97

Chapter 5 Moderation of factor XII- factor XI interactions in surface activation by protein-adsorption competition.....	100
5.1 Introduction .....	100
5.2 Materials and methods.....	102
5.3 Results.....	103
5.4 Discussion.....	105
5.5 Conclusions.....	108
5.6 Literature citations.....	108
Chapter 6 Contact activation of blood coagulation at low-fouling surfaces: poly(ethylene glycol)-grafted and zwitterion-terminated.....	110
6.1 Introduction .....	110
6.2 Materials and methods.....	113
6.2.1 Plasma and proteins.....	113
6.2.2 Preparation of test surfaces.....	114
6.2.3 In vitro coagulation assay.....	117
6.2.4 Mathematical modeling.....	117
6.2.5 Protein adsorption measurements.....	118
6.3 Results.....	119
6.3.1 Water-wettability of test surfaces.....	119
6.3.2 Protein adsorption studies .....	120
6.3.3 Titration of exogenous FXIIa .....	121
6.3.4 Surface area titration of model surfaces .....	122
6.4 Discussion.....	124
6.5 Conclusions.....	126
6.6 Literature citations.....	126
Chapter 7 Summary .....	130
Appendix A Mathematical model for material-induced coagulation .....	137
A.1 Quantitative analysis of coagulation response to exogenous FXIIa.....	137
A.2 Quantitative analysis of material-induced coagulation.....	138
A.3 Literature citations .....	141
Appendix B Plasma coagulation response to surfaces containing dual chemical groups .....	142
B.1 Objective.....	142
B.2 Materials and methods .....	142
B.2.1 Preparation of test surfaces.....	142
B.2.2 Coagulation assay .....	143
B.2.3 Mathematical modeling of coagulation response .....	143
B.3 Results.....	143

B.4 Literature citations .....	147
Appendix C Material-induced whole-blood coagulation.....	148
C.1 Objective .....	148
C.2 Materials and methods .....	148
C.2.1 Preparation of test surfaces.....	148
C.2.2 Coagulation assay using whole bovine blood.....	149
C.3 Results and Discussion .....	149
C.4 Literature citations .....	151



## LIST OF FIGURES

- Figure 1-1: Blood coagulation cascades: the intrinsic and extrinsic pathways (enclosed within labeled lined boxes) converge into the common pathway, ultimately producing a fibrin clot. (The solid box indicates the surface-mediated steps.) ..... 3
- Figure 1-2: The surface-mediated interactions in contact activation complex according to traditional biochemistry involving the four participating proteins: prekallikrein (PK), high molecular weight kininogen (HMWK), factor XII (FXII), factor XI (FXI), kallikrein (Kal), suffixes “a” and “f” represent activated and fragmented forms, respectively. .... 7
- Figure 2-1: FXIIa titration in platelet poor plasma (PPP) showing experimental coagulation time (CT) values vs. concentration of exogenous FXIIa introduced in various forms: soluble FXIIa (open triangles,  $\nabla$ ), and immobilized on: COOH (solid circles,  $\bullet$ ), APS (open circles, o), and OTS surfaces (closed triangles,  $\blacktriangledown$ ). The smooth curve shows the best fit of a mathematical model to the data for soluble FXIIa titration. (All data shown as mean  $\pm$  S.D. for  $n \geq 3$ ). ..... 35
- Figure 2-2: Surface area titration (SAT) in PPP showing experimental CT vs. surface area of three different procoagulant materials. Data for COOH particles (solid circles  $\bullet$ ), APS particles (open circles o), CMETS particles (closed triangles  $\blacktriangledown$ ) and OTS particles (open triangles  $\nabla$ ) are shown along with the smooth lines representing the best fit to the previously developed mathematical model. (All data expressed as mean  $\pm$  S.D. for  $n \geq 3$ ). ..... 38
- Figure 2-3: Surface area titration (SAT) in PPP showing experimental CT vs. surface area of three different BSA-coated procoagulant materials. Data for BSA immobilized on COOH (solid circles  $\bullet$ ), APS (open circles o), and OTS (closed triangles  $\blacktriangledown$ ) surfaces are shown along with the smooth lines representing the best fit to the previously developed mathematical model. (All data expressed as mean  $\pm$  S.D. for  $n \geq 3$ ). ..... 42
- Figure 2-4: FXIIa titration in FXII-deficient platelet poor plasma ( $d_{XII}$ PPP) showing experimental CT values vs. concentration of exogenous FXIIa introduced in different forms: soluble (solid circle  $\bullet$ ) and as immobilized enzyme onto COOH (open triangles  $\nabla$ ), APS (closed triangles  $\blacktriangledown$ ) and OTS (open circles o) surfaces. The solid lines represent best fit of the data to the mathematical model: soluble enzyme (smooth line) and as immobilized enzyme onto COOH (dotted line), APS (short-dashed line) and OTS (dashed line). (All data expressed as mean  $\pm$  S.D. for  $n \geq 3$ ). ..... 44

- Figure 3-1: FXIIa titration in PK-deficient PPP ( $d_{PK}PPP$ ) (solid circles, ●), and reconstituted  $d_{PK}PPP$  ( $Rd_{PK}PPP$ ) (open circles, ○) showing experimental coagulation time (CT) values vs. concentration of exogenous soluble FXIIa. The smooth curve shows the best fit of a mathematical model to the data for soluble FXIIa titration. (All data is shown as mean  $\pm$  S.D. for  $n \geq 3$ )..... 60
- Figure 3-2: Surface area titration (SAT) in  $d_{PK}PPP$  and  $Rd_{PK}PPP$  showing experimental CT vs. added surface area of three different procoagulant materials. Data for glass-particles (circles ●, ○), APS particles (triangles ▼, ▽) and OTS particles (squares ■, □) are shown, where solid and open symbols represent measurements in  $Rd_{PK}PPP$  and  $d_{PK}PPP$ , respectively. The smooth lines represent CT values calculated from the model using the mean  $K_I$  values listed in Table 3-2. (All data expressed as mean  $\pm$  S.D. for  $n \geq 3$ ). ..... 63
- Figure 3-3: FXIIa produced in total and via the autoactivation and reciprocal-activation pathways at three surface area values for the each of the three solid test procoagulants: (top) glass, (middle) APS and (bottom) OTS. The bars show in groups of three at each surface area the total amount of enzyme (solid bar), enzyme produced by autoactivation (hatched bar) and enzyme produced by reciprocal-activation (dotted bar). ..... 65
- Figure 3-4: A compilation of values from the different surface presented using a semi-log plot for ease of comparison among the procoagulants showing glass (white background), APS (gray background) and OTS (black background) from left to right at each surface area. .... 66
- Figure 3-5: FXIIa produced per unit surface area in total and via the individual pathways at three surface area values for each of the three solid test procoagulants: (top) glass, (middle) APS and (bottom) OTS. The bars show in groups of three at each surface area the total amount of enzyme (solid bar), enzyme produced by autoactivation (hatched bar) and enzyme produced by reciprocal-activation (dotted bar). ..... 67
- Figure 3-6: A compilation of values from the different surface presented using a semi-log plot for ease of comparison among the procoagulants showing glass (white background), APS (gray background) and OTS (black background) from left to right at each surface area. .... 68
- Figure 4-1: Temporal changes in Kal generation in solutions of 20  $\mu\text{g/mL}$  PK and  $5 \times 10^{-2}$   $\mu\text{g/mL}$  FXIIa at glass (closed circles ●), OTS (closed triangles ▼) and OTS-BSA (open triangles ▽) surfaces up to 10 min. Also shown is Kal generation in glass vials containing 500  $\text{mm}^2$  OTS beads (open circles ○). Guidelines are drawn to highlight the profound differences in trends. The symbols # and \* represent statistical significance with respect to Kal

concentrations in glass vials containing OTS beads and OTS vials, respectively, at each time point. (Data expressed as mean  $\pm$  S.D. for  $n \geq 3$ ). ..... 86

**Figure 4-2:** Temporal changes in Kal generation in solutions of 20  $\mu\text{g/mL}$  PK and  $5 \times 10^{-2}$   $\mu\text{g/mL}$  of FXII at glass (closed circle ●), OTS (closed triangle ▼) and OTS-BSA (open triangle ▽) surfaces. Data are plotted using same y-scale as Figure 2 for ease of comparison. Guidelines are drawn to highlight the differences in trends. The symbols \* and # represent statistical significance with respect to OTS vials and OTS-BSA surfaces, respectively, at a given time point. (Data expressed as mean  $\pm$  S.D. for  $n \geq 3$ ). ..... 87

**Figure 4-3:** Temporal changes in Kal generation in solutions of 20  $\mu\text{g/mL}$  PK and 4  $\mu\text{g/mL}$  FXII in OTS vials (closed circle ●). The effects of addition of BSA at 5 mg/mL (open triangle ▽), 1 mg/mL (closed triangle ▼), or 0 mg/mL, (PBS alone, open circle o) at 10.5 min are also presented. The symbols \* and # represent statistical significance with respect to 0 mg/mL and 1 mg/mL BSA, respectively, at given time points. (Data expressed as mean  $\pm$  S.D. for  $n \geq 3$ ). ..... 89

**Figure 4-4:** Alternate model for the sequence of events involving PK and FXII at solid procoagulant surfaces. Contact activation is initiated by autoactivation of FXII at the interphase and is not specific to negatively-charged surfaces. Subsequent interactions involving reciprocal-activation of PK and FXII do not occur by direct assembly on the surface but rather require displacement from the surface. .... 96

**Figure 5-1:** Temporal changes in FXIa generation in solutions of 4  $\mu\text{g/mL}$  FXII and 5  $\mu\text{g/mL}$  FXI in glass (dotted squares ■) and OTS (closed circles ●) vials. Statistical analyses were performed by two-tailed p-value using InStat software (GraphPad). Means were compared pair-wise and the differences were considered statistically significant for  $p < 0.05$ . Significant differences are denoted by one symbol ( $p < 0.05$ ) and two symbols ( $p < 0.01$ ). The symbol \* represents statistical significance at a given time point. (Data expressed as mean  $\pm$  S.D. for  $n \geq 3$ ). ..... 104

**Figure 5-2:** Temporal changes in FXIa generation in solutions of 4  $\mu\text{g/mL}$  FXII and 5  $\mu\text{g/mL}$  FXI in OTS (closed circles ●) vials. The effects of addition of BSA at 12.5 mg/mL (closed triangles ▲) or 0 mg/mL, (PBS alone, open triangles △) at 10.5 min to the OTS vials are also presented. Statistical analyses described in Figure 5-1. The symbol # represent statistical significance between OTS vials with BSA 12.5 mg/mL and PBS at a given time point. (Data expressed as mean  $\pm$  S.D. for  $n \geq 3$ ). ..... 105

- Figure 5-3: Alternate model for the sequence of events involving FXII and FXI at solid procoagulant surfaces. Contact activation is initiated by autoactivation of FXII at the interphase and is not specific to anionic hydrophilic surfaces. Subsequent FXIIa-mediated FXI hydrolysis does not occur by direct assembly on the surface but rather require displacement from the surface..... 107
- Figure 6-1: Chemical structure of methoxy(polyethyleneoxy)propyltrimethoxysilane (PEGS, top) and n-(trimethoxysilylpropyl)ethylenediamine triacetic acid, trisodium (ZWITS, bottom)..... 116
- Figure 6-2: FXIIa titration in platelet poor plasma (PPP) showing experimental coagulation time (CT) values vs. concentration of exogenous FXIIa. The smooth curve shows the best fit of a mathematical model to the data. (All data shown as mean  $\pm$  S.D. for  $n \geq 3$ )...... 122
- Figure 6-3: Surface area titration (SAT) in PPP showing experimental CT vs. surface area of different solid procoagulants. Measured data for clean-glass particles (solid circles ●), COOH particles (open circles ○), ZWITS particles (closed triangles ▼), APS particles (open triangles ▽), BTS particles (solid squares ■) and PEGS particles (open squares □) are shown along with the smooth lines representing the best fit to a mathematical model for material-induced coagulation. (All data shown as mean  $\pm$  S.D. for  $n \geq 3$ )...... 123
- Figure 7-1: Proposed sequence of events for contact activation of blood-plasma coagulation at material surfaces. Contact activation is initiated by autoactivation of FXII at the interphase and is not specific to anionic surfaces. Subsequent reactions involving reciprocal-activation and FXI hydrolysis do not occur by direct assembly on the surface but rather require displacement from the surface. .... 134
- Figure B-1: Surface area titration (SAT) in PPP showing experimental CT vs. added surface area of six different procoagulant materials prepared from a dual component silane solution containing CMETS:BTS in varying proportions. Data for 0.00:1.00 (solid circles ●), 0.25:0.75 (open circles ○), 0.5:0.5 (closed triangles ▼), 0.67:0.33 (open triangles ▽), 0.75:0.25 (closed squares ■), and 1.00:0.00 (open squares □) are shown. (All data expressed as mean  $\pm$  S.D. for  $n \geq 3$ ). .... 145
- Figure B-2: Plot showing the relationship between  $K_I$  (a measure of catalytic efficiency) and the water adhesion tension (surface energy) of test surfaces from mixtures of CMETS and BTS in different proportions. .... 146
- Figure C-1: Surface area titration (SAT) in whole bovine blood showing experimental CT vs. added surface area of three different procoagulant

materials. Data for glass-particles (solid circles ●), APS particles (open circles o) and OTS particles (closed triangles ▼) are shown. (All data expressed as mean  $\pm$  S.D. for  $n \geq 3$ ). ..... 150

## LIST OF TABLES

Table <b>2-1</b> : Parameters describing processing of a FXIIa dose as generated by best fit of the measured CT response to an enzyme kinetics model. ....	36
Table <b>2-2</b> : Catalytic efficiency of solid procoagulants and BSA-coated procoagulants.....	37
Table <b>2-3</b> : Protein Coverage of FXIIa and BSA on the solid procoagulants .....	40
Table <b>3-1</b> : Parameters describing the gray box processing of FXIIa .....	61
Table <b>3-2</b> : $K_I$ values for the solid procoagulants.....	62
Table <b>3-3</b> : Estimated fraction of enzyme generation via reciprocal-activation.....	72
Table <b>4-1</b> : Water contact angles and the measured CT response to PPP .....	84
Table <b>6-1</b> : Surface water-wettability and values of $K_I$ for the test surfaces .....	120
Table <b>6-2</b> : Parameters describing processing of FXIIa dose in PPP as generated by best fit of the measured CT response to a mathematical model. ....	121
Table <b>B-1</b> : $K_I$ values for the solid procoagulants .....	144

## ACKNOWLEDGEMENTS

I am grateful to my thesis advisor Dr. Christopher Siedlecki and Dr. Erwin Vogler with whom I had an opportunity to closely work for their mentoring efforts during my graduate research. They have been very patient and supportive in helping me finding my way through this “labyrinth” called coagulation cascade.

I am also grateful to my other committee members- Drs. Alan Snyder, Ira Ropson and William Hancock- for their feedback and their truly enthusiastic support for my work.

Over the years I had the privilege of working with a great group of people as part of the Hematology at Biomaterial Interfaces research group across both campuses. I have also enjoyed my time in the lab with fellow lab mates and thank everyone for their support.

Without the support of my family and friends I would not have completed my journey through graduate school. I dedicate my thesis to my parents for their constant support and love over the years.

## **Chapter 1**

### **Introduction**

#### **1.1 Problems of coagulation and thrombosis in blood-contacting medical devices**

An ever-increasing number of blood-contacting medical devices are being used in patients for treatment of cardiovascular diseases every year. For example, it is estimated that over a thousand left-ventricular-assist-devices, nearly two million stents and over two hundred thousand heart valves were implanted in US patients in the year 2000 alone (Lysaght 2000; Ratner 2000). In addition, use of peripheral devices like hemodialysis membranes and cardiopulmonary bypass oxygenators is also routine medical practice. However, thrombosis and coagulation arising from adverse blood-material interactions persist as serious risk to patient health and a major cause for device failure. Large doses of anticoagulants administered to these patients fail to completely prevent thrombosis while increasing the risk of uncontrolled bleeding and hemorrhage (Galloway 1999; McBride 1999). There is a need for improved blood-compatible materials for use in devices that contact blood. Towards this objective, we have been studying the molecular mechanism underlying hemocompatibility of biomaterials.

Interaction of blood components and biomaterial surface leads to thrombus formation via a combination of two different pathways, (i) initiation of the coagulation cascade and (ii) activation, adhesion and aggregation of platelets. These biological responses are mediated by the interaction of blood components at the biomaterial surface



and are largely influenced by protein adsorption events. The following sections provide a short review of mechanisms of hemostasis and theories in protein adsorption as background to the work presented in this dissertation on molecular events at the blood-material interface.

## **1.2 Blood hemostasis**

Blood is a suspension of formed elements, or cells, in plasma, an aqueous solution containing a variety of organic and inorganic constituents (Williams 1987). Normally, blood flows through the vascular system lined by endothelial cells, which help to maintain blood fluidity. However, blood may clot in response to vascular injury or during pathological conditions forming an intravascular thrombus. A complex physiological system is involved in hemostasis and thrombosis, and consists of two major pathways broadly grouped as cellular (involving platelets) and humoral (involving soluble plasma proteins) components.

### **1.2.1 Blood coagulation cascades**

The humoral component involves a series of enzyme activation steps referred to as the blood coagulation cascades that acts as a “biochemical amplifier” (MacFarlane 1964). Each cascade step involves a limited proteolytic cleavage of a zymogen to an activated enzyme. These blood coagulation reactions are classically grouped in two major pathways— the extrinsic and intrinsic cascades that converge into the common

pathway to ultimately generate a fibrin clot, as illustrated in Figure 1-1. The intrinsic and extrinsic pathways are not wholly independent and interact through multiple reactions providing feedback.

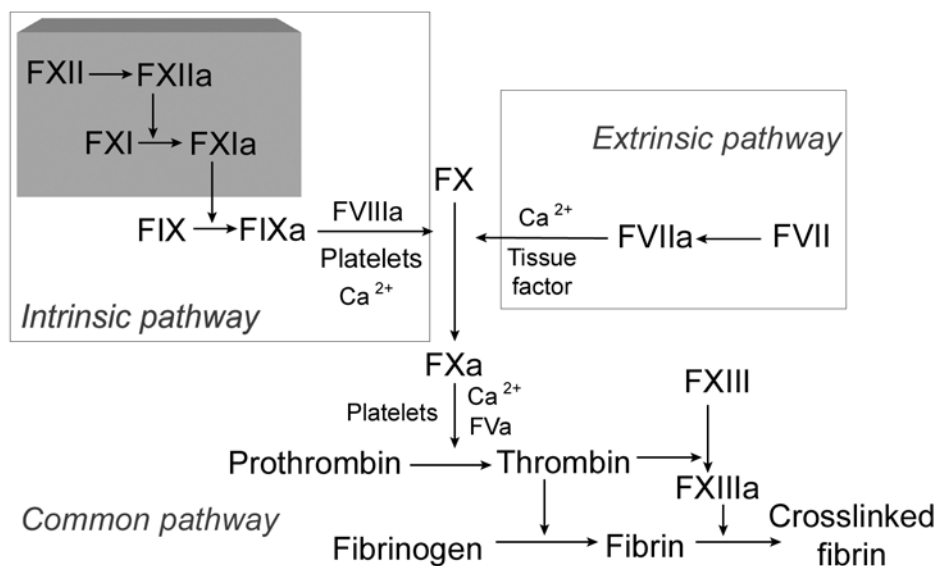


Figure 1-1: Blood coagulation cascades: the intrinsic and extrinsic pathways (enclosed within labeled lined boxes) converge into the common pathway, ultimately producing a fibrin clot. (The solid box indicates the surface-mediated steps.)

### 1.2.2 Extrinsic coagulation cascade

The extrinsic cascade is triggered when blood contacts tissue factor (TF), a non-enzymatic lipoprotein expressed on membranes of sub-endothelial cells, and therefore is “extrinsic” to the vascular system. During injury or damage to a vessel wall, blood contacts TF triggering the extrinsic coagulation cascade, which along with activated

platelets results in a hemostatic plug that stems blood loss. TF acts as a complex with activated factor VII (FVIIa) in presence of phospholipids to convert factor X (FX)→FXa as well as factor IX (FIX)→FIXa, which in turn generates more FXa. Further, in the presence of phospholipids, FXa activates prothrombin (factor II) to produce thrombin. Thrombin cleaves fibrinogen (factor I) releasing fibrinopeptides A and B to produce fibrin monomers, which auto-polymerize into fibrin strands. Thrombin also activates factor XIII, which chemically cross-links these fibrin strands ultimately producing an insoluble fibrin mesh, or the fibrin clot that entraps platelets and strengthens the hemostatic plug.

### **1.2.3 Intrinsic coagulation cascade**

The other pathway to a fibrin clot is the intrinsic cascade in which all the participating factors are contained within the vascular system (plasma) and is initiated upon contact with an activating surface. The central step of contact activation triggering the intrinsic cascade is the activation of factor XII (FXII), which in turn activates factor XI (FXI). FXIa activates FIX and converges into the reactions of the common pathway with the subsequent activation of FX by FIXa as described above to generate a fibrin clot as the ultimate product.

The intrinsic pathway of coagulation is reportedly initiated on contact of blood/blood-plasma with a wide variety of non-physiological surfaces and soluble agents such as glass, kaolin, dextran sulfate, ellagic acid, etc. (Colman 2001a; Kaplan 1978; Sainz 2007). Some investigators have suggested that activated platelet surfaces (Walsh

1984) and collagen on subendothelial cells (Furie 1988) serve as activating surface in vivo, but there is no conclusive evidence. Further, only FXI deficiency has been associated with mild to moderate bleeding disorders but not deficiencies of the other factors of this pathway (Colman 2001b; Gorbet 2004). This has led to the proposition that the role of the intrinsic cascade in coagulation is limited to in vitro conditions with little in vivo significance. In fact, a modified scheme of the coagulation cascade reactions that bypasses contact activation reactions of the intrinsic cascade has also been proposed (Gorbet 2004). In this scheme, coagulation is initiated by TF via the extrinsic coagulation cascade initially producing a small amount of thrombin. Activation of FX by the TF-FVIIa complex is also believed to activate FXI and FVIII of the intrinsic pathway providing a sustained dose of thrombin essential for propagation of coagulation reactions. It is argued that such a scheme explains why the deficiency of FXI, but not of other contact activation proteins, leads to bleeding disorders.

Recent data suggest that contact activation may play an important role pathologically via a here-to-fore unknown mechanism even if its role is limited in hemostasis. In sharp contrast to the conventional paradigm that similar molecular mechanisms are involved in both hemostasis and thrombosis, recent work suggests that the underlying mechanisms may be different and that the intrinsic pathway of coagulation may be involved in thrombosis, but not in hemostasis (Kleinschnitz 2006; Renne 2005). According to this new suggested mechanism, during arterial thrombus formation, platelets are activated by subendothelial extracellular matrix proteins at the site of vascular injury. Although TF-FVIIa pathway initially aids in recruitment of additional platelets, TF is rapidly inactivated by TF-pathway-inactivator (TFPI), but thrombin

generation is sustained by contact activation of FXII on activated platelet surfaces. Therefore, the physiological significance of the intrinsic pathway continues to remain controversial and a topic of current research.

However, elevated levels of activated factors of the intrinsic cascade have been observed with the use of blood-contacting medical devices like ventricular assist devices (Himmelreich 1995; Koster 2000; Wagner 2000), hemodialysis membranes (Panichi 1995; Svensson 1996), cardiopulmonary bypass oxygenators (Campbell 2001; Levy 2003; Paparella 2004; Wachtfogel 1989; Wendel 1999), etc. underscoring the physiological significance of this pathway in patients requiring these devices. These activated enzymes not only exacerbate the risk of thrombosis and coagulation but may also adversely perturb other physiological systems like the complement system, fibrinolytic pathway and immune system while generating hypotension-causing vasodilation agents (Colman 2001a; Courtney 1994; Hsu 1997; Janatova 2000; Nilsson 2007; Sainz 2007). There is an obvious need for materials with improved blood compatibility, a goal that remains largely unrealized in biomaterial surface science. It is essential, therefore, to understand blood-material interactions that determine hemocompatibility of biomaterials.

#### **1.2.4 Biochemistry of contact activation**

Initiation of the intrinsic cascade of coagulation on contact with an activating surface is a complex process and is believed to involve four different proteins— FXII, FXI, prekallikrein (PK) and high molecular weight kininogen (HMWK) (Colman 2001a;

Williams 1987). Molecular interactions of contact activation are schematically illustrated in Figure 1-2. It is widely believed that contact activation is specific to negatively-charged surfaces (Colman 2001a; Kaplan 1978; Sainz 2007) so that surfaces lacking the negative charges are essentially “benign”.

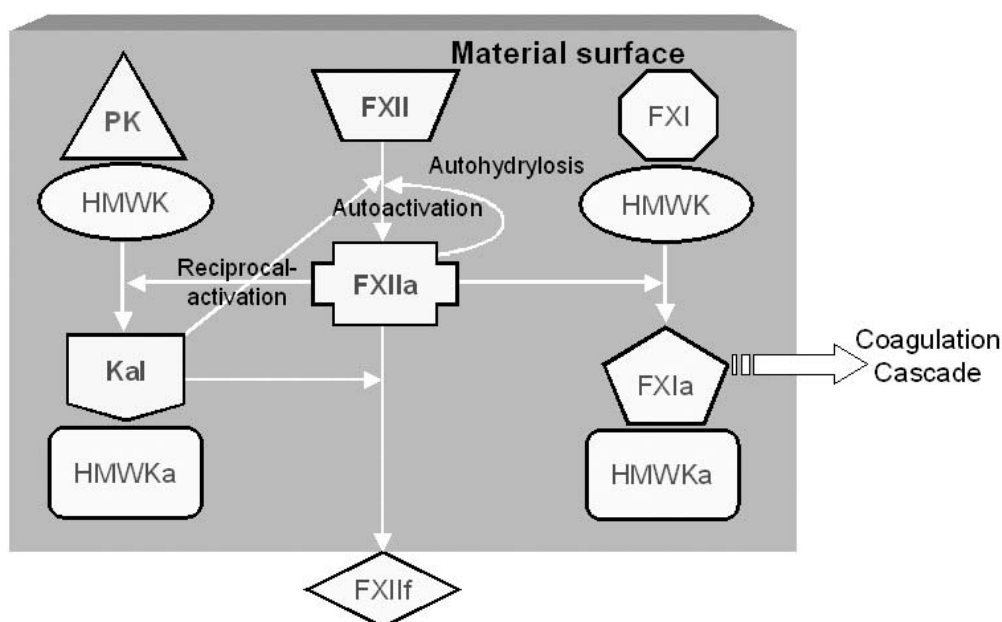


Figure 1-2: The surface-mediated interactions in contact activation complex according to traditional biochemistry involving the four participating proteins: prekallikrein (PK), high molecular weight kininogen (HMWK), factor XII (FXII), factor XI (FXI), kallikrein (Kal), suffixes “a” and “f” represent activated and fragmented forms, respectively.

According to this traditional biochemical theory, FXII can “bind” to negatively-charged surface functional groups via domains rich in positively-charged residues (Pixley 1987; Revak 1974). Binding to these anionic activating surfaces purportedly induces a conformational change in FXII leading to some level of activation and is referred to as

autoactivation (Fair 1977; Vroman 1964). Binding to the surface is also believed to sharply increase susceptibility of activation of FXII to proteolytic cleavage by kallikrein (Kal) (Silverberg 1982). FXIIa generated at the surface in turn cleaves PK bound to the surface as a complex with HMWK (Griffin 1978). This mutual activation of PK and FXII at the surface is known as reciprocal-activation. Some investigators have also observed that FXIIa can also hydrolyze other FXII molecules and is referred to as autohydrolysis or self-amplification (Silverberg 1980; Zhuo 2006). FXIIa activates FXI bound at the surface as a complex with HMWK to generate FXIa leading to propagation of coagulation cascade reactions (Bouma 1977; Ratnoff 1979).

### **1.2.5 Role of platelets in hemostasis**

Platelets, which are discoid-shaped anucleated blood cells originating from the cytoplasm of megakaryocytes, circulate in the vascular system and constitute the cellular component of hemostasis (Colman 2001b). During vascular injury, platelets adhere to the exposed sub-endothelial surface and are activated. Activated platelets secrete stored intercellular components that can locally activate other platelets to recruit into the growing hemostatic plug while providing enzymes such as thrombin that are involved in the coagulation cascade. Activated platelet membrane also serves as a cofactor for the formation of the tenase and prothrombinase complexes of the coagulation cascade (Zwaal 1998). Concurrently, coagulation factors such as thrombin and calcium are known to activate platelets. Thus, the cellular and humoral components of hemostasis synergistically interact to generate a stable hemostatic plug.

### **1.3 Principles of protein adsorption**

Proteins are surface-active and tend to adsorb to materials surfaces (Brash 1995). Protein adsorption is an early event that determines the biological response to materials, both in vitro and in vivo. Water and ions are perhaps the first components of the biological milieu to arrive at the biomaterial surface and are closely followed by proteins (Ratner 2004; Vogler 1999). In fact, cells that are much larger and slower to arrive at the surface essentially respond to the proteins at the surface rather than the native surface of the biomaterial. The nature of the material surface profoundly affects protein adsorption and in turn the biological response. Thus, the study of protein adsorption has been a topic of deep interest and even intense debate in biomaterial surface science research.

A driving force for protein adsorption is the reduction in free energy at an interface between two phases (Nakanishi 2001). A combination of different intermolecular forces are believed to be involved in adsorption, including van der Waals forces, electrostatic double-layer forces, hydration forces and hydrophobic interactions (Blomberg 1998; Brash 1995).

Literature in biomaterial surface science offers few universal principles in protein adsorption making it a difficult proposition to evaluate reported results, further complicated by the use of a multitude of measurement techniques. One useful classification of protein adsorption studies is to group them into two broad categories, namely, the Langmuirian and Gibbsian/Guggenheim paradigms. The former is based on the concept of a two-dimensional (2-D) monolayer model at the surface, whereas the latter envisages a three-dimensional (3-D) “interphase” between two contacting phases,



i.e., the material and the bulk biological fluid in the case of biomaterials. Furthermore, it is worthwhile to recognize surfaces classed into two relative groups “hydrophilic” and “hydrophobic” for the study of protein adsorption. Surfaces exhibiting a water contact angle  $> 65^\circ$  (or pure water adhesion tension of  $< 30$  dyne/cm) are taken to be hydrophobic while surfaces exhibiting water contact angle  $< 65^\circ$  (or pure water adhesion tension of  $> 30$  dyne/cm) are hydrophilic (Vogler 1999).

### **1.3.1 Langmuir model of protein adsorption**

The fundamental premise of the Langmuir model for the adsorption of molecules to an adsorbent is that it occurs as a monolayer on the surface at specified sites and a complete occupancy of these specified sites corresponds to complete coverage. Langmuir isotherm is widely applied to protein adsorption studies, although it is acknowledged that there are many shortcomings (Brash 1995; Horbett 1993).

In the context of material-induced coagulation and thrombosis, Horbett has identified key principles governing adsorption of plasma proteins to biomaterials governing these responses (Horbett 2004). Firstly, monolayer adsorption and limited availability for protein adsorption sites leads to competition and not all plasma proteins are equally represented at the surface. Secondly, composition of the protein monolayer is determined by intrinsic surfactancy of each plasma protein and its bulk concentration. Inherent in this principle is the argument that each protein exhibits different surfactancy that is uniquely determined by its characteristic properties: size, charge, amino-acid sequence and structural stability (“hard” vs. “soft”) (Brash 1995; Nakanishi 2001).

Thirdly, surfaces vary in their selectivity of adsorption and ability to cause conformational change. Finally, coagulation response and platelet activation by the surfaces are mediated not only by the total amounts of protein adsorbed but also the bioreactivity determined by conformational change in adsorbed molecules.

Protein adsorption for a given combination of protein(s) and adsorbent surface is believed to be influenced by the interplay of different interactions including protein-surface and protein-protein interactions in addition to environmental factors like temperature, pH etc. (Brash 1995; Nakanishi 2001).

Structural stability/conformation of adsorbed protein is particularly critical because it affects the reversibility of adsorption, steric effects that determine protein packing in the monolayer and also the biological activity, i.e. availability of epitopes for ligand-receptor interactions in antibody binding, cell adhesion, platelet activation, etc. (Horbett 1993). “Hard” proteins like  $\alpha$ -chymotrypsin, ribonuclease and lysozyme exhibit high internal stability (Nakanishi 2001). These proteins adsorb in small amounts to hydrophilic surfaces except in the presence of strong electrostatic interactions but in larger amounts on hydrophobic surface where they undergo conformational changes. In contrast, “soft” proteins like bovine serum albumin, human serum albumin, hemoglobin, catalase and phytase have low internal stability (Nakanishi 2001). These molecules adsorb to all surfaces, both hydrophilic and hydrophobic, due to the gain in entropy arising from conformational changes upon adsorption (Nakanishi 2001).

In mixed protein solutions (including plasma) selectivity for proteins by a given surface plays a critical role in determining the adsorbed monolayer composition during competitive adsorption. Since only a limited number of “binding sites” are available on

the adsorbent, a limited number of proteins may be accommodated at the interface that is determined by protein-surface and protein-protein interactions and not necessarily by the bulk compositions. This is further complicated by changes in the monolayer composition that may arise due to competitive protein adsorption. For instance, in the so-called Vroman effect that has now been extensively discussed in literature, adsorbed fibrinogen (key factor in platelet activation) is reportedly displaced by activated HMWK, so that the amount of adsorbed fibrinogen passes through a peak along the scale of adsorption time, plasma concentration or spatial distance (Horbett 1993; Slack 1995).

The traditional theory of contact activation is predicated on the principles of selectivity/specificity in protein adsorption arising due to biochemical differences in composition of proteins, although not unequivocally demonstrated experimentally. Proteins involved in contact activation, in particular HMWK, are believed to specifically adsorb (or “bind”) to anionic surfaces (see (Brash 1995) and references therein).

### **1.3.2 Gibbs/Guggenheim model of protein adsorption**

In contrast to the monolayer model of protein adsorption to materials surfaces, the Gibbsian paradigm proposes a 3-D interfacial model. Measuring the decrease in interfacial tension at the liquid/vapor interface, Vogler and co-workers observed a systematic progression with molecular weight of proteins (Krishnan 2003). They proposed that protein molecules adsorb to the “interphase” with dimensions scaling with the size of the adsorbing protein, such that smaller proteins fill a single layer whereas larger proteins form multi-layers. The authors proposed that protein adsorption follows a

homology in size rather than biochemical composition/specificity (Krishnan 2003; Krishnan 2004b).

Applying contact-angle goniometry to measure energetics of protein adsorption at the solid/liquid interface they observed that trends were similar to those reported for liquid/vapor interface (Krishnan 2006; Krishnan 2005). They proposed that adsorption is driven by protein concentration in solution rather than the biochemical specificity. Of particular interest to molecular events of contact activation, they observed that all plasma proteins including those of the contact-activation complex exhibited trends in protein adsorption that were similar to other plasma proteins (Krishnan 2005). The underlying mechanism for these observed trends is based on the argument that the driving force for protein adsorption is the dehydration of the bound water vicinal to the surface (Krishnan 2006; Krishnan 2005). Due to weak binding to water molecules, hydrophobic surfaces are more prone to easy dehydration by the protein molecules facilitating adsorption to these surfaces. In contrast, protein adsorption to “water loving” or hydrophilic surfaces is energetically less favorable, although some proteins may associate with the surface in a manner not requiring the displacement of water molecules (see (Krishnan 2005) and references therein). Thus, these studies highlight the role of the solvent in driving protein adsorption rather than protein-surface and protein-protein interactions as described in **1.3.1.**

Recent results using solution-depletion measurements at hydrophobic surfaces corroborate results of contact-angle goniometry, wherein proteins partitioned into a 3-D interphase that was largely influenced by the size and not the biochemistry of the protein (Noh 2006a; Noh 2006b). Further, studies on competitive protein adsorption to

hydrophobic surfaces indicated that a limited capacity (measured in weight per unit volume) of the interphase to accommodate proteins naturally leads to selective adsorption (Noh 2007), consistent with trends observed at the liquid/vapor interface (Krishnan 2004a). A size discrimination effect, wherein the interphase is richer in smaller proteins (on number or molar basis), arises because fewer large proteins are required to attain the same interfacial concentration than smaller proteins.

#### **1.4 Proposed hypothesis**

Protein adsorption to material surfaces (see 1.3) is undoubtedly a complex process that remains poorly understood. However, one of the few principles generally accepted in the field is that hydrophobic surfaces are more efficient adsorbents than hydrophilic surfaces (Brash 1995; Hoffman 2004; Horbett 1993). Using a plethora of measurement techniques, studies have revealed that hydrophobic surfaces adsorb larger amounts of proteins than hydrophilic surfaces (Goncalves 2005; Noh 2006a; Renner 2005; Roach 2005; Wu 2005). In studies using atomic force microscopy to determine adhesion forces between proteins and surfaces, stronger forces were measured at hydrophobic surfaces than at hydrophilic surfaces (Sethuraman 2004; Xu 2007).

Therefore, if the molecular events of contact activation are indeed facilitated by the direct “binding”, “uptake” or “assembly” of the contact activation proteins on to the activating surface, from the perspective of protein adsorption, hydrophobic surfaces which can more efficiently “bind” or “assemble” (or adsorb) proteins at the surface should be stronger activators. However, the reverse is typically observed in hematology

where poorly-adsorbent hydrophilic surfaces are stronger procoagulants than adsorbent hydrophobic surfaces (Guo 2006; Zhuo 2005). There remains this unresolved paradox between known trends in protein adsorption to material surfaces and the suggested mechanism of contact activation of the plasma coagulation cascade. This has led to a patchwork of mechanistic fixes such as special adsorption specificity for a narrow class of contact activation proteins not shared by the multitude and selective denaturation of these proteins at hydrophobic surfaces. Studies on the interfacial activity of plasma proteins do not support these special properties (Krishnan 2005; Krishnan 2004b). In fact, interfacial activity of contact activation proteins was found to be no different from other plasma proteins such as albumin and immunoglobulin.

In sharp contrast to this traditional biochemical theory of contact activation, which suggests that biochemical specificity for anionic hydrophilic surfaces arises out of negatively-charged functional groups, we propose a new paradigm to incorporate a key role for protein adsorption in the molecular mechanism for contact activation, which is the overarching aim for this work. The central hypothesis of this work may be summarized as follows:

*All material surfaces are activators of the intrinsic coagulation cascade. Adsorption at hydrophobic surfaces moderates these interactions leading to an “apparent specificity” for hydrophilic surfaces.*

### 1.5 Significance of proposed work

In order to engineer improved blood-compatible materials, it is critical to develop a comprehensive understanding interactions between plasma proteins at the blood-contacting surface. The proposed hypothesis upon validation will redefine the problem of material-induced blood coagulation. These studies are also expected to yield a library of “structure-property relationships” relating material surface properties to coagulation response along with an understanding of the molecular mechanism and would offer new avenues to improving hemocompatibility of biomedical materials.

### 1.6 Literature citations

Blomberg, E., P. M. Claesson and J. C. Froberg (1998). "Surfaces coated with protein layers: a surface force and ESCA study." Biomaterials **19**: 371-386.

Bouma, B. N. and J. H. Griffin (1977). "Human blood coagulation factor XI." The Journal of Biological Chemistry **252**: 6432-6437.

Brash, J. L. and T. A. Horbett (1995). Proteins at interfaces: an overview. Proteins at interfaces II: fundamentals and applications. J. L. Brash and T. A. Horbett. Washington DC, American Chemical Society: 1-23.

Campbell, D. J., B. Dixon, A. Kladis, M. Kemme and J. D. Santamaria (2001). "Activation of the kallikrein-kinin system by cardiopulmonary bypass in humans." American Journal of Physiology - Regulatory Integrative & Comparative Physiology **281**: R1059-1070.

Colman, R. W. (2001a). Contact activation pathway: inflammatory, fibrinolytic, anticoagulant, antiadhesive, and antiangiogenic activities. Hemostasis and Thrombosis- Basic Principles and Clinical Practice. R. W. Colman, J. Hirsh, V. J. Marder, A. W. Clowes and J. N. George. Philadelphia, Lippincott William and William. **4**: 103-122.

Colman, R. W., A. W. Clowes, J. N. George, J. Hirsh and V. J. Marder (2001b). Overview of Hemostasis. Hemostasis and Thrombosis- Basic Principles and

Clinical Practice. R. W. Colman, J. Hirsh, V. J. Marder, A. W. Clowes and J. N. George. Philadelphia, Lippincott William and William. **4**: 3-16.

Courtney, J. M., N. M. Lamba, S. Sundaram and C. D. Forbes (1994). "Biomaterials for blood-contacting applications." Biomaterials **15**: 737-44.

Fair, B. D., H. Saito, O. D. Ratnoff and W. B. Rippon (1977). "Detection by fluorescence of structural changes accompanying the activation of Hageman factor (factor XII)." Proceedings of the Society for Experimental Biology and Medicine **155**: 199-202.

Furie, B. and B. C. Furie (1988). "The molecular basis of blood coagulation." Cell **53**: 505-518.

Galloway, A. C., R. V. Anderson, E. A. Grossi, F. C. Spencer and S. B. Colvin (1999). Acquired heart diseases. Principles of Surgery. S. I. Schwartz. New York, McGraw Hill: 845-908.

Goncalves, I. C., M. C. L. Martins, M. A. Barbosa and B. D. Ratner (2005). "Protein adsorption on 18-alkyl chains immobilized on hydroxyl-terminated self-assembled monolayers." Biomaterials **26**: 3891-3899.

Gorbet, M. B. and M. V. Sefton (2004). "Biomaterial-associated thrombosis: roles of coagulation factors, complement, platelets and leukocytes." Biomaterials **25**: 5681-5703.

Griffin, J. H. (1978). "Role of surface in surface-dependent activation of Hageman factor (blood coagulation Factor XII)." Proceedings of the National Academy of Sciences USA **75**: 1998-2002.

Guo, Z., K. M. Bussard, K. Chatterjee, R. Miller, E. A. Vogler and C. A. Siedlecki (2006). "Mathematical modeling of material-induced blood plasma coagulation." Biomaterials **27**: 796-806.

Himmelreich, G., H. Ullmann, H. Riess, R. Rosch, M. Loebe, A. Schiessler and R. Hetzer (1995). "Pathophysiologic role of contact activation in bleeding followed by thromboembolic complications after implantation of a ventricular assist device." ASAIO Journal **41**: M790-794.

Hoffman, A. S. and B. D. Ratner (2004). Nonfouling surfaces. Biomaterials science: an introduction to materials in medicine. B. D. Ratner, A. S. Hoffman, F. J. Schoen and J. E. Lemons. San Diego, Elsevier Science: 197-201.



- Horbett, T. A. (1993). "Principles underlying the role of adsorbed plasma proteins in blood proteins in blood interactions with foreign materials." Cardiovascular Pathology **2**: 137S-148S.
- Horbett, T. A. (2004). The role of adsorbed proteins in tissue response to biomaterials. Biomaterials science: an introduction to materials in medicine. B. D. Ratner, A. S. Hoffman, F. J. Schoen and J. E. Lemons. San Diego, Elsevier Science: 237-246.
- Hsu, L. C. (1997). "Biocompatibility in cardiopulmonary bypass." Journal of Cardiothoracic & Vascular Anesthesia **11**: 376-382.
- Janatova, J. (2000). "Activation and control of complement, inflammation, and infection associated with the use of biomedical polymers." ASAIO Journal **46**: S53-62.
- Kaplan, A. P. (1978). "Initiation of the intrinsic coagulation and fibrinolytic pathways of man: the role of surfaces, Hageman factor, prekallikrein, high molecular weight kininogen, and factor XI." Progress in Hemostasis and Thrombosis **4**: 127-175.
- Kleinschnitz, C., G. Stoll, M. Bendszus, K. Schuh, H. U. Pauer, P. Burfeind, C. Renne, D. Gailani, B. Nieswandt and T. Renne (2006). "Targeting coagulation factor XII provides protection from pathological thrombosis in cerebral ischemia without interfering with hemostasis." Journal of Experimental Medicine **203**: 513-518.
- Koster, A., M. Loebe, R. Hansen, E. V. Potapov, G. P. Noon, H. Kuppe and R. Hetzer (2000). "Alterations in coagulation after implantation of a pulsatile Novacor LVAD and the axial flow MicroMed DeBakey LVAD." Annals of Thoracic Surgery **70**: 533-537.
- Krishnan, A., C. A. Siedlecki and E. A. Vogler (2003). "Traube-Rule Interpretation of Protein Adsorption at the Liquid-Vapor Interface." Langmuir **19**: 10342-10352.
- Krishnan, A., C. A. Siedlecki and E. A. Vogler (2004a). "Mixology of Protein Solutions and the Vroman effect." Langmuir **20**: 5071-5078.
- Krishnan, A., J. Sturgeon, C. A. Siedlecki and E. A. Vogler (2004b). "Scaled interfacial activity of proteins at the liquid-vapor interface." Journal of Biomedical Materials Research. Part A **68**: 544-557.
- Krishnan, A., Y. H. Liu, P. Cha, D. Allara and E. A. Vogler (2005). "Scaled interfacial activity of proteins at a hydrophobic solid/aqueous-buffer interface." Journal of Biomedical Materials Research. Part A **75**: 445-457.
- Krishnan, A., P. Cha, Y. H. Liu, D. Allara and E. A. Vogler (2006). "Interfacial energetics of blood plasma and serum adsorption to a hydrophobic self-assembled monolayer surface." Biomaterials **27**: 3187-3194.

- Levy, J. H. and K. A. Tanaka (2003). "Inflammatory response to cardiopulmonary bypass." Annals of Thoracic Surgery **75**: S715-720.
- Lysaght, M. J. and J. A. O'Loughlin (2000). "Demographic scope and economic magnitude of contemporary organ replacement therapies." ASAIO Journal **46**: 515-521.
- MacFarlane, R. G. (1964). "An enzyme cascade in the blood clotting mechanism, and its function as a biochemical amplifier." Nature **202**: 498-499.
- McBride, L. R., K. S. Naunheim, A. C. Fiore, D. A. Moroney and M. T. Swartz (1999). "Clinical Experience With 111 Thoratec Ventricular Assist Devices." Annals of Thoracic Surgery **67**: 1233-1239.
- Nakanishi, K., T. Sakiyama and K. Imamura (2001). "On the adsorption of proteins on solid surfaces, a common but very complicated phenomenon." Journal of Bioscience and Bioengineering **91**: 233-244.
- Nilsson, B., K. N. Ekdahl, T. E. Mollnes and J. D. Lambris (2007). "The role of complement in biomaterial-induced inflammation." Molecular Immunology **44**: 82-94.
- Noh, H. and E. A. Vogler (2006a). "Volumetric interpretation of protein adsorption: mass and energy balance for albumin adsorption to particulate adsorbents with incrementally increasing hydrophilicity." Biomaterials **27**: 5801-5812.
- Noh, H. and E. A. Vogler (2006b). "Volumetric interpretation of protein adsorption: Partition coefficients, interphase volumes, and free energies of adsorption to hydrophobic surfaces." Biomaterials **27**: 5780-5793.
- Noh, H. and E. A. Vogler (2007). "Volumetric interpretation of protein adsorption: competition from mixtures and the Vroman effect." Biomaterials **28**: 405-422.
- Panichi, V., L. Casarosa, V. Gattai, A. M. Bianchi, B. Andreini, M. Migliori, S. De Pietro, L. Giovannini and R. Palla (1995). "Protein layer on hemodialysis membranes: a new immunohistochemistry technique." International Journal of Artificial Organs **18**: 305-308.
- Paparella, D., S. J. Brister and M. R. Buchanan (2004). "Coagulation disorders of cardiopulmonary bypass: a review." Intensive Care Medicine **30**: 1873-1881.
- Pixley, R. A., L. G. Stumpo, K. Birkmeyer, L. D. Silver and R. W. Colman (1987). "A monoclonal antibody recognizing an icosapeptide sequence in the heavy chain of

- human factor XII inhibits surface-catalyzed activation." Journal of Biological Chemistry **262**: 10140-10145.
- Ratner, B. D. (2000). "Blood compatibility- a perspective." Journal of Biomaterials Science: Polymer edition **11**: 1107-1119.
- Ratner, B. D. (2004). Background concepts to biology, biochemistry and medicine. Biomaterials science: an introduction to materials in medicine. B. D. Ratner, A. S. Hoffman, F. J. Schoen and J. E. Lemons. San Diego, Elsevier Science: 237-237.
- Ratnoff, O. D. and H. Saito (1979). "Interactions among Hageman factor, plasma prekallikrein, high molecular weight kininogen, and plasma antecedent." Proceedings of the National Academy of Sciences USA **76**: 958-961.
- Renne, T., M. Pozgajova, S. Gruner, K. Schuh, H. U. Pauer, P. Burfeind, D. Gailani and B. Nieswandt (2005). "Defective thrombus formation in mice lacking coagulation factor XII." Journal of Experimental Medicine **202**: 271-281.
- Renner, L., T. Pompe, K. Salchert and C. Werner (2005). "Fibronectin displacement at polymer surfaces." Langmuir **21**: 4571-4577.
- Revak, S. D., C. G. Cochrane, A. R. Johnston and T. E. Hugli (1974). "Structural changes accompanying enzymatic activation of human Hageman factor." The Journal of Clinical Investigation **54**: 619-627.
- Roach, P., D. Farrar and C. C. Perry (2005). "Interpretation of protein adsorption: surface-induced conformational changes." Journal of the American Chemical Society **127**: 8168-8173.
- Sainz, I. M., R. A. Pixley and R. W. Colman (2007). "Fifty years of research on the plasma kallikrein-kinin system: From protein structure and function to cell biology and in-vivo pathophysiology." Thrombosis and Haemostasis **98**: 77-83.
- Sethuraman, A., M. Han, R. S. Kane and G. Belfort (2004). "Effect of surface wettability on the adhesion of proteins." Langmuir **20**: 7779-7788.
- Silverberg, M., J. T. Dunn, L. Garen and A. P. Kaplan (1980). "Autoactivation of human Hageman factor. Demonstration utilizing a synthetic substrate." Journal of Biological Chemistry **255**: 7281-7286.
- Silverberg, M. and A. P. Kaplan (1982). "Enzymatic activity of activated and zymogen forms of human Hageman factor (factor XII)." Blood **60**: 64-70.

- Slack, S. M. and T. A. Horbett (1995). The Vroman effect: a critical review. Proteins at interfaces II: fundamentals and applications. J. L. Brash and T. A. Horbett. Washington DC, American Chemical Society: 112-128.
- Svensson, M., P. Friberger, O. Lundstrom and B. Stegmayr (1996). "Activation of FXII during haemodialysis." Scandinavian Journal of Clinical & Laboratory Investigation **56**: 649-652.
- Vogler, E. A. (1999). "Water and the acute biological response to surfaces." Journal of Biomaterials science: Polymer edition **10**: 1015-1045.
- Vroman, L. (1964). "Effects of hydrophobic surfaces upon blood coagulation." Thrombosis et Diathesis Haemorrhagica **10**: 455-493.
- Wachtfogel, Y. T., P. C. Harpel, L. H. Edmunds, Jr. and R. W. Colman (1989). "Formation of C1s-C1-inhibitor, kallikrein-C1-inhibitor, and plasmin-alpha 2-plasmin-inhibitor complexes during cardiopulmonary bypass." Blood **73**: 468-471.
- Wagner, W. R., R. D. Schaub, E. N. Sorensen, T. A. Snyder, C. R. Wilhelm, S. Winowich, H. S. Borovetz and R. L. Kormos (2000). "Blood biocompatibility analysis in the setting of ventricular assist devices." Journal of Biomaterials Science, Polymer Edition **11**: 1239-1259.
- Walsh, P. N., G. P. Tuszyński, J. S. Greengard and J. H. Griffin (1984). "The possible role of platelets in bypassing the contact phase of blood coagulation." Haematologia **17**: 169-178.
- Wendel, H. P., D. W. Jones and M. J. Gallimore (1999). "FXII levels, FXIIa-like activities and kallikrein activities in normal subjects and patients undergoing cardiac surgery." Immunopharmacology **45**: 141-144.
- Williams, D. F. (1987). Blood physiology and biochemistry: hemostasis and thrombosis. Blood Compatibility. D. F. Williams. Boca Raton, Florida, CRC Press. **1**: 5-35.
- Wu, Y., F. I. Simonovsky, B. D. Ratner and T. A. Horbett (2005). "The role of adsorbed fibrinogen in platelet adhesion to polyurethane surfaces: A comparison of surface hydrophobicity, protein adsorption, monoclonal antibody binding, and platelet adhesion." Journal of Biomedical Materials Research Part A **74A**: 722-738.
- Xu, L.-C. and C. A. Siedlecki (2007). "Effects of surface wettability and contact time on protein adhesion to biomaterial surfaces." Biomaterials **28**: 3273-3283.

- Zhuo, R., R. Miller, K. M. Bussard, C. A. Siedlecki and E. A. Vogler (2005). "Procoagulant stimulus processing by the intrinsic pathway of blood plasma coagulation." Biomaterials **26**: 2965-2973.
- Zhuo, R. and E. A. Vogler (2006). "Practical application of a chromogenic FXIIa assay." Biomaterials **27**: 4840-4845.
- Zwaal, R. F., P. Comfurius and E. M. Bevers (1998). "Lipid-protein interactions in blood coagulation." Biochimica et Biophysica Acta **1376**: 433-453.

## **Chapter 2**

### **Procoagulant activity of surface immobilized Hageman factor**

#### **2.1 Introduction**

Millions of blood-contacting medical devices are annually used for the treatment and diagnosis of cardiovascular diseases (Lysaght 2000), yet the risk of thrombosis persists as one of the major hazards to patient health and a cause for device under-performance or failure (Ratner 2000). Administration of large doses of anticoagulants to patients with heart-valves, ventricular assist devices and other blood-contacting implantable devices is used to prevent thrombosis but increases risk of bleeding and hemorrhage (Galloway 1999; McBride 1999). Unfortunately, the development of hemocompatible materials to ameliorate these medical complications has remained largely an unrealized objective. Towards this goal, the study of blood-material interactions has been a much-researched field for many decades, yet there is little understanding of the many facets of this complex phenomenon (Andrade 1981; Ratner 1993; Ratner 2000). Blood-material interactions that lead to the formation of a blood clot consist of two major components: cellular (platelets) and acellular (or humoral) (Williams 1987). While these two components are not independent of each other, this study focuses primarily on the latter in an effort to gain insight into the initial events of blood-material interactions that ultimately lead to clot formation.

The humoral component of biomaterial-induced blood coagulation, generally referred to as the intrinsic pathway of blood plasma coagulation, is by itself a complex process consisting of numerous steps involving conversion of an inactive zymogen to the corresponding active enzyme by limited proteolytic cleavage (Colman 2001). The enzyme cascade acts as biochemical amplifier that generates thrombin, a potent enzyme that cleaves fibrinogen to fibrin leading to fibrin oligomerization, causes activation of FXIII, and ultimately results in formation of a crosslinked fibrin mesh generally referred to as a clot. The initiation events are believed to involve four proteins that comprise the contact activation complex; coagulation factor XII (FXII, Hageman factor), prekallikrein (PK, Fletcher factor), high molecular weight kininogen (HMWK, Fitzgerald factor), and coagulation factor XI (FXI, Plasma Thromboplastin Antecedent) (Williams 1987). Initiation of this intrinsic pathway of blood plasma coagulation is widely believed to occur when FXII “binds” to a negatively-charged surface (Ratnoff 1958; Revak 1977). Binding of the zymogen via “specific interactions” between the negatively-charged surface and some domains of the protein rich in positively-charged residues (Kirby 1983) is believed to result in structural changes in the protein (Samuel 1992; Vroman 1964), sharply increasing its susceptibility to cleavage to form FXIIa (Griffin 1978). The common observation that plasma in contact with glass or kaolin (negatively-charged hydrophilic surfaces) clots rapidly compared to plasma in contact with hydrophobic surfaces is used to argue that binding of the protein to the contacting surface leads to activation (Ratnoff 1966). It is well accepted however that hydrophilic surfaces are not efficient protein-adsorbent materials whereas adsorption to hydrophobic materials is relatively efficient (Goncalves 2005; Horbett 1993; Renner 2005; Roach 2005;

Sethuraman 2004; Wu 2005). If, in fact, direct binding of the proteins to the contacting surface were necessary for activation, then one might expect protein-adsorbent hydrophobic surfaces to be relatively stronger procoagulants than hydrophilic surfaces, in sharp contrast to what is routinely observed. This is clearly an unresolved paradox between known trends in protein adsorption to surfaces and the traditional theory of contact activation of the intrinsic pathway of the coagulation cascade that requires further investigation.

Numerous studies utilizing a variety of experimental techniques have been undertaken in order to study the interaction between the proteins of the coagulation activation complex and underlying solid procoagulants (see for example (Davie 1979; Griffin 1979; Kaplan 1978) and references therein.) These studies have generally focused on interactions between two or three components that comprise only a small portion of the plasma proteome. Results from these investigations have been interpreted in terms of a sequence of molecular events at the blood-material interface that describes the initial events of material-induced blood coagulation. According to this consensus theory (Griffin 1979; Williams 1987), binding of FXII to a negatively-charged surface leads to some level of autoactivation to FXIIa and renders FXII susceptible to proteolytic cleavage by kallikrein to yield FXIIa (Griffin 1978). FXIIa in turn cleaves PK bound to the surface via the HMWK-PK complex (Meier 1977). This reciprocal-activation of FXII and PK causes rapid amplification of the initial zymogen-enzyme conversions of contact activation. The surface-bound FXIIa molecules also cleave FXI bound to the negatively-charged surface via a HMWK-FXI complex. However, neither FXII or FXIIa interact directly with HMWK, whose primary function is to mediate the binding of PK



and FXI to the surface (Wiggins 1983). It remains unclear how these surface-adsorbed molecules could efficiently interact with each other, in the presence of all the other plasma proteins, many of which are present at far higher concentrations than these contact activation proteins. This proposed scheme for contact activation requires that the proteins FXII and/or PK possess some unique ability to undergo repeated adsorption-desorption events adjacent to the surface without diffusing into the bulk fluid phase or that alternatively these protein molecules possess mobility over large distances along the surface, as was suggested by Kaplan (Kaplan 1978). A slightly modified theory was proposed based on the observed cleavage of HMWK by FXIIa in PK-deficient plasma (Griffin 1976; Wiggins 1983). This theory suggests that Hageman factor and HMWK directly interact with each other. However, since HMWK has been suggested to be non-surface-active until it is cleaved (Scott 1984), this would mean that Hageman factor and/or PK must undergo repeated adsorption-desorption and remain in close proximity to the interface for effective activation and propagation of the cascade. Clearly, the sequence of events occurring at the material surface is highly complex with need for further refinement.

In this study, FXIIa was immobilized onto three different solid procoagulant materials having vastly different surface chemistries and water-wettability (a measure of surface energy). Procoagulant activity was assayed *in vitro* (Guo 2006; Zhuo 2005) utilizing platelet-poor human plasma (normal and FXII-deficient). Quantitative analysis of the results indicates that the procoagulant activity of FXIIa is unaffected by the presence or the nature of underlying solid procoagulant. These results suggest that the nature of underlying surface does not significantly affect the enzymatic activity of FXIIa

and it appears to retain its activity when immobilized to all the test surfaces, with no preference for the negatively-charged surface. It was also concluded that repeated adsorption-desorption of the protein molecules at the interface is not a necessary event for the propagation of the coagulation cascade.

## **2.2 Materials and methods**

### **2.2.1 Plasma and proteins**

Detailed procedures for the preparation and storage of human platelet poor plasma are available in (Guo 2006; Miller 2006). Briefly, anticoagulated salvaged human plasma (outdated less than 5 days prior to receipt) was obtained from The Pennsylvania State University Milton S. Hershey Medical Center's Blood Bank. Plasma was pooled from multiple units (eight units for the work described herein), centrifuged at 500 X g for 10 min at 35°C and the resulting plasma supernatant was stored at -20°C. Prior to use in assays, plasma was thawed for ~ 40 min in a 37°C waterbath, and centrifuged as described above. This two-fold centrifugation ensured that the plasma was essentially free of platelets (platelet poor plasma, PPP). Immunodepleted FXII deficient human plasma (d<sub>XII</sub>PPP) was obtained from Haematologic Technologies (Essex Junction, VT) and was stored at -80°C. Prior to use in assays, d<sub>XII</sub>PPP was thawed in a 37°C waterbath, and centrifuged in the same manner as for PPP preparation. For this work, a single lot of d<sub>XII</sub>PPP obtained from a single donor was used. Control experiments performed with a second lot of d<sub>XII</sub>PPP showed similar trends although quantitative values were slightly

different. This is consistent with previous results in which various lots of plasma show slight differences quantitatively but are similar qualitatively (Guo 2006).

Human coagulation FXIIa was obtained commercially from Enzyme Research Laboratories (South Bend, IN). Upon receipt, the enzyme was thawed in a 37°C water-bath, diluted in a 0.1 M phosphate buffer (pH 5.3) and stored as 500 µg/mL aliquots at -80°C. Prior to use, FXIIa was thawed in a 37°C water-bath and diluted with phosphate buffered saline (PBS, pH 7.4, Sigma-Aldrich, St. Louis, MO) to desired concentration. A single lot of the enzyme was used throughout this study, with supplier-provided activity value of 73 PEU/mg. We have shown previously that there is no observable effect for minor variations in activity of the enzyme on the coagulation efficiency as recorded using an in-vitro coagulation assay (Guo 2006). FXIIa concentration is reported in molar units in order to utilize enzyme-kinetic modeling.

Bovine Serum Albumin (BSA, fraction V, Sigma-Aldrich) was stored as received (as lyophilized powder) at 4°C. BSA solution of desired concentration was freshly prepared for immobilization onto the particles (as described below) by dissolving a weighed quantity of the dry protein in a measured volume of PBS (pH 7.4) under ambient conditions.

### **2.2.2 Surface preparation of solid procoagulants**

Surface treatments used herein were minor modifications of previously reported procedures (Guo 2006; Zhuo 2005) and are briefly outlined below, including minor modifications to previous methodology. Glass particles 425-600 µm (Sigma-Aldrich)

were cleaned in a glow-discharge cleaner operated at 100W. The cleaned particles were silanized (all silanes were obtained from Gelest Inc., Morrisville, PA) with 3-aminopropyltriethoxysilane (APS), 2-carbomethylethoxytrichlorosilane (CMETS), or octadecyltrichlorosilane (OTS). Glow-discharge treated particles were incubated for 5 min in a solution of 2% (v/v) APS in acetone in a glass petridish. The petridish was occasionally shaken to facilitate uniform chemical treatment of all particles. The APS solution was aspirated and the particles were rinsed in fresh chloroform by sonication in a glass beaker for 15 min followed by air-drying overnight. CMETS modification was performed using a nearly identical procedure, the difference being the incubation of particles was performed in 2% (v/v) CMETS in ethanol for 10 min. The terminal ester groups of the SAMs of CMETS on the particles were converted to a carboxylic acid group (designated herein as COOH surface) by incubations in 1M NaOH (Sigma-Aldrich) followed by 0.1 N H<sub>2</sub>SO<sub>4</sub> (VWR) for 10 min each, with a water rinse between the two steps. The procedure for OTS modification was also similar, glow-discharge treated particles were incubated for 60 min in a solution of 5% (v/v) OTS in chloroform. After washing in chloroform the particles were annealed overnight in a vacuum-oven at 110°C. Water-wettability of silanized surfaces were measured on 12 mm diameter glass coverslip witness samples (VWR). Contact angles on the resultant surfaces were measured by the horizontal sessile drop method using a Krüss goniometer using 18 MΩ water (Millipore simplicity unit) as the probe liquid.

### 2.2.3 Protein immobilization on solid procoagulants

Protein-coated particles (FXIIa and/or BSA) were prepared by incubation of  $\sim 52$  cm<sup>2</sup> (calculated from the measured weight of dry particles using a nominal diameter of 500  $\mu$ m) of the silane-modified particles in 500  $\mu$ L of protein solution (FXIIa or BSA) in PBS for 2 hr in 2 mL glass vials (12 mm X 35 mm, VWR). Protein-adsorption studies have indicated that proteins adsorb “tighter” onto hydrophobic surfaces but have been shown to loosely associate onto hydrophilic surfaces (Goncalves 2005; Horbett 1993; Renner 2005; Roach 2005; Sethuraman 2004; Wu 2005). To prevent the desorption of the proteins from the hydrophilic COOH and partially-hydrophobic APS surfaces, the proteins were covalently linked through carbodiimide and glutaraldehyde linkages respectively (Hermanson 1992). Fresh solutions of N-(3-dimethylaminopropyl)-N'-ethylcarbodiimide hydrochloride (EDAC, Sigma-Aldrich) in 1,4-Dioxane (Sigma-Aldrich) and N-hydroxysuccinimide (NHS, Alfa Aeser Avocado Research Chemicals Ltd, Waid Hill, MA) in water were prepared and mixed to obtain a solution containing 25 mg/mL EDAC and 25 mg/mL NHS. COOH-functionalized particles of known surface area were incubated in this mixture of EDAC and NHS contained in a glass vial for 30 min. The particles were washed with buffer and incubated with protein (FXII and/or BSA) solution for 2 hr. APS-modified particles were activated by incubation in 25% glutaraldehyde in water (J. T. Baker, Phillipsburg, NJ) for 1 hr and washed with buffer and incubated with protein as above. Aliquots were stored at the start and end of the incubation period for protein assay described below. Protein-coated particles were either used immediately for coagulation studies or stored at 4°C and used within 48 hr.

The amount of protein adsorbed onto the particles was calculated by solution depletion. Protein concentration was measured using a NanoOrange<sup>®</sup> protein quantitation kit (Molecular Probes, Eugene, OR) (Jones 2003) following manufacturer's protocol. NanoOrange<sup>®</sup> is a mercyanine dye that produces a large increase in fluorescence upon interaction with proteins which can detect low protein concentrations ( $0.1 < \mu\text{g/mL} < 10$ ). The sample was mixed (1:20) with the working solution and transferred to a flat bottom, dark walled 96-well plate (VWR) and then heated at 90° C for 10 min. The fluorescence intensity was measured by imaging the well-plate using the FluorImager<sup>®</sup> (Molecular Dynamics, Piscataway, NJ) fitted with a 488 nm excitation laser and a 570 nm reader. All measurements were performed in triplicate and the fluorescent readings calculated using the Molecular Dynamics Image Quant<sup>®</sup> (v. 5.0) software. The initial- and final- protein concentration was determined using a linear calibration curve ( $R^2 > 98\%$ ) generated using standard solutions.

#### **2.2.4 In vitro coagulation assay**

An in vitro coagulation assay was used to measure the coagulation activity of the immobilized enzymes on the solid procoagulants. The assay measured the coagulation response in terms of a coagulation time (CT), defined as the time required from activation of the intrinsic pathway of the coagulation cascade to the appearance of a visible clot, initiated by a dose of enzyme and/or solid procoagulant. The assay has been described extensively in previous publications (Guo 2006; Vogler 1995; Zhuo 2005). Briefly, 0.5 mL of plasma (PPP or d<sub>XII</sub>PPP) was mixed with 0.1 mL of 0.1 M calcium chloride

(CaCl<sub>2</sub>, Sigma-Aldrich) and a known dose of procoagulants (surface-modified particles or soluble enzyme) in a 5 mL polystyrene vial (12 mm X 75 mm, VWR). The volume was adjusted by adding 0.01 M PBS (pH 7.4) to obtain a 1 mL solution resulting in a 1:1 dilution of plasma in buffer. The order in which reagents and solid materials were added was varied depending on the assay type, with recalcification of plasma always occurring last to ensure a common zero time CT. Assay vials were capped with parafilm, rotated at 8 rpm on a hematology mixer and the corresponding CT was recorded. Day-to-day consistency of plasma was tested by two sets of control samples: 2 NIH units/mL of thrombin (Sigma-Aldrich) were added to the recalcified plasma-buffer system in 5 mL polystyrene vials and a control in which the recalcified plasma-buffer system was placed in a 2 mL clean glass vial. CT measurements for different doses of FXIIa concentration, solid procoagulant surface area, and the protein-coated solids were measured in PPP and d<sub>XII</sub>PPP with  $n \geq 3$  for each.

### **2.2.5 Mathematical analysis**

The phenomenological mathematical model used in this work (Guo 2006) described processing of an exogenous dose of FXIIa that leads to the formation of a fibrin clot in human PPP (see **A.1** and **A.2** for summary). The model simplified the cascade into three modules: an input dose (exogenous FXIIa), the gray box (containing the numerous intermediate reactions) and the output response (the clot). The analytical relationship was used to fit experimental CT values at different values of FXIIa using three adjustable parameters. Contact activation due to the addition of a solid procoagulant to PPP was

modeled as a two-step process: 1) the generation of FXIIa from endogenous FXII with the amount produced being in response to a catalytic potential of the surface and 2) the processing of this procoagulant-generated FXIIa through the gray box to form a clot. The values of the parameters were obtained by statistical non-linear least-squares fit using the commercial Sigmaplot<sup>®</sup> 8 (Systat Software Inc., Point Richmond, CA).

## **2.3 Results**

This study addresses two important questions in activation of the contact activation complex of blood coagulation. First, what is the role of the substrate in events subsequent to activation of FXII to FXIIa, and second, is it necessary that FXIIa undergo repeated adsorption and desorption events for the propagation of the cascade? FXIIa was immobilized to surfaces with different surface chemistry and the procoagulant efficiency of these enzyme-modified materials was measured. These values were compared to soluble protein doses as well as solid procoagulants with immobilized BSA.

### **2.3.1 Soluble FXIIa titration in PPP**

Figure 2-1 plots decreasing CT values arising from increasing amounts of enzyme activator (both soluble and surface-immobilized) in PPP. The data corresponding to varying dose of soluble FXIIa was fit to an analytical relationship developed previously and briefly described above and is shown by the solid line ( $R^2 > 97\%$ ). The shape of the curve is consistent with previous work (Guo 2006). Table 2-1 compiles the values of the



parameters  $a$ ,  $b$ , and  $c$  that describe propagation of the dose through the cascade as generated from the best fit of the model to experimental data (see **A.1** and **A.2** for background). The parameters  $b$  and  $c$  account for background activation during the assay, comprised primarily of contact activation due to the polystyrene vial but also from other potential sources of activator in the test system including trace amounts of active enzyme, remnant platelets and platelet-derived microparticles. The model parameters also take into account the role that trace platelets, microparticles or other cell types might have in promoting amplification of the cascade by providing cofactor for the prothrombinase and tenase complexes. In fact, we do find that different lots of plasma yield quantitatively different values but qualitatively similar results and therefore we carefully determine the  $a$ ,  $b$ , and  $c$  parameters for each lot of plasma used.

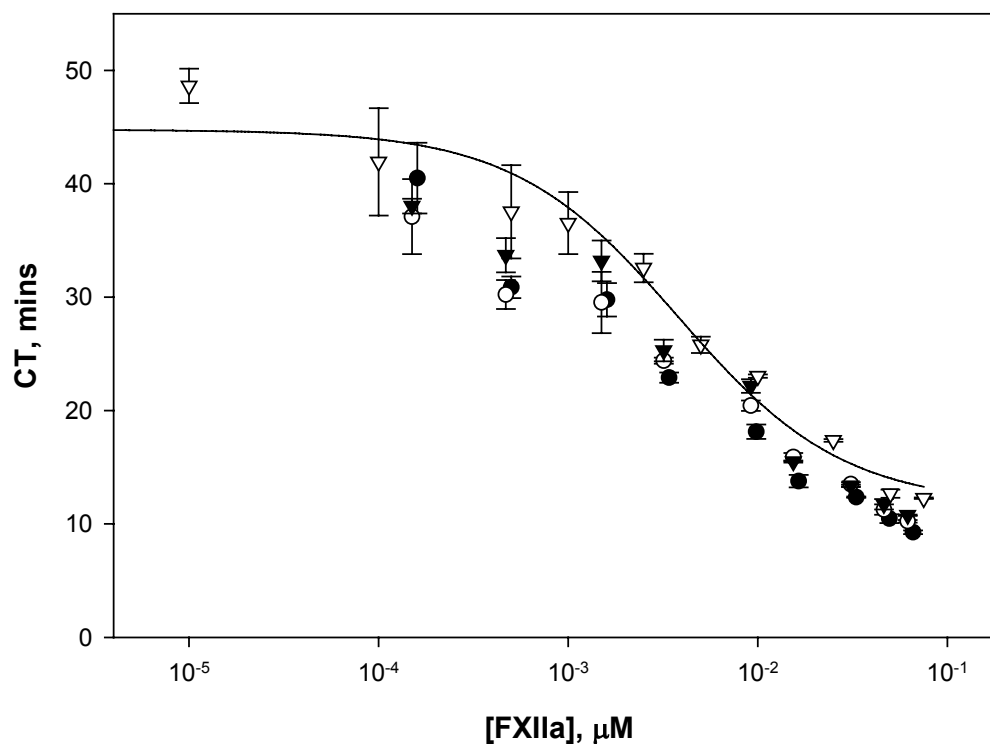


Figure 2-1: FXIIa titration in platelet poor plasma (PPP) showing experimental coagulation time (CT) values vs. concentration of exogenous FXIIa introduced in various forms: soluble FXIIa (open triangles,  $\nabla$ ), and immobilized on: COOH (solid circles,  $\bullet$ ), APS (open circles,  $\circ$ ), and OTS surfaces (closed triangles,  $\blacktriangledown$ ). The smooth curve shows the best fit of a mathematical model to the data for soluble FXIIa titration. (All data shown as mean  $\pm$  S.D. for  $n \geq 3$ ).

Table 2-1: Parameters describing processing of a FXIIa dose as generated by best fit of the measured CT response to an enzyme kinetics model.

FXIIa (surface/ plasma type)	$a$ (min)	$b \times 10^{-4}$ ( $\mu\text{M min}$ )	$c \times 10^{-5}$ ( $\mu\text{M}$ )
Soluble/ PPP	11.7 $\pm$ 1.8	170 $\pm$ 40	38 $\pm$ 10
Soluble/ d <sub>XII</sub> PPP	12.4 $\pm$ 2.3	2.0 $\pm$ 0.5	2.7 $\pm$ 0.7
OTS/ d <sub>XII</sub> PPP	14.0 $\pm$ 2.0	2.1 $\pm$ 0.4	2.8 $\pm$ 0.7
APS/ d <sub>XII</sub> PPP	13.1 $\pm$ 1.8	2.6 $\pm$ 0.5	3.5 $\pm$ 0.7
COOH/ d <sub>XII</sub> PPP	12.6 $\pm$ 1.9	2.7 $\pm$ 0.5	3.7 $\pm$ 0.8

Values are displayed as mean  $\pm$  S.D.

### 2.3.2 Procoagulant efficiency of solid procoagulants

Three model solid procoagulants with different surface energy were prepared by silane-modification of glass particles. The water-wettability (a measure of the surface energy) of the monolayer formed was assessed by measuring the nominal contact angles on identically-modified glass coverslips by the sessile drop method on a goniometer using 18 M $\Omega$  Millipore water as a probe liquid. The contact angles measured are consistent with previous results (Guo 2006; Zhuo 2005) and are listed as mean values and standard deviation in Table 2-2. The data is in good agreement with the expected trend of increasing water-wettability for the OTS, APS and COOH surfaces respectively.

Table 2-2: Catalytic efficiency of solid procoagulants and BSA-coated procoagulants.

Procoagulant Surface	Sessile Drop Contact Angle	Catalytic efficiency $K_I \times 10^{-2}$ ( $\mu\text{M}/\text{min}$ )
OTS	$108^\circ \pm 3^\circ$	$1.2 \pm 0.6$
APS	$59^\circ \pm 4^\circ$	$3.4 \pm 1.3$
CMETS	$52^\circ \pm 2^\circ$	$2.0 \pm 0.5$
COOH	$<10^\circ$	$28.3 \pm 5.4$
BSA/OTS	N/A	$0.5 \pm 0.1$
BSA/APS	N/A	$0.6 \pm 0.1$
BSA/COOH	N/A	$1.2 \pm 0.2$

The procoagulant efficiency of these silane-modified particles was assayed in PPP by measuring the coagulation response to varying doses (surface area) of the solid procoagulants. As described above and in (Guo 2006), the coagulation response of solid procoagulants in PPP is modeled as a two-step process consisting of generation of FXIIa from the endogenous FXII due to the catalytic potential (termed herein as  $K_I$ ) of the surface and the processing of this FXIIa resulting in formation of a clot. The analytical relationship for the titration of the solid procoagulant data involves four parameters:  $K_I$  for the solid procoagulant in addition to  $a$ ,  $b$ , and  $c$ . By utilizing the  $a$ ,  $b$ , and  $c$  values determined from the FXIIa titration in PPP (Figure 2-1 and Table 2-1)  $K_I$  values for each of the solid procoagulants were determined by best fit analysis to the surface area titration plots, as shown in Figure 2-2. These  $K_I$  values are collected in Table 2-2 and are

consistent with previously observed trends showing scaling of the catalytic efficiency of a surface with hydrophilicity (Guo 2006; Vogler 1995).

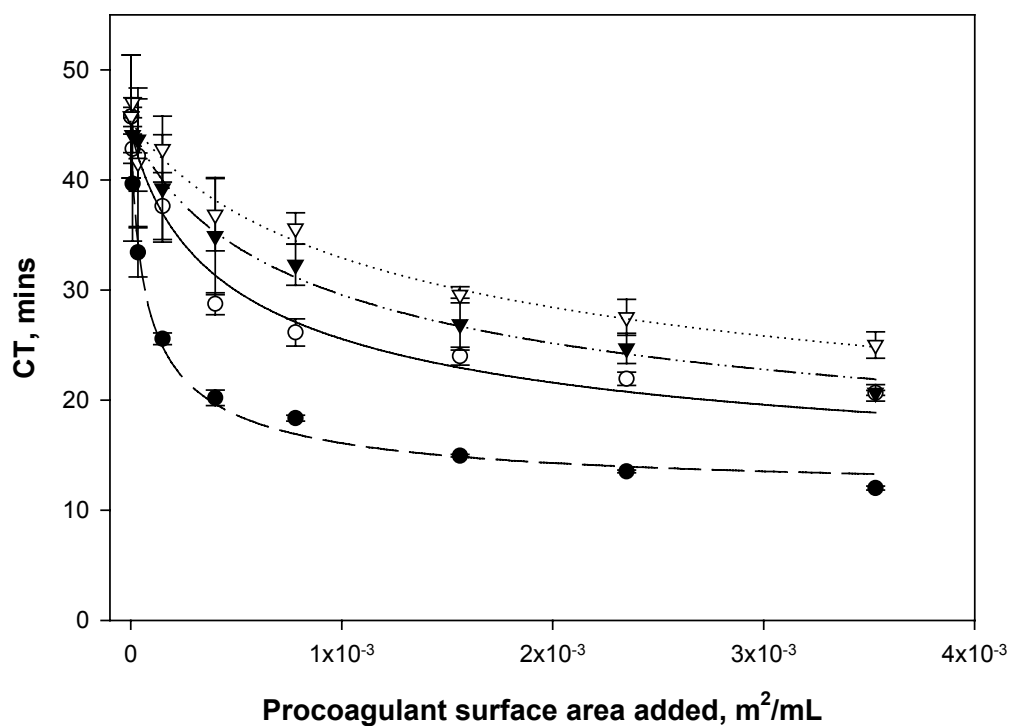


Figure 2-2: Surface area titration (SAT) in PPP showing experimental CT vs. surface area of three different procoagulant materials. Data for COOH particles (solid circles ●), APS particles (open circles ○), CMETS particles (closed triangles ▼) and OTS particles (open triangles ▽) are shown along with the smooth lines representing the best fit to the previously developed mathematical model. (All data expressed as mean  $\pm$  S.D. for  $n \geq 3$ ).

### 2.3.3 Titration of FXIIa-coated-particles in PPP

The calculated protein coverage on each solid procoagulant is listed in Table 2-3.

Incubation of protein solution for 2 hr in vials in the absence of particles resulted in no

observable difference between initial- and final- concentration values (data not shown), indicating that adsorption of protein to vial is negligible in comparison to amounts immobilized to the particles. These protein-coated particles were titrated in PPP and the data for the immobilized FXIIa on the particles is plotted in Figure 2-1. The dose of surface-immobilized FXIIa is expressed as  $\mu\text{M}$  for consistency, and is calculated from the protein coverage on the surfaces and the number of particles introduced into the 1 mL plasma system in the vial for the assay. Current models of material- and enzyme-induced coagulation are inadequate to describe this data due to a “double dose” effect in these experiments. In this case a first dose comes from the immobilized enzyme molecules and the second dose is provided by the procoagulant surface. A qualitative assessment of the data shows that the coagulation response of FXIIa on each of the three surfaces (with very different water-wettability) exhibits remarkably similar procoagulant activity. Without thorough quantitative analysis using a robust mathematical model (beyond the scope of this work) it is difficult to determine if the response of the immobilized enzymes is similar-to or slightly-faster than a corresponding dose of soluble enzyme. It would not be surprising to find a somewhat faster response (shorter CT for equivalent [FXIIa]) for the immobilized enzymes compared to soluble FXIIa due to the double-dose effect described above (and further described in the following section on observations for the titration of BSA-coated procoagulants in PPP).

Table 2-3: Protein Coverage of FXIIa and BSA on the solid procoagulants

Protein/Surface	Protein coverage (mg/m <sup>2</sup> )	Protein concentration in plasma system for in vitro assay (μM/m <sup>2</sup> )
FXIIa/OTS	2.0 ± 0.4	25 ± 5
FXIIa/APS	2.0 ± 0.3	25 ± 4
FXIIa/COOH	2.2 ± 0.5	28 ± 7
BSA/OTS	2.0 ± 0.6	25 ± 8
BSA/APS	1.6 ± 0.6	20 ± 8
BSA/COOH	1.8 ± 0.4	23 ± 5

Desorption of FXIIa from OTS surfaces was a concern, as it was important that the FXIIa remained surface-bound similar to enzyme covalently linked to hydrophilic surfaces. In a separate series of experiments (data not shown) an OTS-modified glass vial was precoated with FXIIa and used in 5 consecutive coagulation assays with washing between each. There was no change in CT for these experiments, demonstrating that FXIIa seems to be quite tenaciously adsorbed to these hydrophobic surfaces. This observation was consistent with other experiments where FXII/FXIIa was observed to be tenaciously adsorbed onto OTS surfaces despite repeated washings (Zhuo 2006).

### 2.3.4 Titration of BSA-coated particles in PPP

Figure 2-3 displays results for surface area titration plots utilizing the three BSA-coated solid procoagulants in PPP. Guidelines correspond to fits to the mathematical model for surface procoagulant activation and the calculated procoagulant efficiency ( $K_I$ ) of these three solid procoagulants are listed in Table 2-2. These  $K_I$  values indicate that the BSA-coated particles (with protein coverage equivalent to FXIIa-coated particles) are much less procoagulant than the bare solid procoagulants surfaces or the corresponding FXIIa-immobilized solid materials. Apparently BSA modification reduces the availability of surface area to interact with the contact activation proteins causing a reduction in the measured catalytic efficiency. Interestingly, the  $K_I$  values of the BSA-coated surfaces, shown in Table 2-2, continue to scale with the water-wettability of the underlying solid substrate, suggesting sub-monolayer coverage of the surface by BSA. Theoretical calculations suggest a coverage of 3.5 to 8 mg/m<sup>2</sup> for a monolayer of BSA (Wagner 2003). These values would indicate that the protein coverage on these BSA-coated particles (~ 2 mg/m<sup>2</sup>) will result in exposed underlying material over some fraction of the surface. This would explain the observation that the procoagulant efficiency of these BSA-coated surfaces varies as a function of the water-wettability of the underlying solid procoagulant. Because FXIIa and BSA are similar in molecular weight and therefore should be of roughly similar size (Teller 1976), these proteins will have similar surface coverage. It seems quite likely then that the data for FXIIa-coated particles in Figure 2-1 includes the “double dose” effect described previously, with the presence of an underlying solid surface contributing to the coagulation activity in



addition to the immobilized enzymes. To overcome the difficulty in modeling the double-dose effect of immobilized enzymes in PPP, another series of experiments using plasma devoid of FXII ( $d_{XII}PPP$ ) was performed.

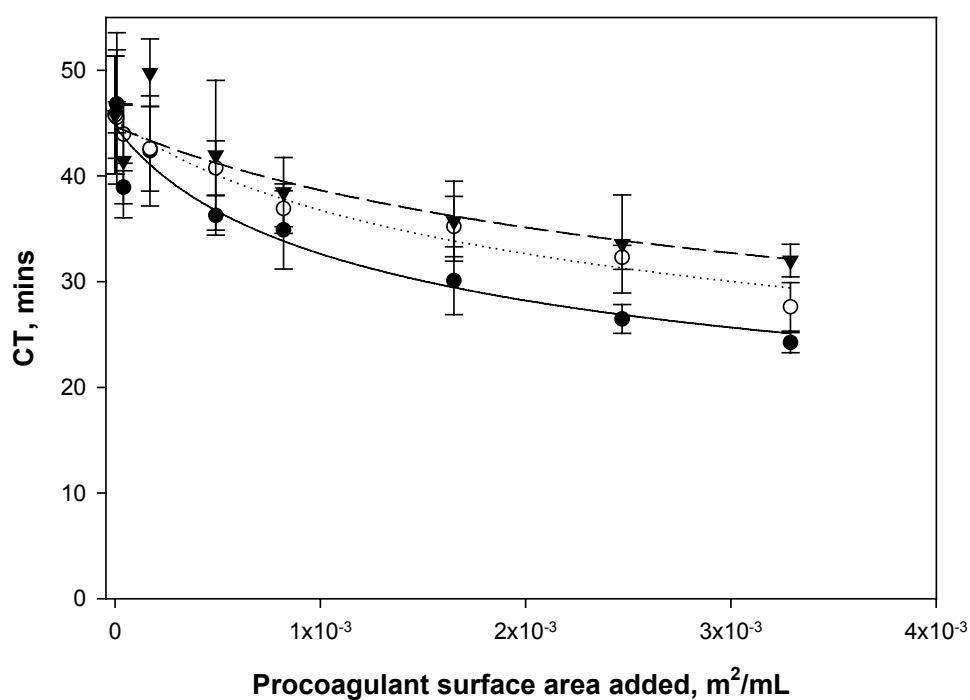


Figure 2-3: Surface area titration (SAT) in PPP showing experimental CT vs. surface area of three different BSA-coated procoagulant materials. Data for BSA immobilized on COOH (solid circles ●), APS (open circles ○), and OTS (closed triangles ▼) surfaces are shown along with the smooth lines representing the best fit to the previously developed mathematical model. (All data expressed as mean  $\pm$  S.D. for  $n \geq 3$ ).

### 2.3.5 FXIIa titration in $d_{XII}PPP$

Figure 2-4 illustrates the coagulation response to exogenous FXIIa titrations in  $d_{XII}PPP$ . In this FXII-deficient test system the only dose applied to the plasma comes from immobilized enzyme and therefore the double dose problem is removed. The plots correspond to four different types of FXIIa doses: soluble FXIIa and FXIIa immobilized onto the three different solid procoagulants (COOH, APS and OTS). Each set of experimental data was fit to the mathematical model developed for FXIIa titration in plasma. The parameters  $a$ ,  $b$ , and  $c$  generated from the best fit (indicated by the smooth lines) of the analytical equation for FXIIa titration to the plotted data are listed in Table 2-1. A comparison of the  $a$ ,  $b$ , and  $c$  values indicates no difference between the four types of FXIIa doses suggesting that soluble FXIIa and FXIIa immobilized on all the three solid procoagulants exhibit similar coagulation activity independent of the underlying substrate properties.

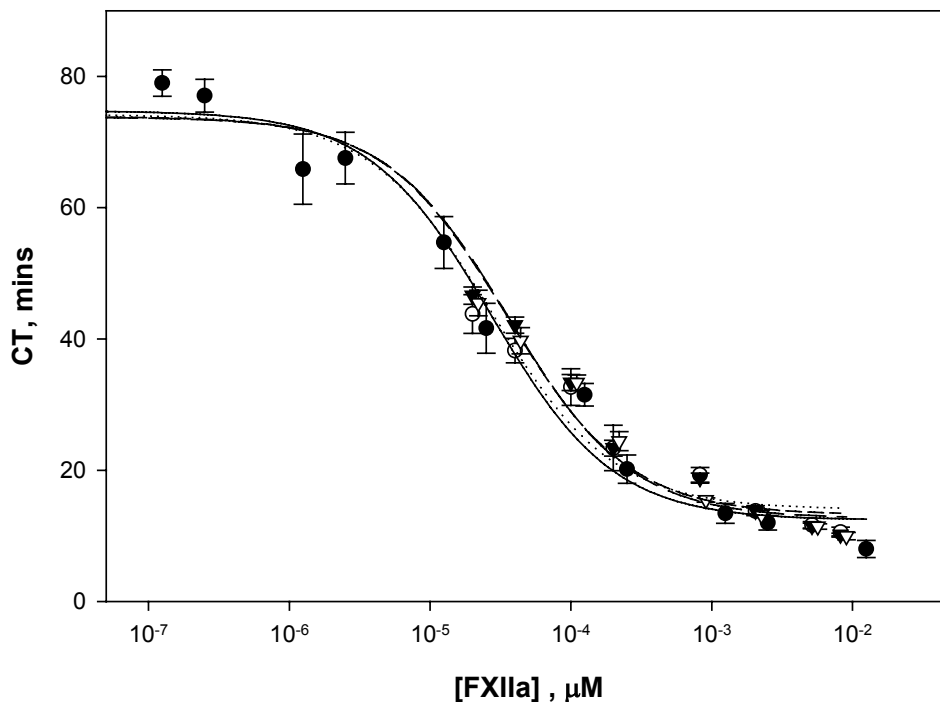


Figure 2-4: FXIIa titration in FXII-deficient platelet poor plasma ( $d_{XII}PPP$ ) showing experimental CT values vs. concentration of exogenous FXIIa introduced in different forms: soluble (solid circle ●) and as immobilized enzyme onto COOH (open triangles ▽), APS (closed triangles ▼) and OTS (open circles ○) surfaces. The solid lines represent best fit of the data to the mathematical model: soluble enzyme (smooth line) and as immobilized enzyme onto COOH (dotted line), APS (short-dashed line) and OTS (dashed line). (All data expressed as mean  $\pm$  S.D. for  $n \geq 3$ ).

### 2.3.6 Titration of BSA-coated solid procoagulants in $d_{XII}PPP$

As a negative control for the FXIIa-coated particles, BSA-coated particles were titrated in  $d_{XII}PPP$  (data not shown). The BSA-immobilized surface serves to act as a protein-coated procoagulant surface lacking the specific enzymatic activity of FXIIa. Table 2-3 displays data for protein coverage of BSA immobilized onto the solid

procoagulants. The data indicates that for a given solid procoagulant, the surface coverage of BSA and FXIIa are approximately same. The range of surface area tested is similar to the range used for the FXIIa-coated solid procoagulant titrations and the data indicates that there is no observable effect for addition of BSA-coated particles above the background coagulation response due to the PS vial. Because this control data shows no coagulation arising from introduction of protein-coated particles, we can conclude that the decrease in CT seen in Figure 2-4 arises solely from the enzymatic activity of the FXIIa-coated particles and data can be analyzed using models developed for FXIIa titration.

## 2.4 Discussion

It is well established that water-wettable, high-energy surfaces (e.g. glass, kaolin) are stronger procoagulants than hydrophobic surfaces (Vogler 1995), although the mechanisms of activation are not clear. As described previously, the current theory of contact activation of blood coagulation is in direct conflict with observed trends in protein adsorption that indicate stronger binding of proteins onto hydrophobic surfaces than onto hydrophilic surfaces. In this work, three different glass-based solid procoagulants were prepared by silane-modification. Contact angle measurements confirmed the differences in wettability between the COOH, APS and OTS solids. The procoagulant tendencies or catalytic efficiencies for these surfaces determined using an *in vitro* coagulation assay were consistent with previous trends where catalytic efficiency scaled with hydrophilicity (Vogler 1995; Zhuo 2005).

The solid procoagulants were incubated in FXIIa so as to either chemically-link (for the COOH and APS materials) or physically adsorb (for the OTS procoagulant) the enzyme onto the hydrophilic and partially-hydrophilic surfaces to prevent desorption. Protein quantization indicated sub-monolayer coverage of the protein on these surfaces. BSA (66kDa) was immobilized onto the three solid procoagulants with a nearly equivalent surface coverage to serve as a negative control for FXIIa (80 kDa). Titration of the BSA-coated particles in  $d_{XII}PPP$  indicated there was no significant effect beyond background, whereas titration of immobilized FXIIa in  $d_{XII}PPP$  indicated that the immobilized-enzyme retained activity similar to the soluble FXIIa regardless of the wettability of the underlying substrate.

This result is significant because it is in sharp contrast to the generally accepted theory of contact activation that suggests an essential role for the negatively-charged surface in both the activation and amplification of contact activation. Griffin and Cochrane have suggested three major roles for the underlying negatively-charged surface in the contact activation events including: the ability of the surface to alter the structure of FXII to enhance its susceptibility to cleavage, facilitation of HWMK-PK dependent reciprocal activation and promoting the activation of FXI by the surface-bound FXIIa (Griffin 1979). While the results in this study do not lend insight into the former two observations, the results do indicate that FXIIa in any form (soluble or immobilized onto surfaces of different degree of hydrophilicity) exhibit similar procoagulant activity. In contrast to the previous theories, the data in this study suggests that the presence of a surface or its nature does not affect the ability of FXIIa to propagate the cascade.

Moreover, the FXIIa molecules have been tightly bound to the solid procoagulants (using covalent linkages on the hydrophilic surfaces where proteins would otherwise not be expected to undergo “tight” binding) thereby preventing either large-scale lateral mobility or repeated adsorption/desorption of the protein molecules near the interface. The ability of these immobilized enzymes to exhibit similar coagulation activity as soluble enzymes indicate quite clearly that FXIIa need not undergo the complex sequence of events vicinal to the interface as suggested by traditional theories.

Although this study does not provide insight into the mechanisms of FXII activation, it does indicate that the key to material-induced blood coagulation must lie in the activation step. The remarkably similar parameters describing processing of FXIIa through the cascade as illustrated by the parameters *a*, *b*, and *c* in Table 2-1 for the various presentations of the enzyme indicate that once FXIIa is produced, be it immobilized or free, it will be processed by the cascade with equal efficiency. Therefore, the suggestion that a hydrophilic anionic surface is necessary for binding of the cofactors involved in the contact activation complex is not supported by this work. In fact, the data suggests that once FXIIa is generated the material is a passive bystander to the activation of FXI and release of enzyme to the common pathway of coagulation.

## 2.5 Conclusions

The enzyme FXIIa and the nonenzymatic-control molecule BSA were immobilized on a series of model biomaterial surfaces having varying levels of water-wettability. Surface area titrations with these materials present increasing amounts of

immobilized protein to plasma test solutions. Results generated by calculating the parameters describing processing of the enzymatic dose by the coagulation cascade demonstrate that FXIIa retains similar enzymatic potential whether presented as a soluble enzyme or linked to any of the three different test materials having contact angle ranging from  $< 10^\circ$  to  $100^\circ$ . Once the enzyme is formed, the surface does not serve as a cofactor for propagation of the cascade, it is not necessary to have repeated adsorption/desorption events as suggested by the traditional mechanism, and the surface seems to play the role of a passive observer to the process of FXI activation and continuation of the cascade to the common pathway. The results suggest that the role of the surface in biomaterial-mediated coagulation is simply production of enzyme, but once that enzyme is produced, the nature of the underlying substrate does not play a role in subsequent coagulation cascade events.

## 2.6 Literature citations

Andrade, J. D., D. L. Coleman, P. Didisheim, S. R. Hanson, R. Mason and E. Merrill (1981). "Blood-materials interaction - 20 years of frustration." Transactions of the American Society of Artificial Internal Organs **27**: 659-662.

Colman, R. W. (2001). Contact activation pathway: inflammatory, fibrinolytic, anticoagulant, antiadhesive, and antiangiogenic activities. Hemostasis and Thrombosis- Basic Principles and Clinical Practice. R. W. Colman, J. Hirsh, V. J. Marder, A. W. Clowes and J. N. George. Philadelphia, Lippincott William and William. **4**: 103-122.

Davie, E. W., K. Fujikawa, K. Kurachi and W. Kisiel (1979). "The role of serine proteases in the blood coagulation cascade." Advances in Enzymology & Related Areas of Molecular Biology **48**: 277-318.

- Galloway, A. C., R. V. Anderson, E. A. Grossi, F. C. Spencer and S. B. Colvin (1999). Acquired heart diseases. Principles of Surgery. S. I. Schwartz. New York, McGraw Hill: 845-908.
- Goncalves, I. C., M. C. L. Martins, M. A. Barbosa and B. D. Ratner (2005). "Protein adsorption on 18-alkyl chains immobilized on hydroxyl-terminated self-assembled monolayers." Biomaterials **26**: 3891-3899.
- Griffin, J. H. and C. G. Cochrane (1976). "Mechanisms for the involvement of high molecular weight kininogen in surface-dependent reactions of Hageman factor." Proceedings of the National Academy of Sciences of the United States of America **73**: 2554-2558.
- Griffin, J. H. (1978). "Role of surface in surface-dependent activation of Hageman factor (blood coagulation Factor XII)." Proceedings of the National Academy of Sciences USA **75**: 1998-2002.
- Griffin, J. H. and C. G. Cochrane (1979). "Recent advances in the understanding of contact activation reactions." Seminars in Thrombosis and Hemostasis **5**: 254-273.
- Guo, Z., K. M. Bussard, K. Chatterjee, R. Miller, E. A. Vogler and C. A. Siedlecki (2006). "Mathematical modeling of material-induced blood plasma coagulation." Biomaterials **27**: 796-806.
- Hermanson, G. T., A. K. Mallia and P. Smith (1992). Immobilized affinity ligand techniques. New York, Academic Press.
- Horbett, T. A. (1993). "Principles underlying the role of adsorbed plasma proteins in blood proteins in blood interactions with foreign materials." Cardiovascular Pathology **2**: 137S-148S.
- Jones, L. J., R. P. Haugland and V. L. Singer (2003). "Development and characterization of the NanoOrange (R) protein quantitation assay: A fluorescence-based assay of proteins in solution." Biotechniques **34**: 850-861.
- Kaplan, A. P. (1978). "Initiation of the intrinsic coagulation and fibrinolytic pathways of man: the role of surfaces, Hageman factor, prekallikrein, high molecular weight kininogen, and factor XI." Progress in Hemostasis and Thrombosis **4**: 127-175.
- Kirby, E. P. and P. J. McDevitt (1983). "The binding of bovine factor XII to kaolin." Blood **61**: 652-659.



- Lysaght, M. J. and J. A. O'Loughlin (2000). "Demographic scope and economic magnitude of contemporary organ replacement therapies." ASAIO Journal **46**: 515-521.
- McBride, L. R., K. S. Naunheim, A. C. Fiore, D. A. Moroney and M. T. Swartz (1999). "Clinical Experience With 111 Thoratec Ventricular Assist Devices." Annals of Thoracic Surgery **67**: 1233-1239.
- Meier, H. L., J. V. Pierce, R. W. Colman and A. P. Kaplan (1977). "Activation and function of human Hageman factor. The role of high molecular weight kininogen and prekallikrein." The Journal of Clinical Investigation **60**: 18-31.
- Miller, R., Z. Guo, E. A. Vogler and C. A. Siedlecki (2006). "Plasma coagulation response to surfaces with nanoscale chemical heterogeneity." Biomaterials **27**: 208-215.
- Ratner, B. D. (1993). "The blood compatibility catastrophe." Journal of Biomedical Materials Research **27**: 283-287.
- Ratner, B. D. (2000). "Blood compatibility- a perspective." Journal of Biomaterials Science: Polymer edition **11**: 1107-1119.
- Ratnoff, O. D. and J. M. Rosenblum (1958). "Role of Hageman factor in the initiation of clotting by glass." American Journal of Medicine **25**: 160-168.
- Ratnoff, O. D. (1966). "The biology and pathology of the initial stages of blood coagulation." Progress in Hematology **2**: 204-245.
- Renner, L., T. Pompe, K. Salchert and C. Werner (2005). "Fibronectin Displacement at Polymer Surfaces." Langmuir **21**: 4571-4577.
- Revak, S. D., C. G. Cochrane and J. H. Griffin (1977). "The binding and cleavage characteristics of human Hageman factor during contact activation." The Journal of Clinical Investigation **59**: 1167-1175.
- Roach, P., D. Farrar and C. C. Perry (2005). "Interpretation of protein adsorption: surface-induced conformational changes." Journal of the American Chemical Society **127**: 8168-8173.
- Samuel, M., R. A. Pixley, M. A. Villanueva, R. W. Colman and G. B. Villanueva (1992). "Human factor XII (Hageman factor) autoactivation by dextran sulfate. Circular dichroism, fluorescence, and ultraviolet difference spectroscopic studies." Journal of Biological Chemistry **267**: 19691-19697.

- Scott, C. F., L. D. Silver, M. Schapira and R. W. Colman (1984). "Cleavage of human high molecular weight kininogen markedly enhances its coagulant activity. Evidence that this molecule exists as a procofactor." Journal of Clinical Investigation **73**: 954-962.
- Sethuraman, A., M. Han, R. S. Kane and G. Belfort (2004). "Effect of Surface Wettability on the Adhesion of Proteins." Langmuir **20**: 7779-7788.
- Teller, D. C. (1976). "Accessible area, packing volumes and interaction surfaces of globular proteins." Nature **260**: 729-731.
- Vogler, E. A., J. C. Graper, G. R. Harper, H. W. Sugg, L. M. Lander and W. J. Brittain (1995). "Contact activation of the plasma coagulation cascade I. Procoagulant surface chemistry and energy." Journal of Biomedical Materials Research **29**: 1005-1016.
- Vroman, L. (1964). "Effects of hydrophobic surfaces upon blood coagulation." Thrombosis et Diathesis Haemorrhagica **10**: 455-493.
- Wagner, M. S., M. Shen, T. A. Horbett and D. G. Castner (2003). "Quantitative analysis of binary adsorbed protein films by time of flight secondary ion mass spectrometry." Journal of Biomedical Materials Research Part A **64A**: 1-11.
- Wiggins, R. C. (1983). "Kinin release from high molecular weight kininogen by the action of Hageman factor in the absence of kallikrein." Journal of Biological Chemistry **258**: 8963-8970.
- Williams, D. F. (1987). Blood physiology and biochemistry: hemostasis and thrombosis. Blood Compatibility. D. F. Williams. Boca Raton, Florida, CRC Press. **1**: 5-35.
- Wu, Y., F. I. Simonovsky, B. D. Ratner and T. A. Horbett (2005). "The role of adsorbed fibrinogen in platelet adhesion to polyurethane surfaces: A comparison of surface hydrophobicity, protein adsorption, monoclonal antibody binding, and platelet adhesion." Journal of Biomedical Materials Research Part A **74A**: 722-738.
- Zhuo, R., R. Miller, K. M. Bussard, C. A. Siedlecki and E. A. Vogler (2005). "Procoagulant stimulus processing by the intrinsic pathway of blood plasma coagulation." Biomaterials **26**: 2965-2973.
- Zhuo, R., C. A. Siedlecki and E. A. Vogler (2006). "Autoactivation of blood factor XII at hydrophilic and hydrophobic surfaces." Biomaterials **27**: 4325-4332.

## **Chapter 3**

### **Contributions of contact activation pathways of coagulation factor XII in plasma**

#### **3.1 Introduction**

Development of truly blood-compatible materials remains a largely unrealized objective of biomaterial surface science (Andrade 1981; Ratner 1993; Ratner 2000). Coagulation and thrombosis persist as major risks to patient health associated with the use of blood-contacting medical devices (Galloway 1999; McBride 1999). An improved understanding of the molecular basis of hemocompatibility is essential to the prospective engineering of advanced cardiovascular biomaterials.

The intrinsic cascade of blood plasma coagulation is a complex process linking a series of limited proteolytic conversions of zymogens to active enzymes (Colman 2001). This enzyme cascade acts as a biochemical amplifier that converts a procoagulation signal to thrombin, a potent enzyme that cleaves fibrinogen to fibrin and activates FXIII, ultimately resulting in the formation of a cross-linked fibrin mesh that is generally referred to as a fibrin clot.

Molecular interactions at the blood-material interface involved in the activation of the intrinsic cascade, often referred to as contact activation, have been extensively investigated. These results have been compiled into a mechanistic sequence of molecular events at the blood-material interface (see (Davie 1979; Griffin 1979; Kaplan 1978) and references therein) that describes initiation of material-induced blood coagulation.

According to this traditional biochemical theory of contact activation, negatively-charged surfaces are efficient activators of the coagulation cascade because these materials can bind to one-or-more proteins of the so-called contact activation complex. This binding induces zymogen-enzyme conversions through poorly-understood surface chemistry. The contact activation complex is believed to involve four proteins; coagulation factor XII (FXII, Hageman factor), prekallikrein (PK, Fletcher factor), high-molecular weight kininogen (HMWK, Fitzgerald factor), and coagulation factor XI (FXI, Plasma Thromboplastin Antecedent) (Williams 1987) that somehow preferentially adsorb to procoagulant surfaces in the presence of overwhelming concentrations of other blood proteins such as albumin. It is thought that FXIIa can be produced by at least three different biochemical reactions. Autoactivation produces FXIIa by contact of FXII with an activating surface ( $FXII \xrightarrow{\text{surface}} FXIIa$ ), presumably due to a “conformational change” upon binding of FXII to the surface (Samuel 1992; Vroman 1964). Binding of FXII to a negatively-charged surface is also believed to render it susceptible to cleavage by kallikrein (Kal) presumably generated by FXIIa-mediated hydrolysis of PK (Griffin 1978). This mutual activation of PK and FXII is known as reciprocal-activation, the second known reaction route to FXIIa. Finally, autohydrolysis or self amplification produces FXIIa by the action of FXIIa on FXII ( $FXIIa + FXII \rightarrow 2FXIIa$ ) (Miller 1980; Wiggins 1979; Zhuo 2006b).

Interestingly, while each of these three biochemical reactions can be observed in defined solutions containing one-or-more components of the contact activation complex, apparently all three reactions do not occur in plasma to the same extent as in defined solutions. For example, Zhuo and Vogler report that autohydrolysis is a facile reaction in

buffer solutions of FXIIa but that autohydrolysis is not a significant reaction in plasma (Zhuo 2006b). This observation is consistent with mathematical-modeling of the intrinsic cascade predicting that autohydrolysis of FXII was not a significant source of FXIIa following activation with either exogenous FXIIa or solid procoagulants (Guo 2006). Zhuo and Vogler speculated that autohydrolysis is not significant in plasma because PK and FXI are preferred substrates for FXIIa in plasma which are not available in neat-buffer solutions of FXII. Other investigations have reported similar observations demonstrating that hydrolysis of a zymogen by its activated enzymatic form is negligible compared to cleavage by other preferred enzymes. Notably among these reports, Tans et al demonstrated using rigorous enzyme-kinetics measurements that although Kal may autohydrolyze PK in neat solution, the rate constant for this reaction is about three orders of magnitude smaller than that for the cleavage of PK by FXIIa (Tans 1987). Also, Dunn et al made measurements of the time course of generation of activated FXII products to show that the rate of activation of FXII by Kal was much faster than the rate of autohydrolysis (Dunn 1982). Thus, it seems that autohydrolysis can be safely ruled out as a significant contributor to overall FXIIa yield in plasma.

However, it is not at all clear which of the remaining two known chemical reactions that produce FXIIa is most important in contact activation of plasma coagulation. The proportions which these two (or possibly more) reactions contribute to overall FXIIa yield is not known. And it is not clear how these proportions may depend on the surface chemistry of procoagulant surfaces. This lack of clarity is an important impediment to the prospective design of cardiovascular biomaterials with improved hemocompatibility; for if the elementary chemical reactions at a procoagulant surface

producing the first activated enzyme of an enzyme-amplifier cascade are unknown, then evidenced-based surface engineering routes to minimizing or eliminating contact activation of plasma coagulation cannot be proposed. Further complicating a full understanding of contact activation, it has been shown recently that FXII activation is not, in fact, specific for anionic/hydrophilic surfaces as purported by the traditional theory of contact activation (Zhuo 2006a). Rather, apparent specificity for hydrophilic surfaces is actually due to a relative diminution of the FXII→FXIIa yield at hydrophobic surfaces immersed in plasma (Zhuo 2006a). This finding discounts the specific-binding argument that is central to traditional theory and rivets our attention to biochemical details of how FXIIa is actually produced at procoagulant surfaces with different hydrophilicity. Toward this objective, we report herein semi-quantitative determination of the contributions of different FXII activation pathways to the total FXIIa enzyme produced by blood plasma contact with three model surfaces spanning the full range of observable water-wettability (surface energy). Results indicate that reciprocal-activation is the principal biochemical pathway to FXIIa. Autoactivation and reciprocal activation increase in the same proportion with procoagulant surface energy (water-wettability), while total amount of FXIIa produced per-unit-area procoagulant remains roughly constant for any particular procoagulant.

## **3.2 Materials and methods**

### **3.2.1 Plasma and proteins**

Frozen PK-deficient plasma from a human donor with a congenital deficiency was obtained commercially from George King Biomedical (Overland Park, KS) and stored at  $-80^{\circ}\text{C}$ . Prior to use, the plasma was thawed in a water-bath at  $37^{\circ}\text{C}$  for  $\sim 40$  min, centrifuged at  $500 \times g$  for 10 min at  $35^{\circ}\text{C}$  to remove remnant platelets. This was designated as PK-deficient platelet-poor plasma ( $d_{\text{PK}}\text{PPP}$ ). For this work, a single lot of  $d_{\text{PK}}\text{PPP}$  obtained from a single donor was used.

Human FXIIa and human PK were obtained commercially from Enzyme Research Laboratories (South Bend, IN). Upon receipt, the proteins were thawed in a  $37^{\circ}\text{C}$  water-bath, distributed into small aliquots without dilution and stored at  $-80^{\circ}\text{C}$ . Prior to use, proteins were thawed in a water-bath at  $37^{\circ}\text{C}$  and adjusted to desired concentration by serial dilution of stock solutions with phosphate buffered saline (PBS, pH 7.4, Sigma-Aldrich, St. Louis, MO) based on supplier-provided values. Single lots of FXIIa and PK were used throughout this study, with supplier-provided activity values of 73 PEU/mg and 28 PEU/mg, respectively. FXIIa concentration is reported in molar units in order to utilize enzyme-kinetic modeling described below.

### **3.2.2 Surface preparation of solid procoagulants**

Model biomaterial surfaces with controlled chemistry and water-wettability were prepared by surface-treatment of borosilicate glass particles. The procedures were

detailed previously (Chatterjee 2006; Guo 2006) and are briefly outlined here. Glass particles of diameter 425-600  $\mu\text{m}$  (nominal diameter = 500  $\mu\text{m}$ , Sigma-Aldrich, St. Louis, MO) were cleaned by sonication in chloroform for at least 15 min and subsequently cleaned in a glow-discharge chamber at 100W power for 30 min. The clean glass particles were either used as-is or following silanization with 3-aminopropyltriethoxysilane (APS) or n-octadecyltrichlorosilane (OTS, both silanes obtained from Gelest Inc., Morrisville, PA). Glow-discharge cleaned particles were incubated for 5 min in a solution of 2% (v/v) APS in ethanol in a glass petri dish. The APS solution was aspirated and the particles were rinsed in fresh chloroform by sonication in a glass beaker for 15 min followed by air-drying overnight. For OTS modification, glow-discharge cleaned particles were incubated for 60 min in a solution of 5% (v/v) OTS in chloroform. After washing in chloroform the particles were annealed overnight in a vacuum-oven at 110°C. Water-wettability for each surface was measured on 12 mm diameter glass coverslip witness samples (VWR). Contact angles on the resultant surfaces were measured by the horizontal sessile drop method using a Krüss goniometer with 18 M $\Omega$  water (Millipore simplicity unit) as the probe liquid.

### **3.2.3 In vitro coagulation assay**

An in vitro coagulation assay was used to measure the response of plasma to a dose of exogenous enzyme or solid procoagulants (Chatterjee 2006; Guo 2006; Zhuo 2005). The coagulation response was measured in terms of a coagulation time (CT), where CT was defined as the time required from activation of the intrinsic pathway of the



coagulation cascade by a dose of enzyme and/or solid procoagulant to the appearance of a visible clot. Prior experience with the assay has shown that while the trends of measured coagulation responses for different procoagulants are consistent across different batches of plasma used, the absolute values of CT may be affected by variations in plasma batches, possibly arising from donor differences. Therefore, all PPP used for this work was prepared by reconstituting  $d_{PK}PPP$  with PK at physiological concentration, and was designated as  $Rd_{PK}PPP$ .

Briefly, 0.5 mL of  $d_{PK}PPP$  was mixed with 0.1 mL of 0.1 M calcium chloride ( $CaCl_2$ , Sigma-Aldrich) and a known dose of procoagulants (either surface-treated particles or soluble enzyme) in a 5 mL polystyrene vial (12 mm X 75 mm, VWR). For measurements performed in  $Rd_{PK}PPP$ , PK was added at 20  $\mu g/mL$ , assuming a nominal physiological  $[PK] = 40 \mu g/mL$  (Dobrovolsky 2002; Williams 1987) and accounting for the 50% dilution of plasma in the assay. The volume was adjusted by adding PBS to obtain a 1 mL solution resulting in a 1:1 dilution of plasma in buffer. Assay vials were capped with parafilm, rotated at 8 rpm on a hematology mixer at room temperature (22°-25° C) and the corresponding CT was recorded. CT measurements for different doses of exogenous FXIIa or solid procoagulants area were measured in  $d_{PK}PPP$  and  $Rd_{PK}PPP$  with  $n \geq 3$  for each dose.

### **3.2.4 Mathematical analysis**

Quantitative analysis of enzyme production in this work utilized a previously-published mathematical model of the intrinsic cascade of coagulation (Guo 2006) (see

**A.1** and **A.2** for a summary). The model is based on the premise that the role of the solid surface is limited to the generation of FXIIa from the endogenous plasma FXII, which is then processed by a gray box containing all the intermediate steps to ultimately generate the output fibrin clot (Guo 2006). The values of the parameters of the gray box were obtained by statistical non-linear least-squares fit using the commercial Sigmaplot<sup>®</sup> 8 software (Systat Software Inc., Point Richmond, CA).

### **3.3 Results**

The objective of this work was to quantitatively determine the amounts of FXIIa generated via the autoactivation and reciprocal-activation pathways at model surfaces spanning a wide-range of surface water-wettability. Experiments performed may be broadly grouped into two categories: (i) measurement of the coagulation response to exogenous FXIIa in PK-deficient and reconstituted PK-deficient plasma ( $d_{PKPPP}$  and  $Rd_{PKPPP}$ , respectively) or (ii) coagulation response to three solid procoagulants with different surface water-wettability in both  $d_{PKPPP}$  and  $Rd_{PKPPP}$ . Mathematical modeling was used in both cases to calculate the amount of FXIIa generated.

#### **3.3.1 FXIIa titration of $d_{PKPPP}$ and $Rd_{PKPPP}$**

Figure **3-1** plots observed CT measured in response to exogenous FXIIa enzyme doses to  $d_{PKPPP}$  and  $Rd_{PKPPP}$ . Note that CT is a much sharper function of FXIIa for  $Rd_{PKPPP}$  compared to  $d_{PKPPP}$ , especially at low FXIIa concentrations. Mathematical

analysis of coagulation yields the parameters  $a$ ,  $b$  and  $c$  that describe the propagation of the exogenous FXIIa dose through the cascade. These parameters were obtained by statistical best fit of the model to these experimental data are compiled in Table 3-1 from which it is evident that error in estimated parameters was between 10-25%. Lines through the data of Figure 3-1 represent the statistical best fit to the analytical relationships. Note that the coagulation response induced by the surface of the polystyrene vial and other possible sources like remnant platelets are incorporated into the gray box model and accounted for by the parameters  $b$  and  $c$ , in particular.

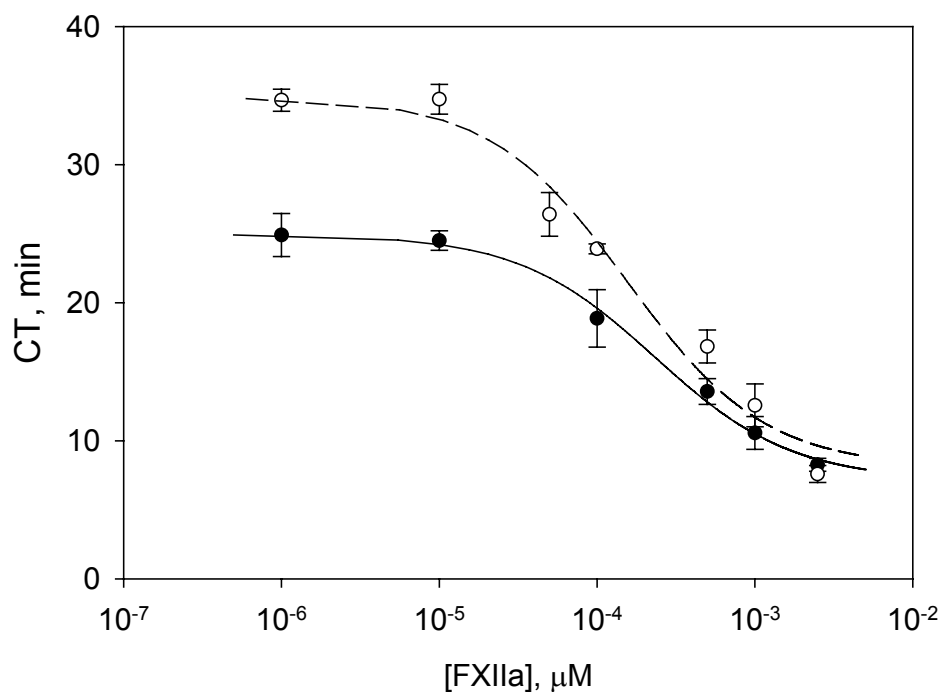


Figure 3-1: FXIIa titration in PK-deficient PPP ( $d_{PK}PPP$ ) (solid circles, ●), and reconstituted  $d_{PK}PPP$  ( $Rd_{PK}PPP$ ) (open circles, ○) showing experimental coagulation time (CT) values vs. concentration of exogenous soluble FXIIa. The smooth curve shows the best fit of a mathematical model to the data for soluble FXIIa titration. (All data is shown as mean  $\pm$  S.D. for  $n \geq 3$ ).

Table 3-1: Parameters describing the gray box processing of FXIIa

Plasma type	$a$ (min)	$b \times 10^{-3}$ ( $\mu\text{M}\cdot\text{min}$ )	$c \times 10^{-4}$ ( $\mu\text{M}$ )
$d_{\text{PKPPP}}$	$8.1 \pm 2.0$	$5.4 \pm 1.9$	$1.6 \pm 0.6$
$\text{Rd}_{\text{PKPPP}}$	$7.1 \pm 0.8$	$5.8 \pm 1.2$	$2.3 \pm 0.5$

Values are displayed as mean  $\pm$  S.D.

### 3.3.2 Surface area titration of solid procoagulants

Glow-discharge cleaned and silane-treated glass particles were used as solid procoagulants spanning the full range of surface water-wettability. The measured contact angles (listed in Table 3-2 as mean and standard deviation) are in good agreement with the expected trend of increasing water-wettability for the OTS, APS, and glass surfaces, respectively. Figure 3-2 collects surface-area-titration (SAT) plots for each of the three test surfaces in  $d_{\text{PKPPP}}$  and  $\text{Rd}_{\text{PKPPP}}$ , illustrating CT values measured in response to variable surface area of solid procoagulant. Utilizing the corresponding gray box parameters ( $a$ ,  $b$  and  $c$ ) generated from FXIIa titration (Figure 3-1 and Table 3-1), mathematical modeling material-induced coagulation was used to solve for  $K_I$ , a characteristic parameter that measures the “catalytic efficiency” of the test procoagulant in the corresponding plasma type (Guo 2006). Table 3-2 lists the mean  $K_I$  values for each solid procoagulant/plasma combination along with estimated uncertainty. Error in  $K_I$  increased with decreasing procoagulant hydrophilicity, ranging from about 35% uncertainty in glass  $K_I$  to 70% uncertainty in OTS, reflecting the diminishing

procoagulant activity induced by glass, APS, and OTS. As such,  $K_I$  values compiled in Table 3-1 were interpreted as best estimates. Lines through the data of Figure 3-2 were calculated from the model using the mean  $K_I$  values listed in Table 3-2.

Table 3-2:  $K_I$  values for the solid procoagulants

Procoagulant Surface	Sessile Drop Contact Angle	Plasma type	$K_I$ ( $\mu\text{M}/\text{min}$ )
Glass	$<5^\circ$	$d_{\text{PK}}\text{PPP}$	$(7.7 \pm 2.7) \times 10^{-2}$
		$\text{Rd}_{\text{PK}}\text{PPP}$	$(1.5 \pm 0.4) \times 10^0$
APS	$63^\circ \pm 3^\circ$	$d_{\text{PK}}\text{PPP}$	$(2.6 \pm 1.1) \times 10^{-3}$
		$\text{Rd}_{\text{PK}}\text{PPP}$	$(1.7 \pm 1.4) \times 10^{-2}$
OTS	$108^\circ \pm 3^\circ$	$d_{\text{PK}}\text{PPP}$	$(1.3 \pm 0.9) \times 10^{-3}$
		$\text{Rd}_{\text{PK}}\text{PPP}$	$(7.0 \pm 5.3) \times 10^{-3}$

Values are displayed as mean  $\pm$  S.D.

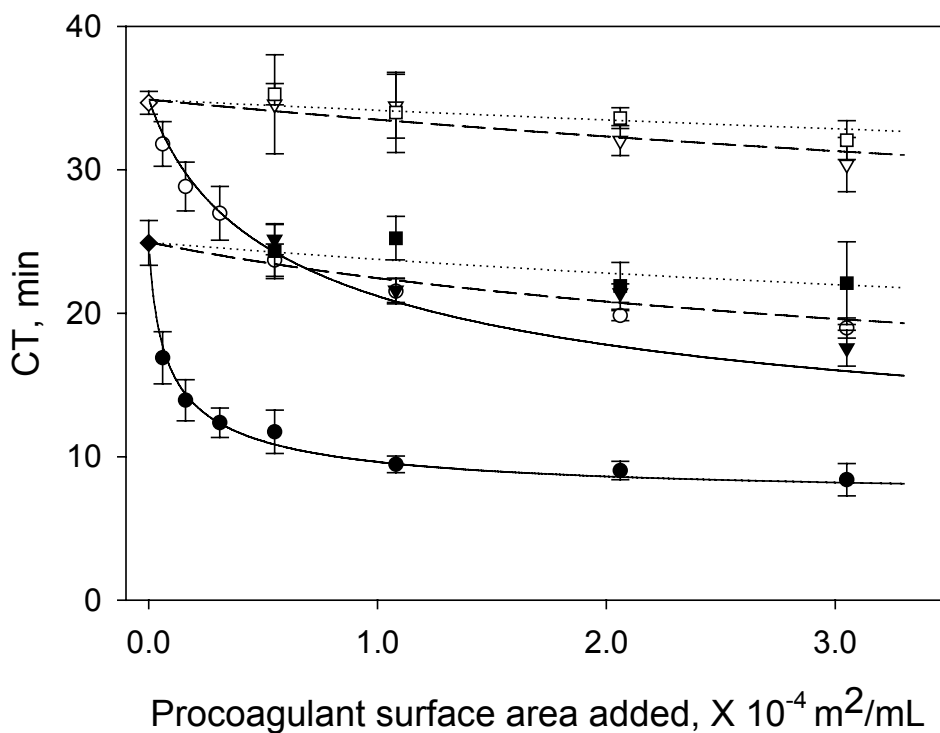


Figure 3-2: Surface area titration (SAT) in  $\text{d}_{\text{pKPPP}}$  and  $\text{Rd}_{\text{pKPPP}}$  showing experimental CT vs. added surface area of three different procoagulant materials. Data for glass-particles (circles ●, ○), APS particles (triangles ▼, ▽) and OTS particles (squares ■, □) are shown, where solid and open symbols represent measurements in  $\text{Rd}_{\text{pKPPP}}$  and  $\text{d}_{\text{pKPPP}}$ , respectively. The smooth lines represent CT values calculated from the model using the mean  $K_I$  values listed in Table 3-2. (All data expressed as mean  $\pm$  S.D. for  $n \geq 3$ ).

### 3.3.3 Calculation of FXIIa generation

The total amounts of FXIIa generated by each solid procoagulant were calculated using the nominal  $K_I$  values listed in Table 3-2. Although autohydrolysis of FXII by FXIIa may be a significant reaction in neat protein solutions, it has been observed to be insignificant in plasma (Guo 2006; Zhuo 2006b), thereby eliminating it as a possible

pathway of FXII activation in material-induced plasma coagulation. Thus, the calculated yield of FXIIa in  $Rd_{PK}PPP$  (equivalent to PPP) represents the total amount of enzyme produced by both the autoactivation and reciprocal-activation pathways, while enzyme produced in response to procoagulants in  $d_{PK}PPP$  yields the amount of FXIIa generated via autoactivation alone as reciprocal-activation cannot occur in the absence of PK. The difference between these two quantities represents the amount of FXIIa produced by reciprocal-activation at a given surface area of solid procoagulant.

Figure 3-3 compares in bar-graph form the total amounts of FXIIa generated for the three model surfaces at three different surface area values as well as the amounts generated individually by the autoactivation and reciprocal-activation pathways. Note the vastly different scales on the y-axis for the three different materials. Figure 3-4 is compilation of data from Figure 3-3 presented as a semi-log plot in order to more clearly illustrate the trends in enzyme production due to change in water-wettability of the activating surface. Experimental error obviates accurate estimates of the amounts of FXIIa generated by autoactivation and reciprocal-activation, especially due to contact with the weaker, more hydrophobic procoagulants, as illustrated by the error bars in Figure 3-4. Nevertheless, nominal values were found to be of interpretive value as described in 3.4.

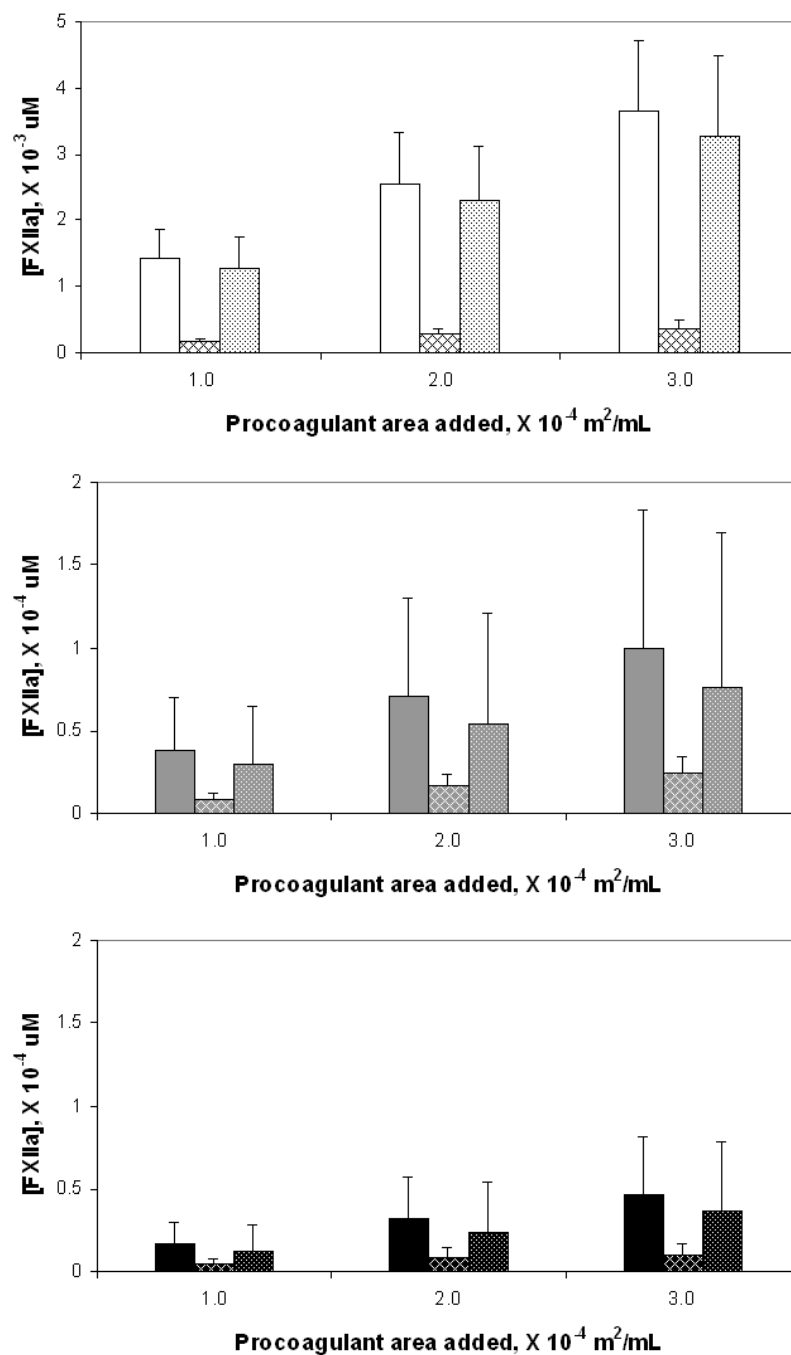


Figure 3-3: FXIIa produced in total and via the autoactivation and reciprocal-activation pathways at three surface area values for the each of the three solid test procoagulants: (top) glass, (middle) APS and (bottom) OTS. The bars show in groups of three at each surface area the total amount of enzyme (solid bar), enzyme produced by autoactivation (hatched bar) and enzyme produced by reciprocal-activation (dotted bar).



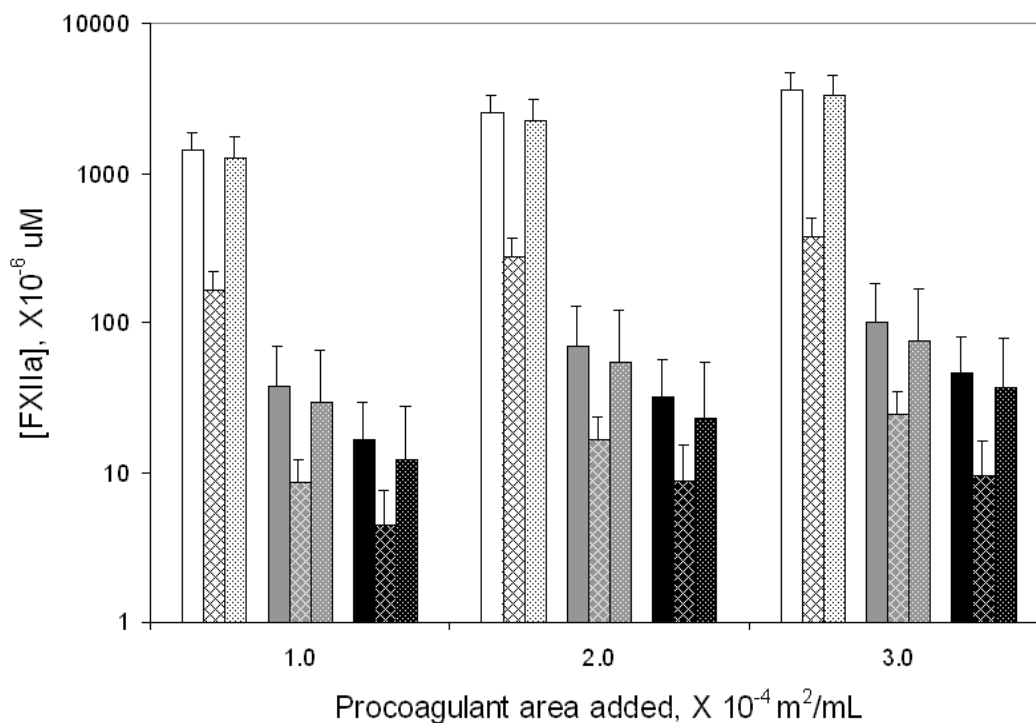


Figure 3-4: A compilation of values from the different surface presented using a semi-log plot for ease of comparison among the procoagulants showing glass (white background), APS (gray background) and OTS (black background) from left to right at each surface area.

Figures 3-5 and 3-6 plot the nominal amount of enzyme produced under each condition and normalized to the procoagulant surface area using the same illustrative scheme as Figure 3-3 and 3-4. Note the declining relationship between enzyme production in total and along each of the pathways with decreasing water-wettability of the activating surface, consistent with catalytic efficiency scaling exponentially with the surface water-wettability (Vogler 1995).

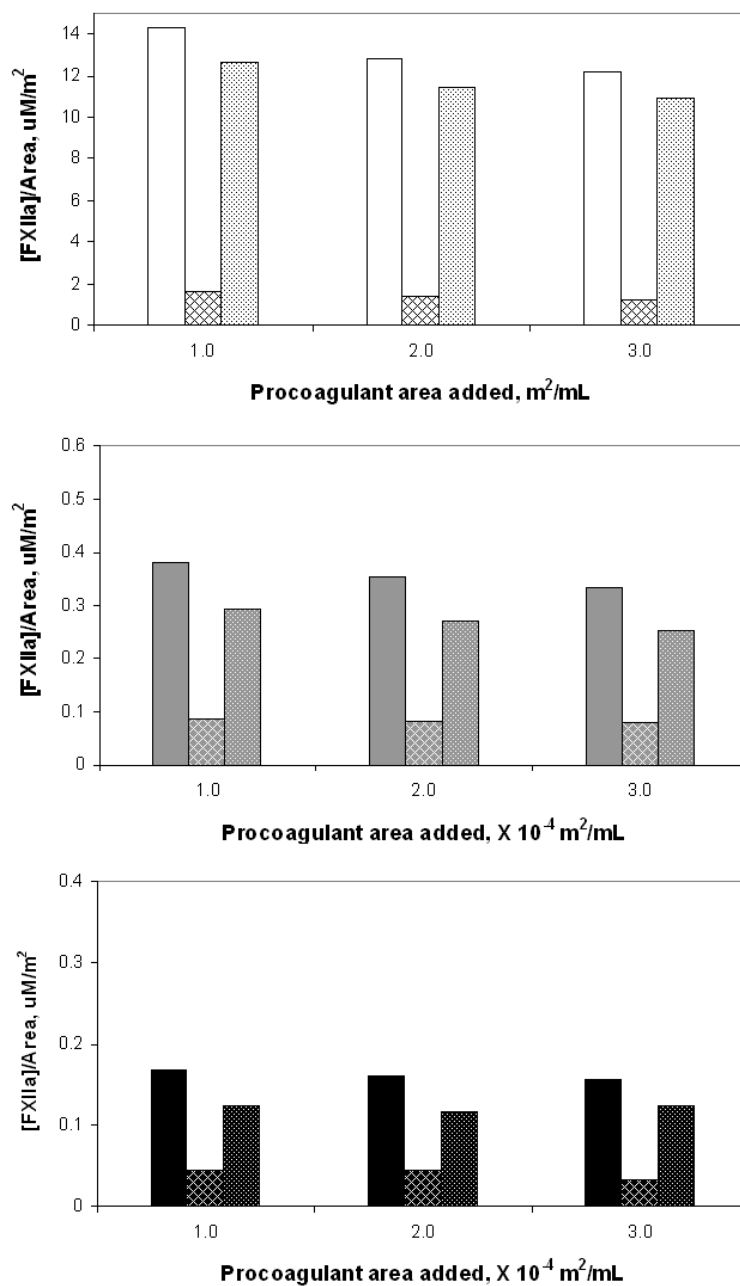


Figure 3-5: FXIIa produced per unit surface area in total and via the individual pathways at three surface area values for each of the three solid test procoagulants: (top) glass, (middle) APS and (bottom) OTS. The bars show in groups of three at each surface area the total amount of enzyme (solid bar), enzyme produced by autoactivation (hatched bar) and enzyme produced by reciprocal-activation (dotted bar).

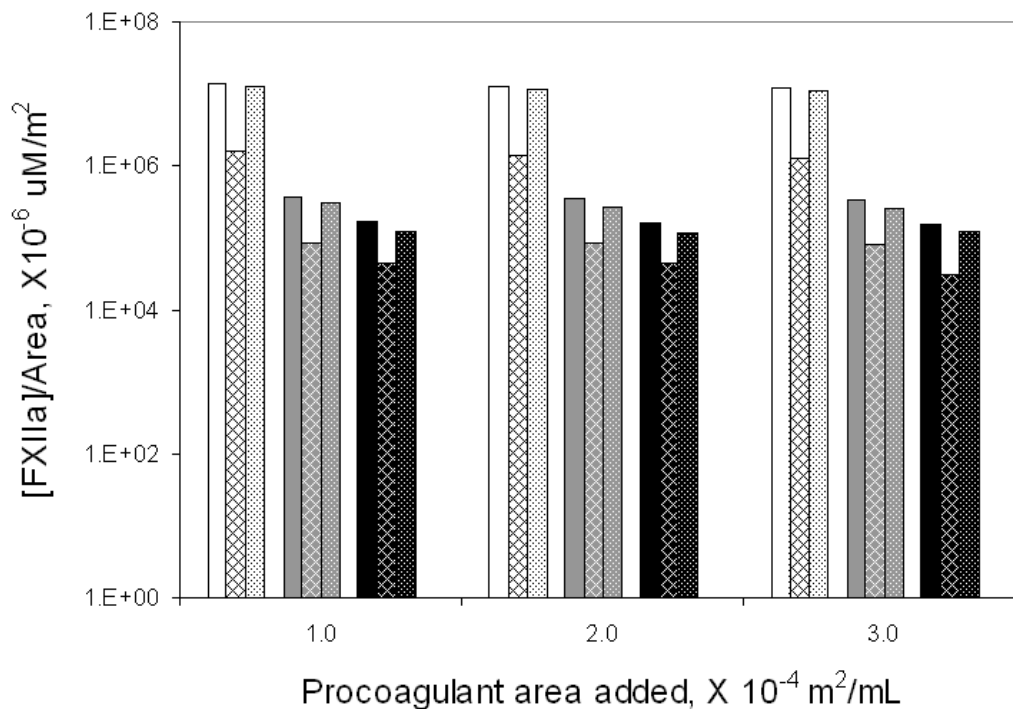


Figure 3-6: A compilation of values from the different surface presented using a semi-log plot for ease of comparison among the procoagulants showing glass (white background), APS (gray background) and OTS (black background) from left to right at each surface area.

### 3.4 Discussion

Prospective surface engineering of cardiovascular biomaterials with improved hemocompatibility requires a secure understanding of the biochemical reactions leading to contact activation of blood plasma. Recent investigations suggest that the traditional mechanism of contact activation requires substantial revision. In particular, the finding that FXII autoactivation is not specific to hydrophilic surfaces (Zhuo 2006a) refocuses attention on the chemical reactions that generate the FXIIa that triggers the intrinsic cascade of plasma coagulation. Our results suggest that of the three known chemical

reactions leading to FXIIa, autoactivation and reciprocal-activation are important in plasma and that reciprocal-activation is the dominant source of FXIIa.

### 3.4.1 Modeling material-induced coagulation

Material-induced coagulation is modeled as a two-step process in this study utilizing a model that has been described previously (Guo 2006). The first step in this process is the activation of plasma FXII by either autoactivation (in both plasma types) or reciprocal-activation (in Rd<sub>PK</sub>PPP alone) in response to interactions with procoagulant materials, and the newly-formed FXIIa is subsequently processed by the cascade leading to formation of a fibrin clot.

The parameters  $a$ ,  $b$  and  $c$  that describe the processing of FXIIa in the model were determined from FXIIa titration experiments performed in d<sub>PK</sub>PPP and Rd<sub>PK</sub>PPP. These new and unique sets of parameters for the two plasma systems were calculated in order to minimize the differences in background response due to the test vial surface and possible changes in the processing of FXIIa in the presence and absence of PK. The change in the background response between the two plasma types is easily observed as reduced CT values at zero dose of activator in Rd<sub>PK</sub>PPP (Figure 3-1 and 3-2), arising from increased FXIIa activation by the vial surface in the presence of PK.

### 3.4.2 Calculation of FXIIa generation

The  $K_I$  values listed in Table 3-2 indicate that catalytic efficiency of these surfaces increases with increasing water-wettability in both  $d_{PK}PPP$  and  $Rd_{PK}PPP$ , consistent with trends previously observed in whole plasma (Chatterjee 2006; Guo 2006). The amounts of enzyme generated along the different pathways at each solid procoagulant surface were then determined from the  $K_I$  values as described in 3.3. When the amount of FXIIa generated is very small, the measured coagulation response is only marginally faster than the background response, and as a result the errors associated with these small values are relatively large on a percent basis. However, we contend that nominal trends provide useful information regarding coagulation at hydrophobic surfaces where activation appears to be all-but absent in plasma. Although activation at hydrophobic surfaces is clearly weak, it is measurable, implying that chronic coagulation activation by hydrophobic cardiovascular materials could be a significant factor underlying the hemocompatibility of all known biomaterials. Furthermore, in light of recent findings that contact activation of FXII is not specific to hydrophilic materials, the important mechanistic question of whether activation by hydrophobic surfaces in plasma is different than activation by relatively hydrophilic counterparts remains to be answered.

In this latter regard, we note that when nominal FXIIa yield is normalized to the surface area used to activate the cascade, we find that the amount enzyme produced on a unit area basis for a given procoagulant material remains constant. Bearing in mind the large experimental uncertainty involved in measuring weak procoagulation, this data suggests that the surface does not play a significant role in propagating the

procoagulation signal down the intrinsic pathway, but only in activating FXII in a manner proportional to surface area and wettability. Otherwise, we would anticipate an increasing amount of FXIIa to be generated per unit area of procoagulant cofactor as a result of enhanced processing through the gray box if in fact the surface was an active participant in subsequent activation reactions as suggested by the traditional mechanism of contact activation. Taken together, the evidence leads us to the conclusion that the surface only generates FXIIa and does not affect any subsequent biochemical reactions of FXIIa, corroborating our previous findings (Chatterjee 2006; Guo 2006).

The consistent trends in scaling of FXIIa production with wettability provide useful insight into the difficult problem of understanding the contact activation process. Perhaps not surprisingly, the results indicate that the total amount of FXIIa generated (the sum of all activation pathways) scales with increasing surface area for a given solid procoagulant although the normalized values (enzyme produced per surface area) remain relatively constant. Furthermore, for a given surface area, FXIIa yield from the autoactivation and reciprocal-activation pathways individually scale with procoagulant water-wettability. Table 3-3 lists the estimated fraction of FXIIa yield from reciprocal-activation (calculated using the mean values for each pathway), showing that Kal-mediated reciprocal-activation is the dominant FXII activation pathway for each of the three different model procoagulant materials. Although experimental error precludes definitive interpretation of Table 3-3, the trend in nominal values hints at a modest increase in reciprocal-activation with increasing procoagulant water-wettability. If so, then these results show that autoactivation becomes a slightly more important activation pathway for hydrophobic procoagulants lacking any negative charges than for

hydrophilic procoagulants bearing the anionic surface functionalities believed to be critical for autoactivation to occur.

Table 3-3: Estimated fraction of enzyme generation via reciprocal-activation

Surface	Sessile Drop Contact Angle	[reciprocal-FXIIa] / [total-FXIIa] (%)
Glass	<5°	~ 89
APS	63° ± 3°	~ 76
OTS	108° ± 3°	~ 72

The results determined from this study demonstrate that the underlying mechanisms for FXII activation in plasma are largely similar for each of these three test surfaces spanning a wide range of water-wettability while the absolute amounts enzyme generated by each of the pathways scales with the wettability. Kallikrein-mediated reciprocal-activation is the dominant FXII activation pathway for each of the materials tested, accounting for no less than roughly 72% of the total FXIIa production. These results then suggest that reciprocal-activation occurs in proportion to the amount of FXIIa produced by auto-activation. These new results further suggest that hydrophobic surfaces are poor procoagulants not because any particular pathway is selectively attenuated at these non-wettable surfaces, but rather that FXII activation along all the individual activation pathways is diminished at hydrophobic surfaces in plasma.

### 3.5 Conclusions

The amounts of FXIIa produced in plasma by autoactivation and reciprocal-activation routes were calculated by mathematical-modeling of plasma coagulation induced by contact with model procoagulant surfaces spanning the full range of observable hydrophilicity. Results broadly indicate the following trends for the FXII activation at biomaterial surfaces in plasma:

- (i) Total FXIIa yield scales with increasing surface area of a particular solid procoagulant, so that the normalized amount of enzyme produced per unit area is constant.
- (ii) At any given surface area, the total amount of FXIIa generated increases with increasing surface water-wettability.
- (iii) Kal-mediated reciprocal-activation pathway is the principal contributor to FXIIa generation at all procoagulant test surfaces studied and the amount of enzyme generated via this pathway scales with water-wettability.
- (iv) Autoactivation produces no more than about 25% of the total FXIIa produced by the intrinsic pathway. FXIIa production by autoactivation scales with surface water-wettability.

### 3.6 Literature citations

Andrade, J. D., D. L. Coleman, P. Didisheim, S. R. Hanson, R. Mason and E. Merrill (1981). "Blood-materials interaction - 20 years of frustration." Transactions of the American Society of Artificial Internal Organs **27**: 659-662.



- Chatterjee, K., E. A. Vogler and C. A. Siedlecki (2006). "Procoagulant activity of surface-immobilized Hageman factor." Biomaterials **27**: 5643-5650.
- Colman, R. W., A. W. Clowes, J. N. George, J. Hirsh and V. J. Marder (2001). Overview of Hemostasis. Hemostasis and Thrombosis- Basic Principles and Clinical Practice. R. W. Colman, J. Hirsh, V. J. Marder, A. W. Clowes and J. N. George. Philadelphia, Lippincott William and William. **4**: 3-16.
- Davie, E. W., K. Fujikawa, K. Kurachi and W. Kisiel (1979). "The role of serine proteases in the blood coagulation cascade." Advances in Enzymology & Related Areas of Molecular Biology **48**: 277-318.
- Dobrovolsky, A. B. and E. V. Titaeva (2002). "The fibrinolysis system: regulation of activity and physiologic functions of its main components." Biochemistry-Russia **67**: 99-108.
- Dunn, J. T., M. Silverberg and A. P. Kaplan (1982). "The cleavage and formation of activated human Hageman factor by autodigestion and by kallikrein." Journal of Biological Chemistry **257**: 1779-1784.
- Galloway, A. C., R. V. Anderson, E. A. Grossi, F. C. Spencer and S. B. Colvin (1999). Acquired heart diseases. Principles of Surgery. S. I. Schwartz. New York, McGraw Hill: 845-908.
- Griffin, J. H. (1978). "Role of surface in surface-dependent activation of Hageman factor (blood coagulation Factor XII)." Proceedings of the National Academy of Sciences USA **75**: 1998-2002.
- Griffin, J. H. and C. G. Cochrane (1979). "Recent advances in the understanding of contact activation reactions." Seminars in Thrombosis and Hemostasis **5**: 254-273.
- Guo, Z., K. M. Bussard, K. Chatterjee, R. Miller, E. A. Vogler and C. A. Siedlecki (2006). "Mathematical modeling of material-induced blood plasma coagulation." Biomaterials **27**: 796-806.
- Kaplan, A. P. (1978). "Initiation of the intrinsic coagulation and fibrinolytic pathways of man: the role of surfaces, Hageman factor, prekallikrein, high molecular weight kininogen, and factor XI." Progress in Hemostasis and Thrombosis **4**: 127-175.
- McBride, L. R., K. S. Naunheim, A. C. Fiore, D. A. Moroney and M. T. Swartz (1999). "Clinical Experience With 111 Thoratec Ventricular Assist Devices." Annals of Thoracic Surgery **67**: 1233-1239.

- Miller, G., M. Silverberg and A. P. Kaplan (1980). "Autoactivatability of human Hageman factor (factor XII)." Biochemical & Biophysical Research Communications **92**: 803-810.
- Ratner, B. D. (1993). "The blood compatibility catastrophe." Journal of Biomedical Materials Research **27**: 283-287.
- Ratner, B. D. (2000). "Blood compatibility- a perspective." Journal of Biomaterials Science: Polymer edition **11**: 1107-1119.
- Samuel, M., R. A. Pixley, M. A. Villanueva, R. W. Colman and G. B. Villanueva (1992). "Human factor XII (Hageman factor) autoactivation by dextran sulfate. Circular dichroism, fluorescence, and ultraviolet difference spectroscopic studies." Journal of Biological Chemistry **267**: 19691-19697.
- Tans, G., J. Rosing, M. Berrettini, B. Lammle and J. H. Griffin (1987). "Autoactivation of human plasma prekallikrein." Journal of Biological Chemistry **262**: 11308-11314.
- Vogler, E. A., J. C. Graper, G. R. Harper, H. W. Sugg, L. M. Lander and W. J. Brittain (1995). "Contact activation of the plasma coagulation cascade I. Procoagulant surface chemistry and energy." Journal of Biomedical Materials Research **29**: 1005-1016.
- Vroman, L. (1964). "Effects of hydrophobic surfaces upon blood coagulation." Thrombosis et Diathesis Haemorrhagica **10**: 455-493.
- Wiggins, R. C. and C. G. Cochrane (1979). "The autoactivation of rabbit Hageman factor." Journal of Experimental Medicine **150**: 1122-1133.
- Williams, D. F. (1987). Blood physiology and biochemistry: hemostasis and thrombosis. Blood Compatibility. D. F. Williams. Boca Raton, Florida, CRC Press. **1**: 5-35.
- Zhuo, R., R. Miller, K. M. Bussard, C. A. Siedlecki and E. A. Vogler (2005). "Procoagulant stimulus processing by the intrinsic pathway of blood plasma coagulation." Biomaterials **26**: 2965-2973.
- Zhuo, R., C. A. Siedlecki and E. A. Vogler (2006a). "Autoactivation of blood factor XII at hydrophilic and hydrophobic surfaces." Biomaterials **27**: 4325-4332.
- Zhuo, R. and E. A. Vogler (2006b). "Practical application of a chromogenic FXIIa assay." Biomaterials **27**: 4840-4845.

## **Chapter 4**

### **Moderation of prekallikrein-factor XII interactions in surface activation of coagulation by protein-adsorption competition**

#### **4.1 Introduction**

The use of blood-contacting medical devices for diagnosis and treatment of disease leads to the activation of blood factors that initiate blood coagulation and thrombosis. Enzymes activated by contact with cardiovascular biomaterials can also perturb the immune system, the complement system, and fibrinolytic pathways as well as generate vascular permeability factors that are detrimental to patient health (Janatova 2000). Despite decades of research, development of improved hemocompatible materials has remained a largely unrealized objective (Ratner 2000), stymied in part by the lack of a fundamental understanding of the role of the material surface in influencing these responses.

It is believed that the intrinsic coagulation cascade has little physiological significance in comparison to the extrinsic cascade that dominates coagulation in vivo (Colman 2001). Despite the lack of conclusive evidence of a physiological role for the intrinsic pathway in hemostasis and thrombosis, elevated levels of activated intrinsic pathway enzymes reported in patients where there is blood-biomaterial contact underscores the in vivo significance of this pathway with the use of medical devices (Campbell 2001; Koster 2000; Paparella 2004).

The intrinsic pathway of blood coagulation is a cascade of limited proteolytic conversions of an inactive zymogen to an active enzyme (Colman 2001). It is believed that negatively-charged surfaces, such as that of glass, are specific initiators of the coagulation cascade (Ratnoff 1958; Revak 1977). This traditional biochemical theory asserts that the intrinsic pathway is initiated by binding coagulation factor XII (FXII, Hageman factor) to the negatively-charged surface via specific interactions with protein domains rich in positively-charged amino acids (Kirby 1983; Wiggins 1979). Binding induces conformational changes in the protein, producing autoactivated FXIIa (Samuel 1992; Vroman 1964) and also enhances FXII susceptibility to cleavage by kallikrein (Kal). FXIIa in turn cleaves prekallikrein (PK, Fletcher factor) to Kal (Griffin 1978) in a process known as reciprocal-activation. Further, FXIIa bound to the negatively-charged surface is believed to activate factor XI (FXI, Plasma Thromboplastin Antecedent) (Griffin 1976) leading to propagation of the cascade. There have also been reports of autohydrolysis of FXII by FXIIa (Tankersley 1984; Zhuo 2006b). Figure 1-2 is an illustration of the interactions involved in contact activation. According to this traditional biochemistry, the negatively-charged surface plays an indispensable role in autoactivation and as serves an essential cofactor-like role in subsequent interactions (Kaplan 1978).

Although the physical chemistry of protein adsorption in biomaterial surface science remains a contentious subject, it is generally agreed that hydrophobic surfaces adsorb more protein than an equivalent area of hydrophilic surface (Noh 2006a; Wu 2005). Therefore, if protein adsorption was the primary mediating event in contact activation (Figure 1-2), then logically hydrophobic surfaces should be more activating than hydrophilic surfaces. However, just the opposite is observed; hydrophobic surfaces

are quite nearly inert whereas hydrophilic surfaces are much more potent activators on a per-unit-area basis (Guo 2006). To circumvent this logical conundrum, specific-charge interactions between hydrophilic surfaces and activating factors were built into the consensus mechanism of contact activation. These specific interactions were implicitly supposed not to occur between activating surfaces and the plethora of more concentrated blood proteins, which would otherwise engage in adsorption competition with activating factors. This latter mechanistic fix is not supported by subsequent research into the interfacial activity of blood proteins (Noh 2006b; Noh 2007). In fact, factors and enzymes of the blood coagulation cascade do not exhibit significantly different adsorption behavior than blood proteins such as albumin or immunoglobulin.

This unresolved mechanistic paradox underscores the need to address the role of the surface in contact activation, and is the overarching motivation for our work in contact activation of plasma coagulation. In sharp contrast to expectations of the traditional theory, our research group has observed nearly equal levels of FXII autoactivation at both hydrophobic and hydrophilic surfaces in neat buffer solutions containing only FXII. In sharp contrast, FXIIa generation in plasma is found to be attenuated at hydrophobic surfaces rather than accentuated at hydrophilic surfaces (Zhuo 2006a). In more recent work, we quantified the effects of competitive-protein adsorption in contact activation at hydrophilic and hydrophobic surfaces (Zhuo 2007). FXIIa generation at hydrophilic surfaces from solutions containing a cocktail of proteins including FXII was greater than that obtained under corresponding activation conditions in neat FXII buffer solutions, whereas FXIIa yield at hydrophobic surfaces was significantly lowered in the presence of other proteins compared to neat solution. These

observations strongly implicate an important role for protein-adsorption competition in the overall mechanism of contact activation that is very different from that contemplated by the traditional mechanism.

We report herein on the role of protein-adsorption competition at surfaces in modulating interactions of FXII and PK. We observed that protein adsorption to hydrophobic surface attenuates PK cleavage to Kal by FXIIa but competitive displacement of adsorbed enzymes from these surfaces sharply increases rate and yield of Kal under otherwise identical reaction conditions.

## **4.2 Materials and Methods**

### **4.2.1 Preparation of model material surfaces**

Model hydrophobic and hydrophilic surfaces were prepared from 5 mL borosilicate glass vials (12 mm X 75 mm, Kimble Glass Inc, Vineland, NJ) using procedures reported previously (Guo 2006). Vials were rinsed with chloroform, dried, and treated in a glow-discharge chamber at 100W power for 30 min. Freshly-cleaned glass vials served as model hydrophilic surfaces. Model hydrophobic surfaces were prepared by silanization of glow-discharge-cleaned vials with n-octadecyltrichlorosilane (OTS, Gelest Inc., Morrisville, PA) by filling the vials with 5 % (v/v) OTS in chloroform (Sigma-Aldrich, St. Louis, MO) for 60 min. Vials were rinsed twice with chloroform and annealed overnight at 110°C in a vacuum-oven. OTS-modification of borosilicate glass particles (nominal diameter 500  $\mu\text{m}$ , Sigma-Aldrich) was performed using similar

procedures. Water-wettability of these model surfaces was measured on identically-treated 12 mm diameter glass coverslip witness samples (VWR). Contact angles on the surfaces were measured by the horizontal sessile drop method on a Krüss goniometer using 18 M $\Omega$  water (Millipore Simplicity 185 System) as the probe liquid. Polystyrene vials (VWR) having identical dimensions to the glass vials were used after rinsing with 18 M $\Omega$  water and drying.

#### **4.2.2 Proteins and plasma**

Human PK, human FXIIa, human FXII, human Kal and corn trypsin inhibitor (CTI) were from Enzyme Research Lab (South Bend, IN). Solutions were prepared by serial dilution of supplier-provided stock concentrations with 0.01 M phosphate-buffered saline (PBS, pH 7.4, Sigma-Aldrich). Bovine serum albumin (BSA) solutions in PBS were freshly prepared from lyophilized BSA (fraction V, Sigma-Aldrich).

Human platelet-poor plasma (PPP) was prepared by pooling 5 units of anti-coagulated salvaged human plasma (outdated less than 5 days prior to receipt) from the Blood Bank at the Pennsylvania State University Milton S. Hershey Medical Center. PPP preparation and storage has been described previously (Guo 2006). Pooled plasma was centrifuged 10 min at 500 x g and 35°C. PPP was stored in 12 mL aliquots at -20°C and thawed at 37°C for 40 min prior to use.

### **4.2.3 Coagulation assay**

An in vitro assay was used to measure the coagulation response of the model surfaces following procedures reported previously (Guo 2006; Zhuo 2005). Briefly, 0.5 mL of PPP was mixed with 0.1 mL of 0.1 M calcium chloride (Sigma Aldrich). The volume was adjusted with PBS to obtain 1 mL solution resulting in a 1:1 dilution of plasma in buffer. The vials were capped with parafilm, rotated at 8 rpm on a hematology mixer, and the time required from activation of the intrinsic pathway of the coagulation cascade to the first appearance of a visible clot was designated as the coagulation time (CT).

### **4.2.4 Kallikrein generation assay**

The Kal assay was designed to closely mimic the coagulation assay. Each surface-treated vial contained 1 mL protein solution consisting of PK (20  $\mu\text{g/mL}$ , ~ 50% dilution of normal plasma concentration (Dobrovolsky 2002)) with either FXIIa (at  $5 \times 10^{-2}$   $\mu\text{g/mL}$ ) or FXII (at  $5 \times 10^{-2}$  or 4  $\mu\text{g/mL}$  as noted in the text) in PBS. The FXIIa concentration was determined to elicit a measurable response without reaching minimum CT. Kal production at hydrophilic and hydrophobic surfaces was compared to that at the same surfaces when pre-incubated with BSA. These “blocked” surfaces were prepared by overnight incubation with 100 mg/mL BSA. Prior to use, the BSA was drained and vials were rinsed with PBS. Surfaces were designated as OTS-BSA and glass-BSA and used immediately without drying.



The vials were capped with parafilm and rotated at 8 rpm on a hematology mixer. Kal production for each test condition was determined by removal of 15  $\mu\text{L}$  aliquots of the protein solution from the test vials at discrete time points between 0 and 10 min. The corresponding Kal concentration was determined using a chromogenic assay described below. Proteins putatively adsorbed to hydrophobic surfaces were displaced by spiking vials with 38  $\mu\text{L}$  of BSA solution at  $t = 10.5$  min to yield concentrations of either 1 mg/mL or 5 mg/mL in the vials. Kal generation was measured up to 30 min.

#### **4.2.5 Chromogenic assay**

The concentration of Kal at each time point was determined using the commercially-available chromogenic substrate Pefachrome-PK<sup>®</sup> (Centerchem Inc, Norwalk, CT). Supplier-provided vials containing 10  $\mu\text{moles}$  of the reagent were stored at 4°C and reconstituted to 0.5 mM in 18 M $\Omega$  Millipore water prior to use. 15  $\mu\text{L}$  of protein solution from the Kal generation assay was added to a 1.5 mL disposable polystyrene cuvette (VWR) containing 1066  $\mu\text{L}$  of 50 mM tris-immidazole buffer (pH 7.8, 0.15 mM NaCl) and 150  $\mu\text{L}$  of 0.5 mM Pefachrome-PK solution at 37°C. The reaction was stopped after 10 min by adding 240  $\mu\text{L}$  of 10% glacial acetic acid (Mallinckrodt Baker, Paris, KY). CTI, an FXIIa inhibitor was added at 25X molar concentration of FXIIa to inhibit additional FXIIa hydrolysis of PK during the 10 min incubation period with the chromogenic substrate. Absorbance was measured at 405 nm using a Lambda 25<sup>®</sup> UV/Vis spectrometer (Perkin-Elmer Instruments, Wellesley, MA), and compared to blanks prepared using protein-free PBS aliquots. A standard curve (not

shown) prepared at 405 nm was linear over  $0 < [\text{Kal}] < 50 \mu\text{g/mL}$  ( $R^2 = 96\%$ ). Control experiments (not shown) indicated that FXIIa, BSA, or CTI did not have measurable effects on the reaction of Kal with the chromogenic substrate.

#### 4.2.6 Statistical analyses

Statistical analyses were performed by parametric ANOVA (Tukey's test) using InStat software (GraphPad Software). Means of experimental Kal concentration in test vials at a given time were compared pair-wise and the differences were considered statistically significant for  $p < 0.05$ . Significant differences are denoted by one symbol ( $p < 0.05$ ), two symbols ( $p < 0.01$ ), or three symbols ( $p < 0.001$ ).

### 4.3 Results

#### 4.3.1 Coagulation response to model surfaces

Sessile drop water contact angles measured on coverslip witness samples confirmed the hydrophilic and hydrophobic character of the glass and OTS surfaces, respectively (Table 4-1). The choice of these hydrophilic ( $< 5^\circ$ ) and hydrophobic ( $108^\circ$ ) surfaces was intentional and represents the two extremities of the range of observable water-wettability (a measure of surface energy) of solid surfaces. The coagulation response to recalcified human PPP was assayed and expressed quantitatively in terms of CT, listed in Table 4-1. Lower CT for glass indicates that it is a more efficient

procoagulant than an equivalent surface area of hydrophobic material. CT for OTS materials were similar to those measured in response to an equivalent surface area of polystyrene and consistent with previously-reported results (Guo 2006; Zhuo 2005).

Table 4-1: Water contact angles and the measured CT response to PPP

Surface	Sessile Drop Contact Angle	CT (min)
Glass	< 5°	5.6 ± 0.1
OTS	108° ± 3°	53.3 ± 4.5
Polystyrene	-	43.1 ± 7.5

Values are displayed as mean ± S.D. for  $n \geq 3$

#### 4.3.2 Kallikrein generation in solutions of PK and FXIIa

Kinetics of FXIIa-induced hydrolysis of PK was measured using a Kal chromogenic assay in the presence of either a hydrophobic or hydrophilic procoagulant surface (surface of the vial in which reactions were carried out with or without added particulate activator). Figure 4-1 reports results obtained under 4 different experimental conditions (mean ± S.D. of  $n \geq 3$ ). In hydrophobic vials, a small initial increase in Kal concentration was followed by a steady-state Kal yield. By contrast, Kal rate and yield was significantly higher in glass vials ( $p < 0.05$  at all  $t \geq 4$  min), trending toward a steady state that almost assuredly would have been achieved at  $t > 10$  min. Interestingly, in hydrophobic vials preblocked with BSA, Kal production kinetics were not statistically

different from those obtained in hydrophilic vials. We further observe that Kal generation in preblocked hydrophilic glass vials was not statistically different than that in non-blocked glass surfaces (data not shown). Figure 4-1 also shows that addition of 500 mm<sup>2</sup> hydrophobic particles to hydrophilic vials leads to Kal production that was statistically identical to that obtained in hydrophobic vials. Control experiments showed no Kal production in the absence of FXIIa for either hydrophobic or hydrophilic vials (data not shown).

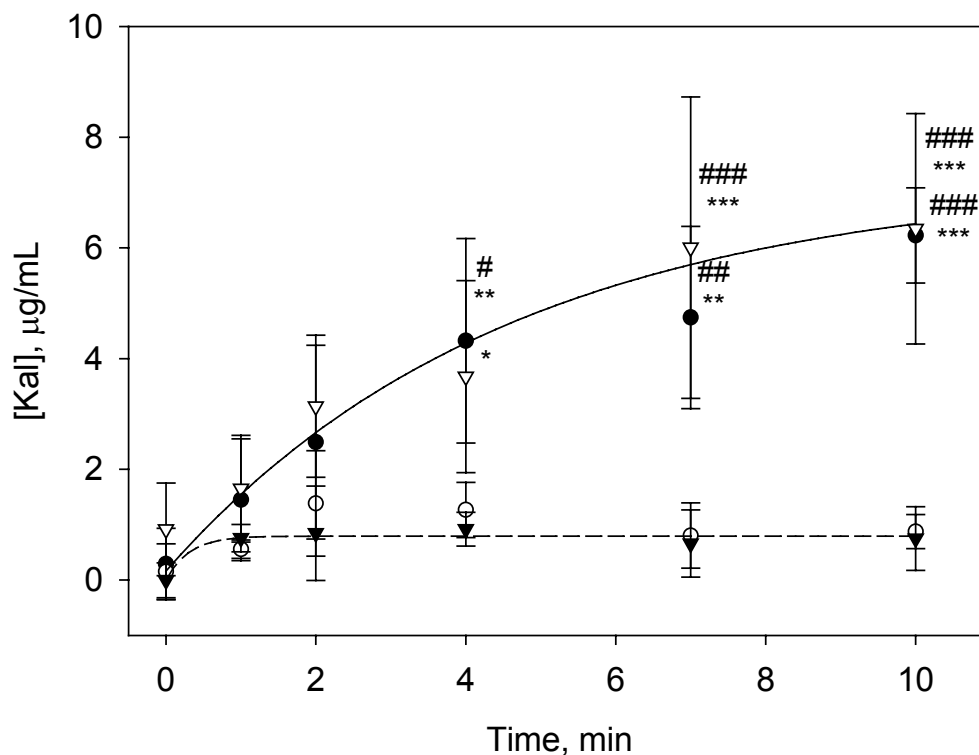


Figure 4-1: Temporal changes in Kal generation in solutions of 20  $\mu\text{g/mL}$  PK and  $5 \times 10^{-2}$   $\mu\text{g/mL}$  FXIIa at glass (closed circles ●), OTS (closed triangles ▼) and OTS-BSA (open triangles ▽) surfaces up to 10 min. Also shown is Kal generation in glass vials containing 500  $\text{mm}^2$  OTS beads (open circles ○). Guidelines are drawn to highlight the profound differences in trends. The symbols # and \* represent statistical significance with respect to Kal concentrations in glass vials containing OTS beads and OTS vials, respectively, at each time point. (Data expressed as mean  $\pm$  S.D. for  $n \geq 3$ ).

#### 4.3.3 Kallikrein generation in solutions of PK and FXII

The Kal chromogenic assay was used to measure Kal arising from PK hydrolysis by agents produced by contacting FXII with either hydrophobic or hydrophilic procoagulant surfaces (putatively FXIIa but possibly including FXIIf and other fragments). Results in Figure 4-2 show that there was no measurable Kal production in

either hydrophobic vials or hydrophobic vials blocked with BSA. In glass vials however, there was an initial lag period followed by a steady rise in Kal concentration that was statistically greater than Kal concentrations for the hydrophobic and BSA-blocked hydrophobic surfaces at all  $t \geq 7$  min. Similar trends were observed for BSA-blocked hydrophilic vials (data not shown).

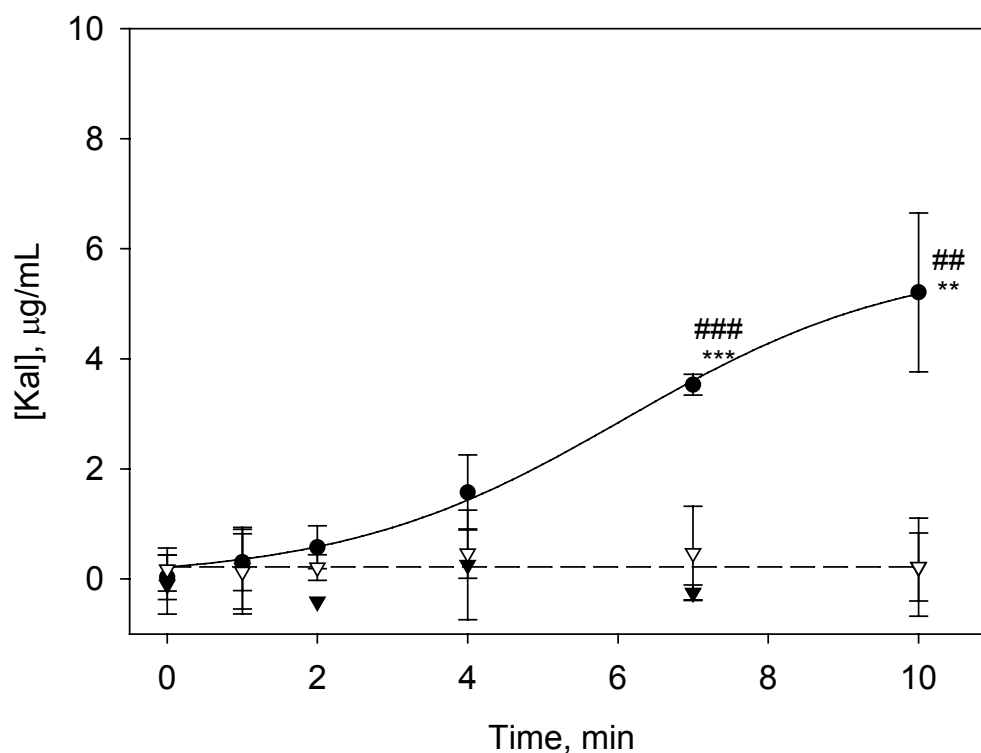


Figure 4-2: Temporal changes in Kal generation in solutions of 20 µg/mL PK and  $5 \times 10^{-2}$  µg/mL of FXII at glass (closed circle ●), OTS (closed triangle ▼) and OTS-BSA (open triangle ▽) surfaces. Data are plotted using same y-scale as Figure 2 for ease of comparison. Guidelines are drawn to highlight the differences in trends. The symbols \* and # represent statistical significance with respect to OTS vials and OTS-BSA surfaces, respectively, at a given time point. (Data expressed as mean  $\pm$  S.D. for  $n \geq 3$ ).

#### 4.3.4 Displacement of adsorbed enzymes at hydrophobic surfaces using BSA

BSA was used to competitively displace adsorbed enzyme from the hydrophobic surfaces. When BSA at 1 mg/mL was added to the Kal assays in hydrophobic vials containing solutions of PK at 20  $\mu\text{g/mL}$  and FXII at  $5 \times 10^{-2} \mu\text{g/mL}$ , there appeared to be a modest increase in Kal concentration but the results were not statistically significant from PBS control (data not shown). When the test solution concentration of FXII was increased to 4  $\mu\text{g/mL}$  (~ an order of magnitude lower than physiologic FXII concentration) there was a rapid increase in Kal (Figure 4-3). Statistically greater Kal concentrations were obtained for both 1 and 5 mg/mL BSA spikes compared to the 0 mg/mL PBS control within  $t \geq 20$  min total reaction time, with the 5 mg/ml spike reaching significance at  $t \geq 15$  min.

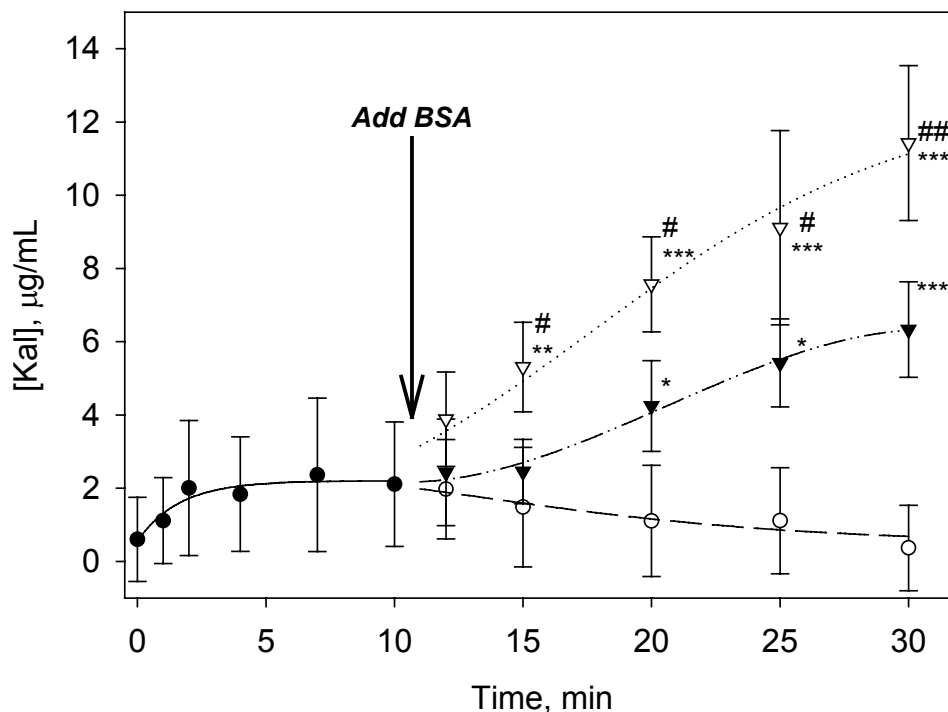


Figure 4-3: Temporal changes in Kal generation in solutions of 20  $\mu\text{g/mL}$  PK and 4  $\mu\text{g/mL}$  FXII in OTS vials (closed circle ●). The effects of addition of BSA at 5 mg/mL (open triangle ▽), 1 mg/mL (closed triangle ▼), or 0 mg/mL, (PBS alone, open circle o) at 10.5 min are also presented. The symbols \* and # represent statistical significance with respect to 0 mg/mL and 1 mg/mL BSA, respectively, at given time points. (Data expressed as mean  $\pm$  S.D. for  $n \geq 3$ ).

#### 4.4 Discussion

Faster coagulation of blood in glass vials than in plastic vials is well known in practical hematology. The traditional biochemical theory explaining this routinely-observed phenomenon is that certain coagulation factors adsorb specifically to negatively-charged surfaces that serve as cofactors for the formation of contact activation complex. In this sense, anionic hydrophilic surfaces are viewed as specific activators and



facilitators of contact activation reactions (Figure 1-2). Effectively, this rationalization of experimental observations confers special properties onto proteins of the activation complex that are conspicuously not shared by other blood proteins. These special properties allow activation-complex proteins to specifically, and yet reversibly when required, adsorb to anionic hydrophilic surfaces in the presence of overwhelming concentrations of other blood proteins. This plethora of other plasma proteins would otherwise competitively adsorb to activating surfaces were it not for the supposed special properties of activation-complex proteins. Moreover, these special properties include resistance to activation by adsorption to hydrophobic surfaces, accounting for the benign activation properties of silanized glass and many plastics.

In sharp contrast to the traditional theory, our recent results underscore the need for a new paradigm to incorporate protein adsorption and protein-adsorption competition into a comprehensive model of contact activation. In particular, we have shown that FXII activation in the presence of proteins unrelated to the plasma coagulation cascade leads to an apparent specificity for hydrophilic surfaces that is actually due to a relative diminution of the FXII→FXIIa reaction at hydrophobic surfaces and an enhancement at hydrophilic surfaces (Zhuo 2006a; Zhuo 2007). This work illuminates in molecular terms how protein-adsorption competition at hydrophobic surfaces leads to this apparent specificity.

#### 4.4.1 Effect of adsorption on interactions of PK and FXII

The objective of the experiments in Figure 4-2 was to evaluate the potential role of a surface in FXIIa hydrolysis of PK and to further evaluate an effect of adsorption on contact activation and enzyme amplification for FXII and PK. Significantly higher amounts of Kal generated in the presence of glass indicates increased FXIIa reaction with PK than is observed to occur at equivalent contact area of hydrophobic or BSA-blocked hydrophobic surfaces. This is consistent with increased autoactivation yield of FXIIa which not only accounts for enhanced PK hydrolysis but also more rapid coagulation as observed at the hydrophilic surfaces. Control experiments verified that Kal generation did not occur at hydrophobic or hydrophilic vials containing neat PK solutions without added FXII/FXIIa, confirming that FXIIa was required for Kal production. At the BSA-blocked hydrophobic surface, solution contact with the substrate was inhibited by the blocking molecules thereby minimizing autoactivation of FXII and subsequent reciprocal-activation processes. At the hydrophobic surfaces, FXIIa molecules potentially generated via autoactivation (Zhuo 2006a) were adsorbed to the surface so that these active enzyme molecules were unable to participate in subsequent reciprocal-activation reactions as reflected by the low Kal yield.

In hydrophilic vials, FXIIa molecules generated via autoactivation near the poorly-adsorbent surface could participate in the subsequent PK→Kal conversion as the molecules are not confined to the surface by adsorption. This resulted in a rapid increase in measured Kal concentrations (Figure 4-2). When glass vials were preblocked with

BSA the response was similar to the unblocked glass because there is no adsorption process to be blocked.

#### 4.4.2 Effect of adsorption on interactions of PK and FXIIa

Results in Figure 4-1 demonstrate the effects of protein adsorption on the PK  $\xrightarrow{\text{FXIIa}}$  KAL reaction carried out in a manner that bypasses FXII autoactivation by direct addition of FXIIa enzyme. Kal yield in hydrophobic vials or hydrophilic vials containing hydrophobic particles was observed to be much lower than in hydrophilic vials, suggesting that loss of proteins through adsorption to the hydrophobic surface moderated the PK hydrolysis. Consistent with this explanation, Kal generation in BSA-blocked hydrophobic surfaces was equivalent to that observed in hydrophilic glass vials that presumably adsorb little-or-no protein. BSA blocking of hydrophilic glass vials had no effect on results because there is no adsorption event to be blocked.

Trends of Figure 4-1 are in sharp contrast to the traditional biochemical mechanism of contact activation which states that FXIIa mediated hydrolysis of PK occurs through assembly of proteins (the so-called activation complex) onto negatively-charged surfaces, where the surface serves as a cofactor (Kaplan 1978). In particular, it is evident that for BSA-blocked hydrophobic surfaces, there is no negatively-charged surface that can serve as a cofactor, unless it is argued that surface-adsorbed albumin itself an activating surface. But then in this latter event, one must anticipate that hydrophobic surfaces immersed in plasma would be activating, which is not observed. Therefore, experiments summarized in Figure 4-1 demonstrate that the PK  $\xrightarrow{\text{FXIIa}}$  KAL

can occur in the absence of an activation complex assembled on an activating surface and that this reaction is not specific to negatively-charged hydrophilic surfaces. Rather, it appears that FXIIa mediated hydrolysis of PK is attenuated by protein adsorption at hydrophobic surfaces.

#### **4.4.3 Competitive displacement of adsorbed enzymes from hydrophobic surfaces**

The above results indicate that adsorption of proteins to hydrophobic vial surfaces moderates molecular interactions necessary for reciprocal-activation, resulting in reduced Kal generation. These results do not, however, directly probe if FXII is activated by the hydrophobic surface to yield surface-adsorbed FXIIa, as reported by us previously (Zhuo 2006a; Zhuo 2007), which cannot react with solution-phase PK. To test this question, BSA, a molecule not involved in the coagulation cascade, was employed to displace putative surface-adsorbed FXIIa by competitive protein adsorption (Krishnan 2005; Krishnan 2003; Noh 2006b). Figure 4-3 shows that addition of BSA at 1 mg/mL results in a significant increase in Kal yield in hydrophobic vials compared to negative controls in which an equivalent volume of buffer (no BSA) was added. Addition of BSA at 5 mg/mL caused an even sharper rise in Kal with statistically greater amounts measured with respect to both the 1 mg/mL BSA and the PBS control within 5 min of introducing BSA. Addition of the competing protein to the test vials therefore resulted in enhanced Kal production, presumably because BSA displaced reactive proteins (FXIIa and/or PK) from the surface which participated in solution-phase reciprocal-activation reactions that generate Kal. These results further show that reactive agents (FXIIa and PK) or products

(Kal) were adsorbed to the surface before BSA displacement but were sequestered from solution where Kal could be detected. In other words, adsorption (assembly) of FXIIa and PK onto a surface is apparently insufficient to produce Kal in solution, either because surface-adsorbed reactants fail to react or because Kal product remains adsorbed. More detailed experiments are required to resolve these two alternatives, but comparison of Figures 4-1 and 4-3 suggest that the rate of Kal production after BSA displacement is not remarkably different than the rate of PK hydrolysis by FXIIa, suggesting that a build-up of surface-adsorbed Kal was not desorbed as a bolus by BSA displacement.

To the best of our knowledge, the only report on the effect of adsorption on contact activation was by Scott et al (Scott 1981) who, in a manner similar to this report, observed reduction in FXIIa hydrolysis of PK in hydrophobic (plastic) tubes. Furthermore, Scott et al noted recovery of activity in the presence of other proteins (high-molecular-weight-kininogen, BSA, fibrinogen) or phospholipids. Unlike us, however, Scott interpreted this recovery to an “enhancement effect” of added proteins that was not further rationalized in molecular terms. We believe that our interpretation in terms of competitive adsorption is a more plausible explanation that does not require invocation of inexplicable enhancement effects and is consistent with the surface science of protein adsorption (see (Noh 2006b) and citations therein).

#### **4.4.4 Role of the material surface in contact activation**

Based on results presented herein and previous work (Zhuo 2006a; Zhuo 2007), we are led to propose a modified sequence of contact-activation events depicted in

Figure 4-4. Autoactivation of FXII is proposed to occur in close vicinity (vicinal) to a solid surface immersed in aqueous solution in what is frequently termed an “interphase”. Unlike the traditional biochemical mechanism, we do not view this step as specific to anionic hydrophilic surfaces. Furthermore, we assert that reciprocal-activation does not require assembly of reactive molecules (FXII and PK) directly on the surface. We further propose that surface-adsorbed FXIIa molecules lack mobility to engage in PK hydrolysis, resulting in reduced Kal production at hydrophobic surfaces. By contrast, FXIIa generated by FXII collisions with non-adsorbent hydrophilic surfaces are readily-available to participate in solution-phase reciprocal-activation reactions. Thus, FXIIa generation and subsequent PK hydrolysis results in an *apparent specificity* relative to the attenuated response observed at hydrophobic surfaces. Competitive displacement of FXIIa and PK by other proteins (or phospholipid) in the system changes this adsorption dynamic at hydrophobic surfaces, resulting in what has been interpreted as reaction enhancement but really is an outcome of solution-phase reactant concentrations.

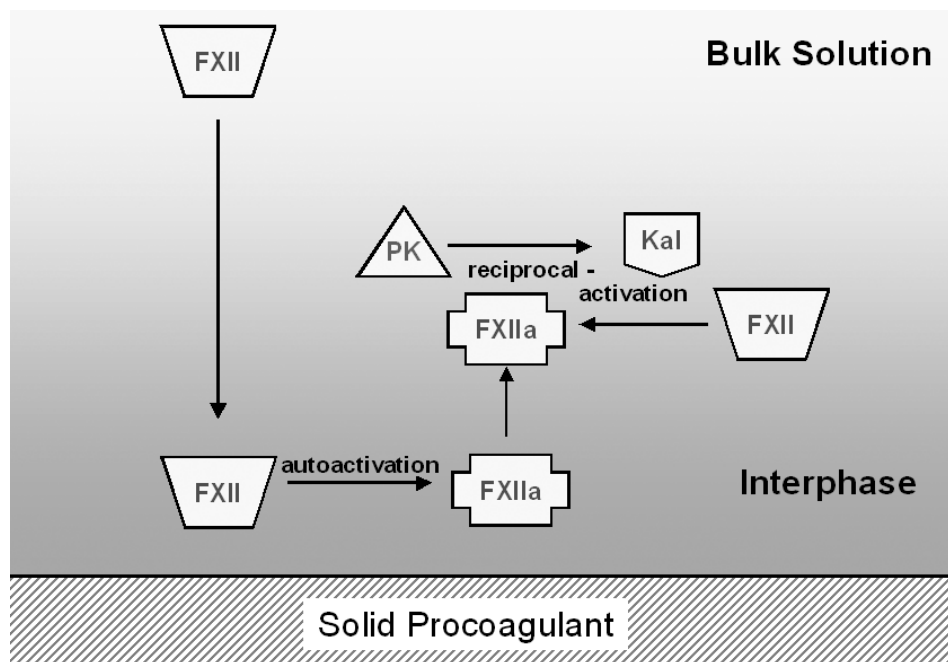


Figure 4-4: Alternate model for the sequence of events involving PK and FXII at solid procoagulant surfaces. Contact activation is initiated by autoactivation of FXII at the interphase and is not specific to negatively-charged surfaces. Subsequent interactions involving reciprocal-activation of PK and FXII do not occur by direct assembly on the surface but rather require displacement from the surface.

#### 4.5 Conclusions

Results presented in this study confirm that (i) an anionic hydrophilic surface is not a necessary cofactor for FXIIa-mediated hydrolysis of PK, (ii) FXIIa hydrolysis of PK can occur in solution and does not require assembly of an activation complex directly on an activating surface, and (iii) contact activation of FXII (autoactivation) is not specific to anionic hydrophilic surfaces. Protein-adsorption competition is an essential component of blood plasma coagulation that must be included in any comprehensive descriptive mechanism.

#### 4.6 Literature citations

- Campbell, D. J., B. Dixon, A. Kladis, M. Kemme and J. D. Santamaria (2001). "Activation of the kallikrein-kinin system by cardiopulmonary bypass in humans." American Journal of Physiology - Regulatory Integrative & Comparative Physiology **281**: R1059-1070.
- Colman, R. W., A. W. Clowes, J. N. George, J. Hirsh and V. J. Marder (2001). Overview of Hemostasis. Hemostasis and Thrombosis- Basic Principles and Clinical Practice. R. W. Colman, J. Hirsh, V. J. Marder, A. W. Clowes and J. N. George. Philadelphia, Lippincott William and William. **4**: 3-16.
- Dobrovolsky, A. B. and E. V. Titaeva (2002). "The fibrinolysis system: regulation of activity and physiologic functions of its main components." Biochemistry-Russia **67**: 99-108.
- Griffin, J. H. and C. G. Cochrane (1976). "Mechanisms for the involvement of high molecular weight kininogen in surface-dependent reactions of Hageman factor." Proceedings of the National Academy of Sciences of the United States of America **73**: 2554-2558.
- Griffin, J. H. (1978). "Role of surface in surface-dependent activation of Hageman factor (blood coagulation Factor XII)." Proceedings of the National Academy of Sciences USA **75**: 1998-2002.
- Guo, Z., K. M. Bussard, K. Chatterjee, R. Miller, E. A. Vogler and C. A. Siedlecki (2006). "Mathematical modeling of material-induced blood plasma coagulation." Biomaterials **27**: 796-806.
- Janatova, J. (2000). "Activation and control of complement, inflammation, and infection associated with the use of biomedical polymers." ASAIO Journal **46**: S53-62.
- Kaplan, A. P. (1978). "Initiation of the intrinsic coagulation and fibrinolytic pathways of man: the role of surfaces, Hageman factor, prekallikrein, high molecular weight kininogen, and factor XI." Progress in Hemostasis and Thrombosis **4**: 127-175.
- Kirby, E. P. and P. J. McDevitt (1983). "The binding of bovine factor XII to kaolin." Blood **61**: 652-659.
- Koster, A., M. Loebe, R. Hansen, E. V. Potapov, G. P. Noon, H. Kuppe and R. Hetzer (2000). "Alterations in coagulation after implantation of a pulsatile Novacor LVAD and the axial flow MicroMed DeBakey LVAD." Annals of Thoracic Surgery **70**: 533-537.



- Krishnan, A., C. A. Siedlecki and E. A. Vogler (2003). "Traube-Rule Interpretation of Protein Adsorption at the Liquid-Vapor Interface." Langmuir **19**: 10342-10352.
- Krishnan, A., Y. H. Liu, P. Cha, D. Allara and E. A. Vogler (2005). "Scaled interfacial activity of proteins at a hydrophobic solid/aqueous-buffer interface." Journal of Biomedical Materials Research. Part A **75**: 445-457.
- Noh, H. and E. A. Vogler (2006a). "Volumetric interpretation of protein adsorption: mass and energy balance for albumin adsorption to particulate adsorbents with incrementally increasing hydrophilicity." Biomaterials **27**: 5801-5812.
- Noh, H. and E. A. Vogler (2006b). "Volumetric interpretation of protein adsorption: Partition coefficients, interphase volumes, and free energies of adsorption to hydrophobic surfaces." Biomaterials **27**: 5780-5793.
- Noh, H. and E. A. Vogler (2007). "Volumetric interpretation of protein adsorption: competition from mixtures and the Vroman effect." Biomaterials **28**: 405-422.
- Paparella, D., S. J. Brister and M. R. Buchanan (2004). "Coagulation disorders of cardiopulmonary bypass: a review." Intensive Care Medicine **30**: 1873-1881.
- Ratner, B. D. (2000). "Blood compatibility- a perspective." Journal of Biomaterials Science: Polymer edition **11**: 1107-1119.
- Ratnoff, O. D. and J. M. Rosenblum (1958). "Role of Hageman factor in the initiation of clotting by glass." American Journal of Medicine **25**: 160-168.
- Revak, S. D., C. G. Cochrane and J. H. Griffin (1977). "The binding and cleavage characteristics of human Hageman factor during contact activation." The Journal of Clinical Investigation **59**: 1167-1175.
- Samuel, M., R. A. Pixley, M. A. Villanueva, R. W. Colman and G. B. Villanueva (1992). "Human factor XII (Hageman factor) autoactivation by dextran sulfate. Circular dichroism, fluorescence, and ultraviolet difference spectroscopic studies." Journal of Biological Chemistry **267**: 19691-19697.
- Scott, C. F., E. P. Kirby, P. K. Schick and R. W. Colman (1981). "Effect of surfaces on fluid-phase prekallikrein activation." Blood **57**: 553-560.
- Tankersley, D. L. and J. S. Finlayson (1984). "Kinetics of activation and autoactivation of human factor XII." Biochemistry **23**: 273-279.
- Vroman, L. (1964). "Effects of hydrophobic surfaces upon blood coagulation." Thrombosis et Diathesis Haemorrhagica **10**: 455-493.

- Wiggins, R. C. and C. G. Cochrane (1979). "The autoactivation of rabbit Hageman factor." Journal of Experimental Medicine **150**: 1122-1133.
- Wu, Y., F. I. Simonovsky, B. D. Ratner and T. A. Horbett (2005). "The role of adsorbed fibrinogen in platelet adhesion to polyurethane surfaces: A comparison of surface hydrophobicity, protein adsorption, monoclonal antibody binding, and platelet adhesion." Journal of Biomedical Materials Research Part A **74A**: 722-738.
- Zhuo, R., R. Miller, K. M. Bussard, C. A. Siedlecki and E. A. Vogler (2005). "Procoagulant stimulus processing by the intrinsic pathway of blood plasma coagulation." Biomaterials **26**: 2965-2973.
- Zhuo, R., C. A. Siedlecki and E. A. Vogler (2006a). "Autoactivation of blood factor XII at hydrophilic and hydrophobic surfaces." Biomaterials **27**: 4325-4332.
- Zhuo, R. and E. A. Vogler (2006b). "Practical application of a chromogenic FXIIa assay." Biomaterials **27**: 4840-4845.
- Zhuo, R., C. A. Siedlecki and E. A. Vogler (2007). "Competitive-protein adsorption in contact activation of blood factor XII." Biomaterials **28**: 4355-4369.

## Chapter 5

### Moderation of factor XII- factor XI interactions in surface activation by protein-adsorption competition

#### 5.1 Introduction

Despite widespread use of blood-contacting medical devices, coagulation and thrombosis persist as major risks arising from unfavorable blood-material interactions (Lamba 2001; Ratner 2000). A comprehensive understanding of the role of the material surface in influencing these responses is an essential prerequisite for engineering improved hemocompatible materials.

Blood factors are activated at the biomaterial surface initiating the intrinsic cascade of coagulation (Lamba 2001). Traditional biochemistry of contact activation suggests that anionic hydrophilic surfaces are specific activators (Colman 2001; Lamba 2001; Sainz 2007; Williams 1987). These surface bind factor XII (FXII) causing a conformational change that leads to activation (autoactivation). These surfaces also serve as cofactors for reciprocal-activation reactions involving FXIIa-mediated prekallikrein (PK)→kallikrein (Kal) hydrolysis and Kal-mediated FXII→FXIIa activation, as well as in FXIIa-mediated activation of factor XI (FXI). As discussed previously, this proposed scheme of molecular events contradicts known trends in protein adsorption to material surfaces (see 1.5 for detailed discussion).

Our recent results suggest a need to incorporate the role of protein adsorption in the molecular events of contact activation. In sharp contrast to the traditional theory, our

group has observed nearly equal levels of FXII activation at both hydrophobic and hydrophilic surfaces in neat solutions (Zhuo 2006). However, FXIIa generation in plasma is attenuated at hydrophobic surfaces rather than being accentuated at hydrophilic surfaces (Zhuo 2006). Further, FXIIa generation at hydrophilic surfaces from solutions containing a cocktail of proteins including FXII was greater than that obtained under corresponding activation conditions in neat FXII buffer solutions, whereas FXIIa yield at hydrophobic surfaces was significantly lowered in the presence of other proteins compared to neat solution (Zhuo 2007). In more recent results, we observed that FXIIa-mediated PK $\rightarrow$ Kal hydrolysis was spontaneously detected at hydrophilic surfaces but not at hydrophobic surfaces unless adsorbed molecules were displaced from the surface (4.4.3). FXIIa molecules generated by autoactivation at strongly-adsorbent hydrophobic surfaces were unable to effectively participate in solution-phase reciprocal-activation reactions, whereas hydrophilic surfaces being poor adsorbents did not attenuate the molecular interactions. However, PK hydrolysis by FXIIa was initiated at hydrophobic surfaces when the adsorbed proteins were displaced by competitive protein desorption using bovine serum albumin (BSA), a molecule not involved in coagulation reactions. Taken together, our results increasingly indicate that protein adsorption events lead to an *apparent specificity* for FXII activation at poorly-adsorbent hydrophilic surfaces relative to the attenuated response at hydrophobic surfaces.

The objective of this study was to investigate the effect of protein adsorption on FXI hydrolysis in solutions of FXII and FXI at test surfaces. Lower FXIa yield was measured in hydrophobic vials than in hydrophilic surfaces. However, displacement of

putatively adsorbed FXIIa from the hydrophobic surfaces caused an increase in FXIa generation.

## 5.2 Materials and methods

In this study, we measured FXIIa-mediated FXI→FXIa hydrolysis at test hydrophobic and hydrophilic surfaces. The experimental design was fundamentally similar to that described previously for the study of FXIIa-mediated PK hydrolysis (4.2). Glow-discharge-treated glass vials and n-octadecyltrichlorosilane (OTS)-modified glass vials served as test hydrophilic and hydrophobic surfaces, respectively (4.2.1). Human FXII and human FXI were obtained commercially (Enzyme Research Lab, South Bend, IN). FXIa-generation assays were designed following the design of Kal-generation assay (4.2.4). Each assay vial contained 1 mL solution of FXI at 5 µg/mL (physiological concentration) and FXII at 4 µg/mL (about an order of magnitude less than physiological concentration) and was rotated at 8 rpm on a hematology mixer. A commercially-available chromogenic substrate Pefachrome-FXIa-3371<sup>®</sup> (Centerchem, Norwalk, CT) was used to detect the concentration of FXIa at set time intervals. At discrete time intervals, 25 µL aliquot from the solution in the test vials was transferred to a 96-well plate (VWR) and incubated with 150 µL of 50 mM tris-immidazole buffer (pH 7.8, 0.15 mM NaCl) and 25 µL of 4 mM Pefachrome-FXIa-3371 solution for 10 min at 37°C. Corn trypsin inhibitor (CTI, Enzyme Research Lab), a FXIIa inhibitor, was added at 25 X molar excess of FXIIa concentration to minimize additional hydrolysis of FXI and the chromogenic substrate during the incubation period. The reaction was stopped by the

addition of 25  $\mu\text{L}$  of 10% glacial acetic acid. Absorbance was measured at 405 nm on a  $\mu\text{Quant}^{\text{®}}$  well-plate reader (Bio-Tek Instruments, Winooski, VT) fitted with KC-Junior<sup>®</sup> software (Bio-Tek Instruments). A standard curve (not shown) prepared at 405 nm was linear over  $0 < [\text{FXIa}] < 5 \mu\text{g/mL}$ .

Proteins putatively adsorbed to hydrophobic OTS surfaces were displaced by spiking with BSA solution (prepared in PBS) to the vials at  $t = 10.5 \text{ min}$ . 95  $\mu\text{L}$  of BSA solution appropriate to yield a BSA concentration of 12.5 mg/mL was added to the 850  $\mu\text{L}$  of solution remaining in the OTS vials.

### 5.3 Results

Figure 5-1 reports FXIa generation in solutions of FXII and FXI at hydrophilic glass and hydrophobic OTS surfaces. In control experiments, no measurable FXIa was detected in neat FXI solution at either surface (data not shown). A steady increase in FXIa concentration following an initial lag was measured in glass vials up to 10 min, whereas in OTS vials FXIa yield remained low after a modest initial increase. FXIa yield in glass was statistically higher than in OTS for all  $t \geq 7 \text{ min}$ .

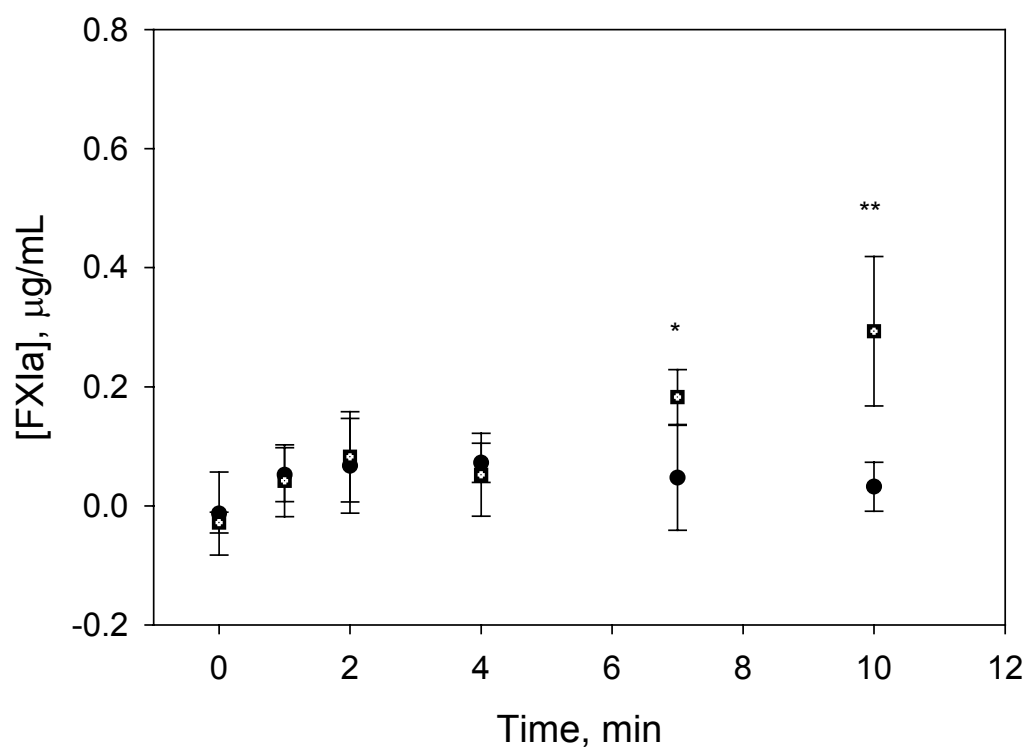


Figure 5-1: Temporal changes in FXIa generation in solutions of 4  $\mu\text{g/mL}$  FXII and 5  $\mu\text{g/mL}$  FXI in glass (dotted squares ■) and OTS (closed circles ●) vials. Statistical analyses were performed by two-tailed p-value using InStat software (GraphPad). Means were compared pair-wise and the differences were considered statistically significant for  $p < 0.05$ . Significant differences are denoted by one symbol ( $p < 0.05$ ) and two symbols ( $p < 0.01$ ). The symbol \* represents statistical significance at a given time point. (Data expressed as mean  $\pm$  S.D. for  $n \geq 3$ ).

Results in Figure 5-2 indicate that spiking the solutions in OTS with BSA caused a rise in FXIa yield. Statistically significant differences in concentration were measured for all  $t \geq 15$  min with respect to the PBS control (BSA = 0 mg/mL). Note that the measurements in OTS vials up to 10 min in Figure 5-2 are identical to data presented in Figure 5-1.

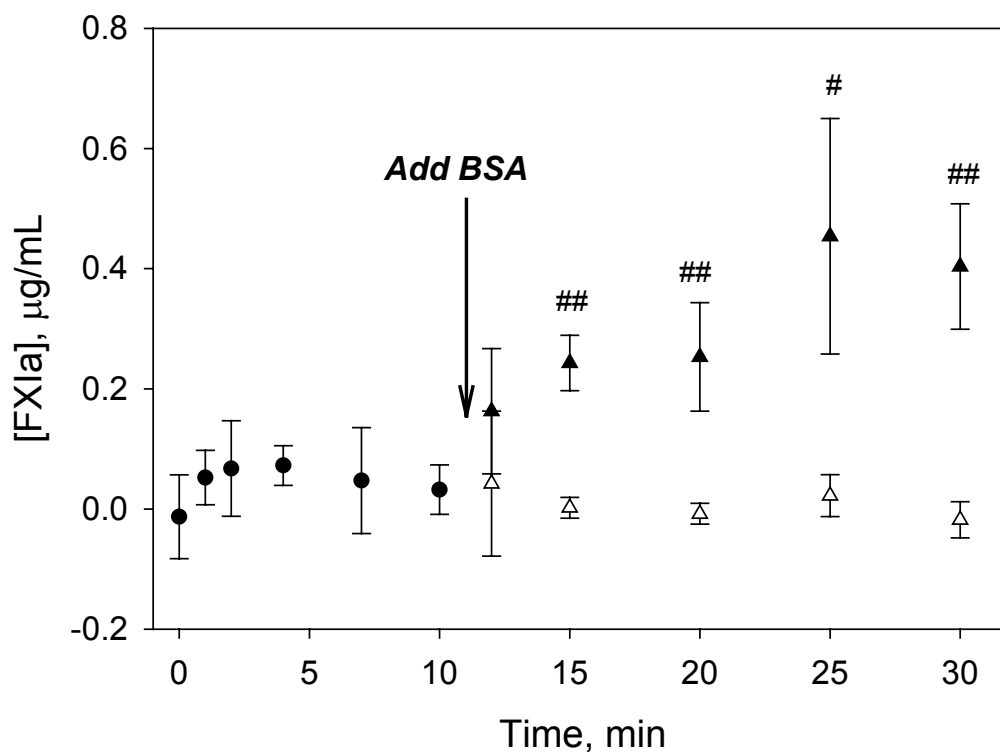


Figure 5-2: Temporal changes in FXIa generation in solutions of 4  $\mu\text{g/mL}$  FXII and 5  $\mu\text{g/mL}$  FXI in OTS (closed circles ●) vials. The effects of addition of BSA at 12.5 mg/mL (closed triangles ▲) or 0 mg/mL, (PBS alone, open triangles  $\Delta$ ) at 10.5 min to the OTS vials are also presented. Statistical analyses described in Figure 5-1. The symbol # represent statistical significance between OTS vials with BSA 12.5 mg/mL and PBS at a given time point. (Data expressed as mean  $\pm$  S.D. for  $n \geq 3$ ).

#### 5.4 Discussion

Results in Figure 5-1 suggest that FXIIa-mediated FXI hydrolysis was more efficient at hydrophilic glass than at hydrophobic OTS surfaces. Since control experiments eliminated autoactivation of FXI as a plausible mechanism of FXIa generation, FXI hydrolysis requires presence of FXIIa putatively generated by surface-



mediated autoactivation. Our group has previously observed nearly equal levels of FXII autoactivation at both hydrophilic and hydrophobic surfaces (Zhuo 2006). Therefore, it seems FXIIa molecules at glass surfaces are more effective in hydrolysis in FXI than the enzymes generated at OTS surfaces.

Since OTS is a stronger adsorbent than glass, putatively adsorbed FXIIa molecules were unable to interact with FXI at OTS, but not so at glass surfaces. When the adsorbed zymogens/enzymes were displaced from the hydrophobic surfaces by competitive protein adsorption/desorption an increase in FXIa yield was observed in the OTS vials (Figure 5-2), demonstrating that adsorption to the hydrophobic surface attenuated FXII-mediated FXI hydrolysis. These observations are consistent with our previous results on FXIIa-mediated PK→Kal activation (4.5), wherein displacement of adsorbed enzymes from the hydrophobic surface caused an increase in Kal yield.

Results presented here indicate that FXIIa-mediated FXI hydrolysis is not specific to anionic hydrophilic surfaces as was suggested by the traditional biochemistry. Further, formation of a complex directly on the activating surface does not appear to facilitate this reaction. In fact, it seems that adsorption to hydrophobic surfaces attenuates this solution-phase interaction. Hydrophilic surfaces being poor adsorbents do not attenuate these molecular interactions leading to an *apparent specificity* for FXII-mediated FXI→FXIa hydrolysis at hydrophilic surfaces arising from protein adsorption events.

We propose a modified sequence of molecular events involving FXII and FXI at an activating surface shown in Figure 5-3 to incorporate our results. FXII autoactivation is proposed to occur in close vicinity to an activating surface (referred to as the “interphase”) and is not limited to anionic surfaces. Subsequent solution-phase FXIIa-

mediated FXI hydrolysis does not occur by the direct assembly of molecules on the surface. Rather adsorption to hydrophobic surfaces attenuates FXI activation by FXIIa so that poorly-adsorbent hydrophilic surfaces that do not attenuate this reaction to appear facilitate it. It would imply that in contrast to the traditional biochemistry of contact activation, an anionic surface does not serve as an essential or active cofactor in this reaction in a manner similar to our observations for reciprocal-activation reactions of FXII and PK.

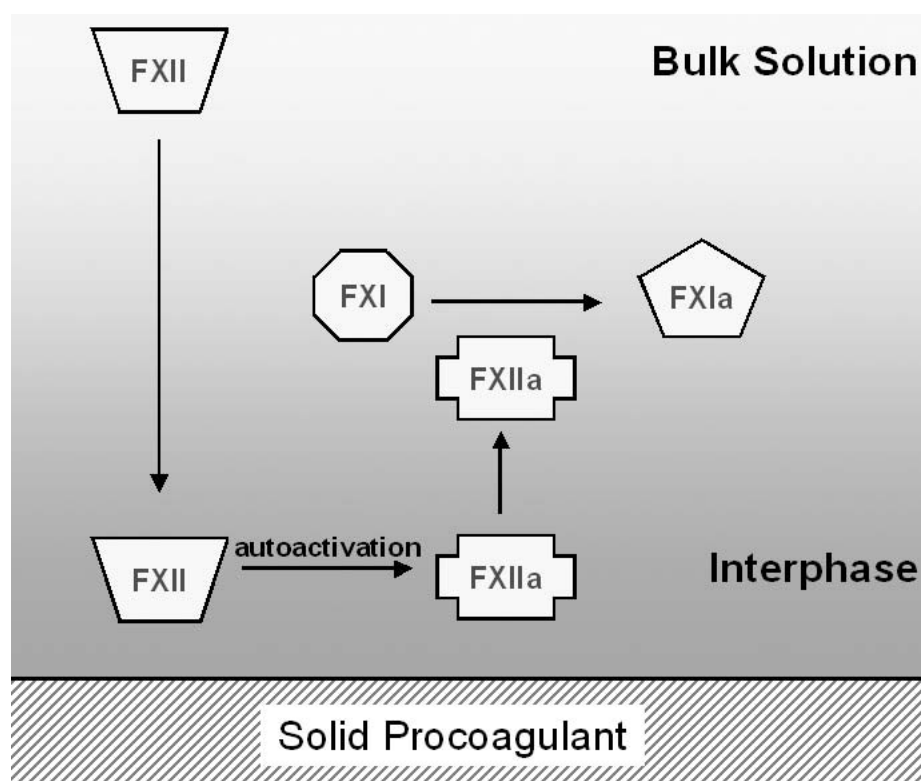


Figure 5-3: Alternate model for the sequence of events involving FXII and FXI at solid procoagulant surfaces. Contact activation is initiated by autoactivation of FXII at the interphase and is not specific to anionic hydrophilic surfaces. Subsequent FXIIa-mediated FXI hydrolysis does not occur by direct assembly on the surface but rather require displacement from the surface.

## 5.5 Conclusions

Results presented in this study (i) demonstrate that a negatively-charged surface is neither essential nor an active cofactor for FXI hydrolysis by FXIIa, (ii) show that FXIIa-mediated FXI hydrolysis does not occur by formation of a contact activation complex directly on the activating surface, (iii) provide further evidence that FXII autoactivation is not limited to anionic hydrophilic surfaces, and (iv) confirm that molecular interactions of contact activation are attenuated by protein adsorption events at hydrophobic surfaces leading to an *apparent specificity* for poorly-adsorbent hydrophilic surfaces. Taken together, our results underscore the need to incorporate events of protein adsorption in any comprehensive mechanism of contact activation.

## 5.6 Literature citations

- Colman, R. W., A. W. Clowes, J. N. George, J. Hirsh and V. J. Marder (2001). Overview of Hemostasis. Hemostasis and Thrombosis- Basic Principles and Clinical Practice. R. W. Colman, J. Hirsh, V. J. Marder, A. W. Clowes and J. N. George. Philadelphia, Lippincott William and William. **4**: 3-16.
- Lamba, N. M. K. and S. L. Cooper (2001). Interaction of blood with artificial surfaces. Hemostasis and Thrombosis- Basic Principles and Clinical Practice. R. W. Colman, J. Hirsh, V. J. Marder, A. W. Clowes and J. N. George. Philadelphia, Lippincott William and William. **4**: 661-672.
- Ratner, B. D. (2000). "Blood compatibility- a perspective." Journal of Biomaterials Science: Polymer edition **11**: 1107-1119.

- Sainz, I. M., R. A. Pixley and R. W. Colman (2007). "Fifty years of research on the plasma kallikrein-kinin system: From protein structure and function to cell biology and in-vivo pathophysiology." Thrombosis and Haemostasis **98**: 77-83.
- Williams, D. F. (1987). Blood physiology and biochemistry: hemostasis and thrombosis. Blood Compatibility. D. F. Williams. Boca Raton, Florida, CRC Press. **1**: 5-35.
- Zhuo, R., C. A. Siedlecki and E. A. Vogler (2006). "Autoactivation of blood factor XII at hydrophilic and hydrophobic surfaces." Biomaterials **27**: 4325-4332.
- Zhuo, R., C. A. Siedlecki and E. A. Vogler (2007). "Competitive-protein adsorption in contact activation of blood factor XII." Biomaterials **28**: 4355-4369.

## Chapter 6

### **Contact activation of blood coagulation at low-fouling surfaces: poly(ethylene glycol)-grafted and zwitterion-terminated**

#### **6.1 Introduction**

A large number of blood-contacting medical devices are used in patients every year (Ratner 2000). However, a number of complications arising out of adverse blood-material interactions continue to be associated with the use of these devices (Ratner 2000). An unavoidable outcome of contact of blood with the surface of the devices is the activation of soluble blood proteins. These activated enzymes initiate reactions of the coagulation cascade greatly exacerbating the risk of coagulation and thrombosis in patients requiring the use of these devices (Lamba 2001). In addition, these activated enzymes are involved in a number of other physiological systems and therefore, may adversely perturb the complement system, immune response and fibrinolytic pathway while generating vasodilating agents causing hypotension (Colman 2001; Sainz 2007). Although large doses of anticoagulants are routinely administered to patients using these devices, it greatly increases the risk of hemorrhage and uncontrolled bleeding. Thus, there persists a need for improved hemocompatible materials for use in the next-generation of cardiovascular medical devices.

Contact of blood with a material surface can lead to thrombus formation via a combination of two pathways: the cellular pathway that involves the activation and aggregation of platelets and the humoral pathway involving the formation of a fibrin clot

from soluble plasma proteins (Lamba 2001). At a biomaterial surface, proteins like fibrinogen, vitronectin, thrombospondin and von Willebrand factor have been observed to activate platelets (Hanson 2004). Receptors on the platelet membrane recognize these adsorbed proteins triggering intracellular events of activation. The activated platelets aggregate to form a platelet plug and along with the fibrin mesh generate a thrombus. An embolized thrombus can lead to potentially fatal brain strokes, kidney infarcts and vascular occlusions.

A widely-attempted strategy in biomaterial surface science for blood-contacting applications is to engineer “low-fouling” surfaces, the underlying principle being that minimizing protein adsorption to surfaces will reduce platelet activation resulting in improved hemocompatibility for these materials (Lamba 2001). Even though principles of protein adsorption to surfaces remain poorly understood and its study highly contentious despite years of research in biomaterial surface science, one of the few trends that have emerged is that hydrophobic surfaces adsorb more protein than hydrophilic surfaces (Brash 1995; Hoffman 2004; Horbett 1993). With decreased protein adsorption one might generally expect decreased thrombosis due to reduced platelet activation, although platelet activation depends not only on the amount of protein adsorbed but also on the availability of exposed epitopes, which is determined by conformational changes upon adsorption (Horbett 2004). Therefore, increasing water-wettability of the surface offers a plausible route to reduced platelet activation towards improving hemocompatibility.

Hydrophilic surfaces tend to be stronger procoagulants than the hydrophobic surfaces. Our group has been investigating the molecular mechanism of contact

activation. Using an *in vitro* assay, we have observed that catalytic efficiency of a surface, a measure of the coagulation response of platelet-poor plasma (PPP) to the surface, scales with the water-wettability (a measure of surface energy) (Guo 2006; Zhuo 2005). Interestingly, we have also observed that it may be possible to engineer surfaces that exhibit deviations from this general trend. A surface with nanoscale chemical heterogeneity was found to exhibit an unexpectedly low catalytic efficiency, possibly arising out of changes in protein adsorption (Miller 2006).

Here, we report on the evaluation of the coagulation responses at “low-fouling” surfaces prepared using two common techniques to minimize protein adsorption. First, we consider the use of poly(ethylene glycol) (PEG) (Hoffman 2004). PEG chains are typically either grafted on a surface or incorporated within the polymer with the expectation that PEG enrichment at the surface will lead to resistance to protein adsorption. These flexible PEG chains are believed to strongly associate with water forming a hydrated “exclusion volume” that resists protein adsorption due to “entropic repulsion” (also referred to as “osmotic effect”) (Hoffman 2004; Lasic 1997). Use of PEG to minimize protein adsorption has been extensively studied using both experimental characterization and theoretical techniques. It has been shown that several factors including molecular weight or length of the PEG molecules, grafting density and temperature affect resistance to protein adsorption (Ivanchemko 1995; Sofia 1997). Despite many successes, PEG modification suffers from certain limitations. PEG chains are prone to easy degradation, especially in the presence of oxygen and transition metal ions that are typical constituents of biological fluids (Ostuni 2001; Shen 2002). Further, PEG brushes are reportedly less effective in resisting protein adsorption at physiological

temperature (37°C) than at 25°C (Leckband 1999) and therefore may not be suited for long-term use in vivo.

An alternate strategy to minimize protein adsorption is the use of zwitterionic functional groups on the surface that purportedly mimic the chemical structure of cell membranes (Chen 2005; Lewis 2000). The zwitterionic groups are also believed to strongly associate with water and therefore reduce protein adsorption by resisting surface dehydration (Lamba 2001).

In this study, we have evaluated the propensity of PEG-grafted and zwitterions-terminated surfaces to induce blood coagulation. Although both surfaces were observed to be poor protein adsorbents, as expected, they exhibited vastly different coagulation responses.

## **6.2 Materials and methods**

### **6.2.1 Plasma and proteins**

Plasma preparation and storage was performed following previous procedures (Chatterjee 2006; Guo 2006). Anticoagulated salvaged human plasma was obtained from The Pennsylvania State University Milton S. Hershey Medical Center's Blood Bank. Plasma was pooled from multiple units (five units for the work described herein), centrifuged at 500 X g for 10 min at 35°C and the resulting plasma supernatant was stored at -20°C in polypropylene tubes (17 X 100 mm, VWR). Prior to use in assays,



plasma was thawed for ~ 40 min in a 37°C waterbath, and centrifuged as described above to generate platelet poor plasma (PPP).

Human coagulation FXIIa (66 PEU/mg) was obtained commercially (Enzyme Research Laboratories, South Bend, IN). Upon receipt, the enzyme was distributed into aliquots and stored at -80°C. Prior to use, FXIIa was thawed in a 37°C water-bath and diluted with phosphate buffered saline (PBS, pH 7.4, Sigma-Aldrich, St. Louis, MO) to desired concentration based on the supplier-provided value.

### **6.2.2 Preparation of test surfaces**

In our previous studies on material-induced coagulation we have prepared model surfaces using glass particles of 425-600 µm diameter (Chatterjee 2006; Guo 2006; Miller 2006; Zhuo 2005). However, in order to utilize the experimental design for depletion studies to measure protein adsorption to these surfaces, here we prepared model surfaces using glass particles < 106 µm diameter (nominal diameter = 80 µm, Sigma-Aldrich, St. Louis, MO). These smaller particles have a larger specific surface area and thereby provide more reliable measurements for the amounts of adsorbed protein in the depletion experiments, as described below.

The as-received glass particles were rinsed using fresh chloroform (Sigma-Aldrich, St. Louis, MO) in an ultrasonic water bath for at least 15 min. After drying the particles were placed in a glow-discharge cleaner operated at 100W for at least 30 min. The cleaned particles were silanized (all silanes were obtained from Gelest Inc., Morrisville, PA) with 3-aminopropyltriethoxysilane (APS), butyltrichlorosilane (BTS), 2-

carbomethylethoxytrichlorosilane (CMETS), n-(trimethoxysilylpropyl)ethylenediamine triacetic acid, trisodium (ZWITS), or methoxy(polyethyleneoxy)propyltrimethoxysilane (PEGS).

APS, CMETS and BTS treatments were performed using procedures described previously (Chatterjee 2006; Guo 2006; Miller 2006). Briefly, glow-discharge treated particles were incubated for 5 min in a solution of 2% (v/v) APS in acetone (Sigma-Aldrich) in a glass petri dish. The APS solution was aspirated and the particles were rinsed in fresh chloroform for 15 min and air-dried. For CMETS modification, the above procedure was repeated except that we used 2% (v/v) CMETS in ethanol for 10 min. The terminal ester groups of the CMETS molecules on the particles were converted to carboxylic acid groups (designated herein as COOH surface) by incubations in 1 M NaOH (Sigma-Aldrich) followed by 0.1 N H<sub>2</sub>SO<sub>4</sub> (VWR) for 10 minutes each, with a water rinse between the two steps. For BTS modification, the glow-discharge treated particles were incubated for 75 min in a solution of 5% (v/v) BTS in chloroform. The particles were washed in fresh chloroform and dried in air, as above.

For PEGS treatment (structure shown in Figure 6-1), we followed published procedures for modification of surface of silicon wafers (Papra 2001). The glow-discharge treated particles were incubated in a solution of 3 mM PEG in toluene (Sigma-Aldrich) containing 0.8 mL HCl / L for 18 hr at room temperature. The silanized particles were rinsed serially in fresh toluene and ethanol (VWR), and finally air-dried. To prepare the ZWITS surfaces (structure shown in Figure 6-1), we followed published procedures (Colic 1998). Here, the glow-discharge treated particles were incubated in a

solution of 1% (v/v) ZWITS in 18 M $\Omega$  water (Millipore Simplicity 185 units) water for 24 hr following which the particles were rinsed in fresh water and air-dried.

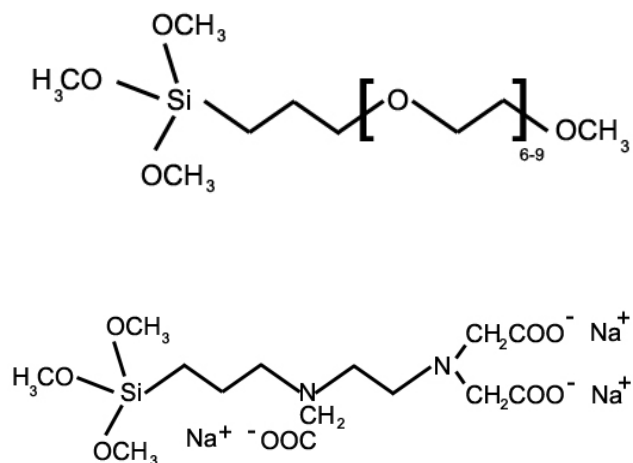


Figure 6-1: Chemical structure of methoxy(polyethyleneoxy)propyltrimethoxysilane (PEGS, top) and n-(trimethoxysilylpropyl)ethylenediamine triacetic acid, trisodium (ZWITS, bottom).

Water-wettability for the different silanized surfaces was measured on 12 mm diameter glass coverslip witness samples (VWR). Contact angles on the dried sample surfaces were measured by the horizontal sessile drop method using a Krüss goniometer using 18 M $\Omega$  water as the probe liquid.

### **6.2.3 In vitro coagulation assay**

An in vitro coagulation assay was used to measure the coagulation response of each of the model surfaces prepared by silanization of glass particles. The assay measured the coagulation response in terms of a coagulation time (CT), defined as the time required from activation of the intrinsic pathway of the coagulation cascade to the appearance of a visible clot, initiated by a known dose of either exogenous enzyme (FXIIa concentration) or surface area of solid procoagulants (calculated from measured weight). The assay has been described previously (Chatterjee 2006; Guo 2006) (Zhuo 2005). Briefly, 0.5 mL of PPP was mixed with 0.1 mL of 0.1 M calcium chloride (CaCl<sub>2</sub>, Sigma-Aldrich) and a known dose of procoagulants in a 5 mL polystyrene vial (12 mm X 75 mm, VWR). The volume was adjusted by adding 0.01 M phosphate-buffered-saline (PBS, pH 7.4, Sigma-Aldrich) to obtain a 1 mL solution resulting in a 1:1 dilution of plasma in buffer. The order in which reagents and solid materials were added was varied depending on the type of assay, with recalcification of plasma always occurring last to ensure a common zero time CT. Assay vials were capped with parafilm, rotated at 8 rpm on a hematology mixer and the corresponding CT was recorded. CT for each dose was measured for at least three individual assays.

### **6.2.4 Mathematical modeling**

A previously-developed mathematical model was used to quantify the measured coagulation responses (Guo 2006) (see **A.1** and **A.2** for a summary of relevant equations). To model the plasma coagulation response to an exogenous dose of FXIIa, the

coagulation cascade is divided into three compartments: an input dose (exogenous FXIIa), the gray box (containing the intermediate steps) and the output response (the formation of the fibrin clot). The analytical relationship derived from a Michaelis-Menten-like scheme was fit to experimental CT values at different values of FXIIa using three adjustable parameters. Coagulation response of PPP induced by a solid procoagulant was modeled as a two-step process: (i) the generation of FXIIa from endogenous FXII where the amount of enzyme activated scales with the catalytic potential of the surface and (ii) the processing of this procoagulant-generated FXIIa through the gray box to form a clot (determined from exogenous FXIIa data). The values of the parameters were obtained by statistical non-linear least-squares fit using the commercial Sigmaplot<sup>®</sup> 8 (Systat Software Inc., Point Richmond, CA).

### **6.2.5 Protein adsorption measurements**

Protein adsorption to these silanized surfaces was measured using solution-depletion method implementing SDS gel electrophoresis and has been detailed previously (Noh 2006a; Noh 2006b). A “concentration-titration” is performed where a fixed surface area of the solid surfaces is exposed to a series of protein solutions of increasing concentration. 50  $\mu\text{g}$  of silanized glass beads were incubated for 1 hr in 30  $\mu\text{L}$  solutions of human serum albumin (HSA, Sigma-Aldrich) prepared in PBS. Aliquots from the supernate removed to determine change in protein concentration in solution.

26-lane NuPAGE Novex Tris-Actetate pre-cast gels (Invitrogen, Carlsbad, CA) were used for protein quantification. Electrophoresis was performed at 150 V for 1 hr

using Xcell SureLock Mini-Cell (Invitrogen). Gels were stained using Simply-Blue-Stain-Safe (Invitrogen) for 1 hr and subsequently destained with 18 M $\Omega$  water. Band intensity was determined by measuring the optical density using a Gel-doc system (Bio-Rad Laboratories, Hercules, CA). For each gel, a standard curve was generated by reserving 8 lanes for solutions of known concentration of the same protein.

### **6.3 Results**

The objective of this study was to evaluate the coagulation response of protein-resistant surfaces prepared using two commonly employed surface modification strategies—grafting of PEG chains and use of zwitterionic terminal groups. These low-fouling surfaces were prepared along with a series of model solid procoagulants that span a wide range of water-wettability with well-characterized coagulation responses.

#### **6.3.1 Water-wettability of test surfaces**

Sessile drop water contact angles were measured on witness samples for each of the prepared surfaces, as listed in Table 6-1. Hydrophilic nature of clean glass and COOH surfaces was indicated by the low angles ( $< 5^\circ$ ), while BTS was strongly hydrophobic ( $93^\circ$ ) with APS exhibiting an intermediate surface water-wettability ( $63^\circ$ ), consistent with previous results. Water contact angle of  $32^\circ$  on PEGS was similar to the value of  $34^\circ$  measured by Papra et al (Papra 2001). While Colic et al did not report water

contact angle for their surfaces, the ZWITS surfaces we prepared were highly hydrophilic ( $< 5^\circ$ ).

Table 6-1: Surface water-wettability and values of  $K_I$  for the test surfaces

Procoagulant Surface	Sessile Drop Water Contact Angle	$K_I$ ( $\mu\text{M}/\text{min}$ )
PEGS	$32^\circ \pm 1^\circ$	$(3.4 \pm 1.6) \times 10^{-2}$
BTS	$92^\circ \pm 2^\circ$	$(3.8 \pm 1.7) \times 10^{-2}$
APS	$62^\circ \pm 3^\circ$	$(1.0 \pm 0.1) \times 10^{-1}$
ZWITS	$< 5^\circ$	$1.1 \pm 0.6$
COOH	$< 5^\circ$	$1.5 \pm 0.6$
Glass	$< 5^\circ$	$2.3 \pm 0.7$

Values are displayed as mean  $\pm$  S.D.

### 6.3.2 Protein adsorption studies

Noh and Vogler have previously demonstrated that protein adsorption can be reliably measured using the gel electrophoresis system we have applied here (Noh 2006b). They have reported results for the glass, APS and octadecyltrichlorosilane (OTS, similar to BTS) surfaces (Noh 2006a). We performed preliminary measurements for the other surfaces— COOH, ZWITS and PEGS— not previously investigated. Preliminary experiments (data not shown) measuring adsorption of HSA to these hydrophilic surfaces (COOH, ZWITS and PEGS) did not indicate any measurable depletion in protein from

adsorption consistent with previous trends for surfaces exhibiting contact angles  $< 65^\circ$  (or water adhesion tension  $> 30$  dynes/cm).

### 6.3.3 Titration of exogenous FXIIa

Coagulation time (CT) in response to a series of exogenous FXIIa enzyme dose is plotted in Figure 6-2. Consistent with previous observations (Chatterjee 2006; Guo 2006), the measured response is sigmoidal in nature. The solid line in the figure denotes fit of the mathematical model to the measured data. The values of model parameters  $a$ ,  $b$  and  $c$  are listed in Table 6-2. The combination of these 3 parameters ( $a$ ,  $b$  and  $c$ ) can be used to describe how a dose of FXIIa is processed by the gray box to generate the fibrin clot. The model parameters  $b$  and  $c$  in particular account for the background response induced by the wall of the polystyrene vial, remnant platelets, etc.

Table 6-2: Parameters describing processing of FXIIa dose in PPP as generated by best fit of the measured CT response to a mathematical model.

$a$ (min)	$b \times 10^{-2}$ ( $\mu\text{M min}$ )	$c \times 10^{-4}$ ( $\mu\text{M}$ )
$6.7 \pm 2.2$	$1.3 \pm 0.3$	$2.7 \pm 0.8$

Values are displayed as mean  $\pm$  S.D.



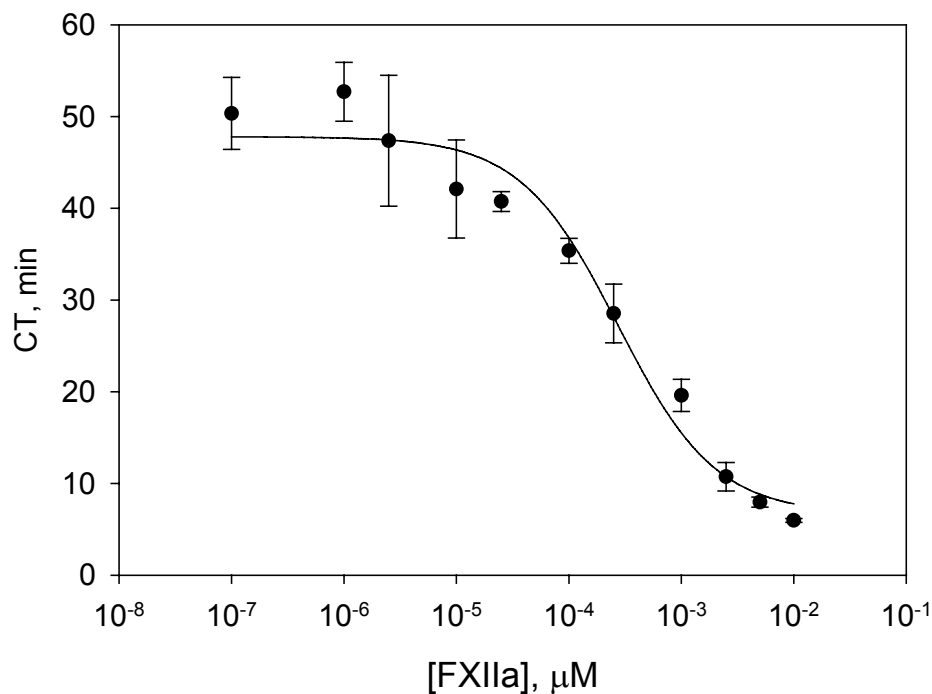


Figure 6-2: FXIIa titration in platelet poor plasma (PPP) showing experimental coagulation time (CT) values vs. concentration of exogenous FXIIa. The smooth curve shows the best fit of a mathematical model to the data. (All data shown as mean  $\pm$  S.D. for  $n \geq 3$ ).

### 6.3.4 Surface area titration of model surfaces

Surface-area-titration (SAT) plots were generated from measurement of coagulation response to a series of surface area values for each solid procoagulant, as plotted in Figure 6-3. A mere qualitative assessment of the data indicates that glass, COOH and ZWITS surfaces are strong procoagulants demonstrated by the short CT values for a given surface area. Longer CT measured for equivalent surface area of APS indicates that APS is a relatively weak procoagulant. Further, the longest CT measured

for equivalent surface area of BTS and PEGS indicate that these surfaces are the weakest procoagulants among the test surfaces evaluated here.

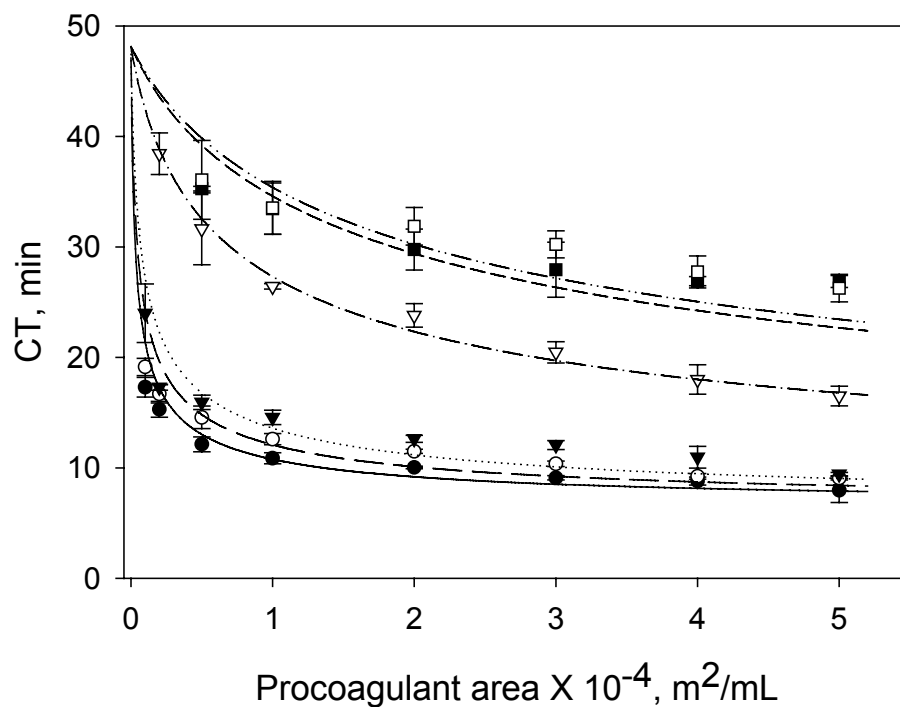


Figure 6-3: Surface area titration (SAT) in PPP showing experimental CT vs. surface area of different solid procoagulants. Measured data for clean-glass particles (solid circles ●), COOH particles (open circles ○), ZWITS particles (closed triangles ▼), APS particles (open triangles ▽), BTS particles (solid squares ■) and PEGS particles (open squares □) are shown along with the smooth lines representing the best fit to a mathematical model for material-induced coagulation. (All data shown as mean  $\pm$  S.D. for  $n \geq 3$ )

Using the gray box parameters ( $a$ ,  $b$  and  $c$ ) determined from the FXIIa titration plot (Figure 6-2, Table 6-2) the mathematical model for material-induced plasma coagulation was solved for an unknown parameter  $K_I$ .  $K_I$  scales linearly with the

“catalytic efficiency” of the solid procoagulant and is essentially a quantitative measure of the coagulation response when plasma contacts the test surface (Guo 2006). Table 6-1 lists the  $K_I$  values with the water contact-angle for each test surface. Glass, COOH and ZWITS surfaces exhibit similarly high catalytic efficiency and are potent activators of the coagulation cascade. The catalytic efficiency of APS is about an order of magnitude less than that for the three strongest procoagulants (glass, COOH, ZWITS), whereas BTS and PEGS surfaces are the weakest procoagulants with catalytic efficiencies nearly two orders of magnitude smaller than for the strongest activators.

#### **6.4 Discussion**

Low-fouling surfaces exhibiting low protein adsorption have immense potential for applications in diverse fields like biology, medicine, food processing, biosensing, microfluidics, etc. As a result different strategies have evolved to engineer such surfaces. Two common strategies investigated here are the use of PEG chains and zwitterions. Some of these have also been tested for blood-contacting applications. Development of blood-contacting surfaces is complicated by the fact that a combination of different mechanisms determines the biological response and each pathway is independently influenced by surface properties. While these low-fouling surfaces have been shown to reduce platelet activation by minimizing the amount of adsorbed proteins (Hoffman 2004; Lamba 2001), it is unclear how these surfaces influence the plasma coagulation cascade. Therefore, in this study we investigated the response of the two low-fouling

surfaces for their propensity to activate the intrinsic coagulation cascade for prospective blood-contacting application.

We prepared model PEG-grafted and zwitterion-terminated surfaces by treating glass particles with commercially-available silanes following procedures previously reported in literature. Preliminary studies measuring adsorption of HSA and Fib reported above confirmed that the ZWITS and PEGS surfaces prepared were indeed poor adsorbents. We assayed the coagulation response in vitro to recalcified PPP by measuring the time for the formation of a fibrin clot. The measured data were further quantified using a model and clearly indicated that while PEGS was a weak procoagulant, ZWITS surface was a strong procoagulant like glass. Our results seem to suggest that the PEG-modified surface may be better suited in blood-contacting applications than zwitterion-terminated surface.

It is important to note that we have evaluated only two specific silane-based molecules for our studies. Since different factors influence protein adsorption events, we cannot eliminate the possibility that using different modification conditions could potentially affect the response. In particular, molecular weight and grafting density of PEG has profound influence on its ability to resist protein adsorption, as does the derivatization of PEG. Similarly, the chemistry of zwitterions used for surface modification could influence the protein adsorption and the coagulation response.

In this regard it is noteworthy to report that we also measured the coagulation response after modification with PEG using triethylamine (TEA) as catalyst (Choi 2006). The measured response (data not shown) was similar to that presented in Figure 6-3, wherein HCl was used as the catalyst. However, when we incubated the clean glass

particles in PEGS solution in the absence of HCl, it was found to be a stronger procoagulant (data not shown) similar to the response of APS but slower than for clean glass. It is perhaps not surprising since in the absence of a catalyst the PEGS was perhaps only physically associated with the surface and not chemically linked.

For the case of ZWITS surfaces, we have used a commercially-available silane that presents zwitterions on the surfaces, but these groups are chemically different from those of phosphorylcholine-based zwitterions that are more commonly applied in biomaterial surface science (Lamba 2001).

Nevertheless, these results underscore the need to develop a comprehensive understanding of the mechanisms involved in protein adsorption at these different surfaces for prospective use in blood-contacting applications.

## 6.5 Conclusions

In summary, we have evaluated the coagulation response of two model low-fouling surfaces and observed that while both surfaces exhibit lower protein adsorption, the coagulation response is vastly different. PEG-modified surface was observed to be a significantly weaker procoagulant than surfaces terminated with zwitterions.

## 6.6 Literature citations

Brash, J. L. and T. A. Horbett (1995). Proteins at interfaces: an overview. Proteins at interfaces II: fundamentals and applications. J. L. Brash and T. A. Horbett. Washington DC, American Chemical Society: 1-23.

- Chatterjee, K., E. A. Vogler and C. A. Siedlecki (2006). "Procoagulant activity of surface-immobilized Hageman factor." Biomaterials **27**: 5643-5650.
- Chen, S., J. Zheng, L. Li and S. Jiang (2005). "Strong resistance of phosphorylcholine self-assembled monolayers to protein adsorption: insights into non-fouling properties of zwitterionic surfaces." Journal of the American Chemical Society **127**: 14473-14478.
- Choi, I., S. K. Kang, J. Lee, Y. Kim and J. Yi (2006). "In situ observation of biomolecules patterned on a PEG-modified Si surface by scanning probe lithography." Biomaterials **27**: 4655-60.
- Colic, M., A. Chien and D. Morse (1998). "Synergistic application of chemical and electromagnetic water treatment in corrosion and scale prevention." Croatica Chemica Acta **71**: 905-916.
- Colman, R. W. (2001). Contact activation pathway: inflammatory, fibrinolytic, anticoagulant, antiadhesive, and antiangiogenic activities. Hemostasis and Thrombosis- Basic Principles and Clinical Practice. R. W. Colman, J. Hirsh, V. J. Marder, A. W. Clowes and J. N. George. Philadelphia, Lippincott William and William. **4**: 103-122.
- Guo, Z., K. M. Bussard, K. Chatterjee, R. Miller, E. A. Vogler and C. A. Siedlecki (2006). "Mathematical modeling of material-induced blood plasma coagulation." Biomaterials **27**: 796-806.
- Hanson, S. R. (2004). Blood coagulation and blood-material interactions. Biomaterials science: an introduction to materials in medicine. B. D. Ratner, A. S. Hoffman, F. J. Schoen and J. E. Lemons. San Diego, Elsevier Science: 332-338.
- Hoffman, A. S. and B. D. Ratner (2004). Nonfouling surfaces. Biomaterials science: an introduction to materials in medicine. B. D. Ratner, A. S. Hoffman, F. J. Schoen and J. E. Lemons. San Diego, Elsevier Science: 197-201.
- Horbett, T. A. (1993). "Principles underlying the role of adsorbed plasma proteins in blood proteins in blood interactions with foreign materials." Cardiovascular Pathology **2**: 137S-148S.
- Horbett, T. A. (2004). The role of adsorbed proteins in tissue response to biomaterials. Biomaterials science: an introduction to materials in medicine. B. D. Ratner, A. S. Hoffman, F. J. Schoen and J. E. Lemons. San Diego, Elsevier Science: 237-246.
- Ivanchemko, M. I., E. A. Kulik and Y. Ikada (1995). Serum protein adsorption and platelet adhesion to polyurethane grafted with methoxypoly(ethylene glycol) methacrylate polymers. Proteins at interfaces II: fundamentals and applications. J.

- L. Brash and T. A. Horbett. Washington DC, American Chemical Society: 463-477.
- Lamba, N. M. K. and S. L. Cooper (2001). Interaction of blood with artificial surfaces. Hemostasis and Thrombosis- Basic Principles and Clinical Practice. R. W. Colman, J. Hirsh, V. J. Marder, A. W. Clowes and J. N. George. Philadelphia, Lippincott William and William. **4**: 661-672.
- Lasic, D. D. (1997). The conformation of polymers at interfaces. Poly(ethylene glycol) chemistry and biological applications. J. M. Harris and S. Zalipsky. Washington DC, American Chemical Society: 31-44.
- Leckband, D., S. Sheth and A. Halperin (1999). "Grafted poly(ethylene oxide) brushes as nonfouling surface coatings." Journal of Biomaterials Science, Polymer Edition **10**: 1125-47.
- Lewis, A. L. (2000). "Phosphorylcholine-based polymers and their use in the prevention of biofouling." Colloids and Surfaces B: Biointerfaces **18**: 261-275.
- Miller, R., Z. Guo, E. A. Vogler and C. A. Siedlecki (2006). "Plasma coagulation response to surfaces with nanoscale chemical heterogeneity." Biomaterials **27**: 208-215.
- Noh, H. and E. A. Vogler (2006a). "Volumetric interpretation of protein adsorption: mass and energy balance for albumin adsorption to particulate adsorbents with incrementally increasing hydrophilicity." Biomaterials **27**: 5801-12.
- Noh, H. and E. A. Vogler (2006b). "Volumetric interpretation of protein adsorption: Partition coefficients, interphase volumes, and free energies of adsorption to hydrophobic surfaces." Biomaterials **27**: 5780-93.
- Ostuni, E., R. G. Chapman, R. E. Holmihl, S. Takayama and G. M. Whitesides (2001). "A survey of structure-property relationships of surfaces that resist the adsorption of protein." Langmuir **17**: 5605-5620.
- Papra, A., N. Gadegaard and N. B. Larsen (2001). "Characterization of ultrathin poly(ethylene glycol) monolayers on silicon substrates." Langmuir **17**: 1457-1460.
- Ratner, B. D. (2000). "Blood compatibility- a perspective." Journal of Biomaterials Science: Polymer edition **11**: 1107-1119.
- Sainz, I. M., R. A. Pixley and R. W. Colman (2007). "Fifty years of research on the plasma kallikrein-kinin system: From protein structure and function to cell biology and in-vivo pathophysiology." Thrombosis and Haemostasis **98**: 77-83.

- Shen, M., L. Martinson, M. S. Wagner, D. G. Castner, B. D. Ratner and T. A. Horbett (2002). "PEO-like plasma polymerized tetraglyme surface interactions with leukocytes and proteins: in vitro and in vivo studies." Journal of Biomaterials Science, Polymer Edition **13**: 367-90.
- Sofia, S. J. and E. W. Merrill (1997). Protein adsorption on poly(ethylene oxide)-grafted silicon surfaces. Poly(ethylene glycol) chemistry and biological applications. J. M. Harris and S. Zalipsky. Washington DC, American Chemical Society: 342-360.
- Zhuo, R., R. Miller, K. M. Bussard, C. A. Siedlecki and E. A. Vogler (2005). "Procoagulant stimulus processing by the intrinsic pathway of blood plasma coagulation." Biomaterials **26**: 2965-2973.



## **Chapter 7**

### **Summary**

In order to develop improved blood-compatible materials for use in the next generation of blood-contacting medical devices, it is essential to understand the molecular basis of hemocompatibility and in particular the role of the surface in influencing these observed biological responses.

Contact of blood with material surfaces leads to activation of plasma proteins that influence many different physiological pathways in patients requiring the use of cardiovascular medical devices. Coagulation and thrombosis arising out of these adverse blood-material interactions are amongst the most significant threats to patient health.

Two different pathways— activation of intrinsic coagulation cascade and activation/adhesion/aggregation of platelets— are involved in the formation of thrombi in vivo during material-induced coagulation and thrombosis. However, each of these pathways is complex and the underlying molecular mechanisms vastly different. We have focused here on the activation of the intrinsic coagulation cascade by studying material-induced coagulation in platelet-poor-plasma (PPP) system, thereby eliminating the contributions of the platelet pathway. This reductionist approach has enabled us to successfully investigate the phenomenon of material-induced coagulation, which is incredibly complex even in the absence of platelets. Preliminary studies (C.1) demonstrate that results from our studies in PPP could be eventually extended to a more complex system of whole blood.

The widely-accepted conventional molecular mechanism for activation of the intrinsic coagulation cascade at a material surface suggests that activation is specific to anionic hydrophilic surfaces. Formation of contact activation complexes by direct binding of select plasma proteins to the negatively-charged groups on the surface causes initiation of the coagulation cascade. Such a proposed scheme is in sharp contradiction to known theories in protein adsorption to material surfaces, as discussed in **1.4**. Further, this scheme which essentially implies that surfaces lacking the anionic groups are “benign” fails to explain how all surfaces are eventually procoagulant, some (typically hydrophobic) are merely weaker than others (typically hydrophilic). In sharp contrast to the traditional biochemistry, we hypothesized that protein adsorption at the material surface plays an important role in contact activation reactions (see **1.4**).

In our initial studies (**2.1**), we assayed coagulation response in PPP and factor XII (FXII)-deficient PPP ( $d_{XII}PPP$ ) to activated FXII (FXIIa) on different test surfaces. In sharp contrast to the traditional theory, we observed that enzymatic activity of FXIIa was incredibly similar irrespective of the nature of solid surface. Specifically, the presence of an anionic hydrophilic surface was not essential for propagation of the coagulation cascade indicating that the role of the surface was only limited to generation of a bolus of FXIIa and not in subsequent events. Having demonstrated that surface was not a cofactor in the enzymatic activity of FXIIa, in studies thereafter, we focused on role of the surface in the molecular events at the surface that lead to the activation of enzymes.

Investigating the different pathways that contribute to the generation of FXIIa, we assayed the coagulation response of test surfaces spanning a wide spectrum of observable water-wettability (surface energy) in prekallikrein (PK)-deficient PPP ( $d_{PK}PPP$ ) and in

PK-reconstituted  $d_{PK}PPP$  ( $Rd_{PK}PPP$ , equivalent to PPP) (see **3.1**). Quantifying the amounts of enzyme production using a previously-developed phenomenological model (**A.1**, **A.2**), we observed that kallikrein (Kal)-mediated reciprocal-activation was the principal pathway of enzyme production at all test surfaces. Surface-mediated autoactivation of FXII was the other contributing pathway of FXII activation at material surfaces in plasma. The amount of enzyme generated in total and along individual pathways was observed to scale with water-wettability. However, enzyme generation per unit area in total or along any given pathway for a specific test surface was nearly constant indicating that the role of the surface was limited to the generation of only an initial bolus of FXIIa via autoactivation and the surface was not involved in subsequent events.

In **4.1**, we investigated the role of the surface water-wettability of reactions of reciprocal-activation, which we had observed to be the principal pathway of enzyme generation at material surface in plasma. Our group had previously reported nearly equal levels of autoactivation of FXII in neat solutions at hydrophilic and hydrophobic surfaces (see **4.1** for discussion and references). Measuring the rate of FXIIa-mediated PK→Kal hydrolysis at test hydrophobic and hydrophilic surfaces using a chromogenic substrate, we observed that adsorbed FXIIa molecules generated via autoactivation at hydrophobic surfaces were unable to cleave PK. At hydrophilic surfaces, FXIIa generated by autoactivation were not adsorbed and solution-phase FXIIa-mediated PK hydrolysis could occur. Competitive displacement of adsorbed FXIIa from the hydrophobic surface using albumin lead to a rapid increase in Kal generation. These results led to a new proposed scheme of reactions involving PK and FXII at the surface (**4.4.4**). FXIIa

generation is proposed to occur in close vicinity of a solid surface, not limited to anionic hydrophilic surface. Reciprocal-activation reactions do not appear to occur by the assembly of molecules at the surface.

In **5.1**, we investigated FXIIa-mediated factor XI (FXI) hydrolysis at test hydrophilic and hydrophobic surfaces using a FXIa-chromogenic substrate. Spontaneous FXI hydrolysis by FXIIa generated via autoactivation was measured at hydrophilic surfaces. In contrast, adsorbed FXIIa molecules at hydrophobic surfaces were unable participate in solution-phase FXI activation. When the adsorbed enzyme molecules were displaced from the hydrophobic surfaces by competitive desorption using albumin, increased yield of FXIa was observed. These results led to a modified scheme of reactions involving FXII and FXI at the material surface (**5.4**). FXII autoactivation was proposed to occur in vicinal to the activating surface, whereas FXI hydrolysis by FXIIa is does not occur by direct binding to the surface.

The proposed schemes based on results from the two studies on reciprocal-activation (**4.4.4**) and FXI hydrolysis (**5.4**) may be combined as shown in Figure **7-1** that schematically presents a modified sequence of surface-mediated molecular events in contact activation of material-induced blood-plasma coagulation. In this scheme, contact activation is initiated by autoactivation of FXII in close vicinity to a material surface and is not limited to anionic hydrophilic surface. Additional amounts of FXIIa are generated by solution-phase reciprocal-activation reactions that do not occur by the assembly/binding of the molecules on the surface. Further, solution-phase FXIIa-mediated FXI hydrolysis also does not occur by the assembly/binding of these proteins on the surface. In fact, adsorption (or “binding” as suggested by the traditional theory) to

the activating surface attenuates these reactions so that hydrophobic surfaces being adsorbent are inhibitory to these reactions leading to an *apparent specificity* at hydrophilic surfaces for contact activation reactions due to protein adsorption events.

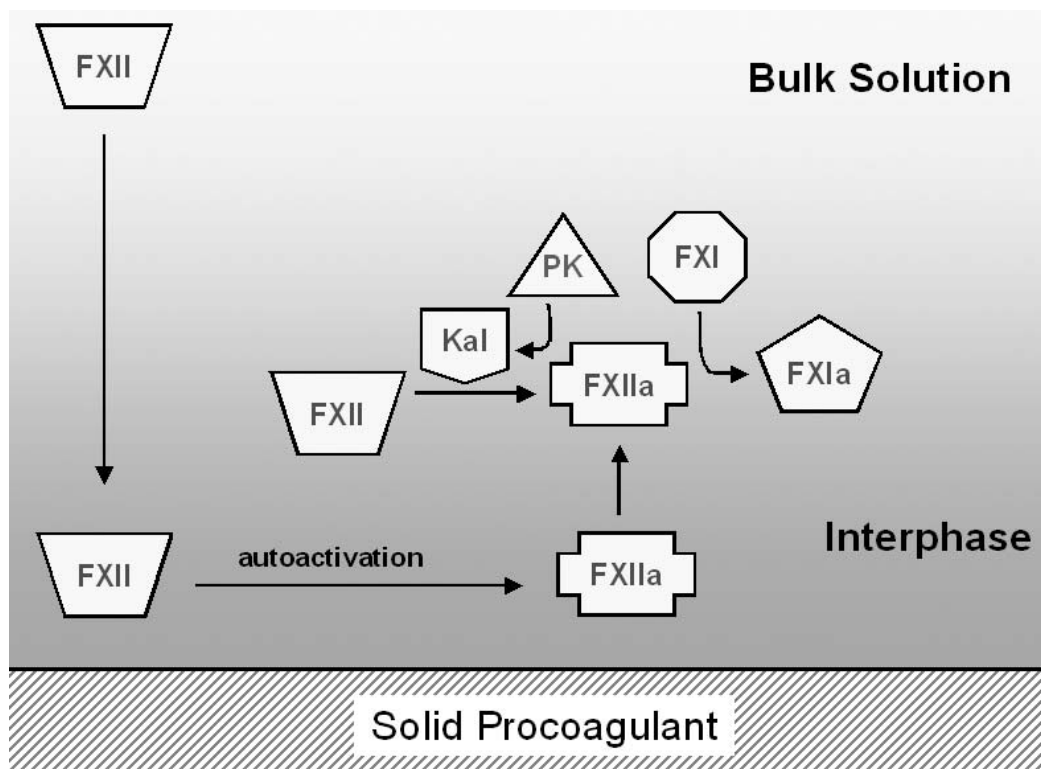


Figure 7-1: Proposed sequence of events for contact activation of blood-plasma coagulation at material surfaces. Contact activation is initiated by autoactivation of FXII at the interphase and is not specific to anionic surfaces. Subsequent reactions involving reciprocal-activation and FXI hydrolysis do not occur by direct assembly on the surface but rather require displacement from the surface.

Taken together with results of 3.5, it becomes apparent why enzyme generation by autoactivation and reciprocal-activation pathways at material surfaces in plasma scale with surface energy. In the presence of other plasma proteins many such as albumin are

present at a significantly higher concentration, adsorption to hydrophobic surface leads reduced autoactivation possibly arising out of reduced contact of FXII with the surface but not so at hydrophilic surfaces. Further, this smaller amount of FXIIa generated at adsorbent hydrophobic surfaces is not efficiently amplified by reciprocal-activation. Therefore, the total amount of enzyme available for FXI hydrolysis necessary for propagation of the cascade is much lower at hydrophobic surfaces than at hydrophilic surfaces, a response largely influenced by protein adsorption. In other words, contact activation is not merely due to biochemical specificity arising from the anionic groups on the surface. It appears that surface chemistry/charge influences surface energy that affects protein adsorption (supporting evidence in **B.3**) that influences contact activation.

Furthermore, the modified sequence of events also explains why both hydrophobic and hydrophilic materials are ultimately procoagulant, a major shortcoming of conventional biochemical scheme.

Since protein adsorption was found to be a key determinant in contact activation, we investigated two commonly-used strategies in biomaterial surfaces science to minimize adsorption to surfaces (**6.1**). Interestingly, we observed test surfaces prepared by either grafting of poly(ethylene glycol) chains or use of zwitterions were poor adsorbents, but the former surfaces were significantly poor adsorbents than the latter. These results highlight the need for careful consideration of surface-modification for biomaterial surfaces in blood-contacting applications.

In summary, our studies demonstrate a need to incorporate protein-adsorption competition at procoagulant surfaces into the mechanism of contact activation to account

for the observed moderation of FXII activation by blood proteins unrelated to the plasma coagulation cascade.

## Appendix A

### Mathematical model for material-induced coagulation

Our group has previously developed a “gray-box” model for quantitative study of material-induced plasma coagulation. The underlying theory for this model is published (Guo 2006) and this appendix summarizes the relevant sections used for analysis in this thesis.

Material-induced coagulation is modeled as a two-step process— activation of endogenous plasma FXII by the surface, which then serves as an input dose to a “gray box” (containing all intermediate steps) that in turn processes the FXIIa dose to produce the output clot.

#### A.1 Quantitative analysis of coagulation response to exogenous FXIIa

The processing of an exogenous dose of FXIIa by the intrinsic coagulation cascade consisting of numerous individual enzyme activation steps can be modeled by abstracting the coagulation cascade into three compartments— an “input” dose of FXIIa, a “gray box” containing all the intermediate steps, and the “output” fibrin clot. This model may be schematically expressed in Eq. A.1 and Eq. A.2 where  $FXIIa$  is the dose of exogenous enzyme,  $GB$  is the substrate (gray box),  $P$  is the product (clot), and  $(FXIIa.GB)$  is the intermediate enzyme-substrate complex.  $K_F$  is the dissociation constant whereas  $k_l$  and  $k_b$  represent reaction rate constants. Eq. A.1 represents the



processing of an exogenous enzyme dose, while Eq. **A.2** represents the background clot production induced by the walls of the tube, remnant platelets and other unknown pathways.



The reaction in scheme Eq. **A.1** may be modeled using a modified version of Michaelis-Menten equation for enzyme kinetics. Solving this equation concurrently with the equation for the background response, leads to a simple parametric equation Eq. **A.3** where  $a$ ,  $b$  and  $c$  are constants that can be determined from the least-squares fit of the model to the data when Eq. **A.3** is applied to measured experimental data.

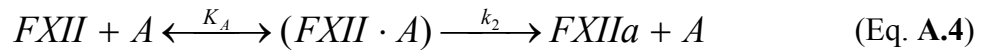
$$CT = \frac{a \cdot [FXIIa] + b}{[FXIIa] + c} \quad (\text{Eq. A.3})$$

## **A.2 Quantitative analysis of material-induced coagulation**

Since experimental data indicated that the addition of the solid procoagulants did not appear to affect the properties of the gray box (Guo 2006), the model for the solid procoagulant-induced plasma coagulation is essentially a two-step process— generation

of FXIIa from endogenous FXII at the surface and its subsequent processing by the gray box similar to the processing of an exogenous FXIIa dose.

The phenomena of autoactivation of FXII by the solid surface and reciprocal-activation by kallikrein and the surface (assuming the system has an abundance of kallikrein for reciprocal-activation) are expressed as Eq. A.4, whereas Eq. A.5 describes autohydrolysis (or self-amplification). In Eqs. A.3 and A.4,  $A$  is the solid procoagulant surface area.  $K_A$  and  $K_{A1}$  denote dissociation constants and  $k_i$  is a reaction rate constant.



The kinetics for the schemes Eq. A.4 and Eq. A.5 can be modeled using a modified version of the Michaelis-Menten kinetics, where the added solid procoagulant surface area is the “effective” enzyme concentration. If only autoactivation and reciprocal-activation (Eq. A.4) are the major FXII activation pathways then FXIIa production may be expressed by Eq. A.6. If, however, only autohydrolysis (or self-amplification, Eq. A.5) is the major FXII activation pathway then, FXIIa production may be expressed by Eq. A.7, where  $K_S$  and  $K_{S1}$  are Michaelis-like constants and  $A$  is the amount of added solid procoagulant ( $\text{m}^2/\text{mL}$ ).

$$\frac{d[FXIIa]}{dt} = \frac{k_2 \cdot [FXII] \cdot A}{K_S + A} \quad (\text{Eq. A.6})$$

$$\frac{d[FXIIa]}{dt} = k_3 \cdot [FXIIa] \cdot \frac{(FXII \cdot A)}{(FXII \cdot A) + K_{S1}} \quad (\text{Eq. A.7})$$

If all three pathways (both reactions Eq. A.6 and Eq. A.7) contribute significantly to FXII activation, then FXIIa production may be expressed as Eq. A.8

$$\frac{d[FXIIa]}{dt} = \frac{k_2 \cdot [FXII] \cdot A}{K_S + A} + k_3 \cdot [FXIIa] \cdot \frac{(FXII \cdot A)}{(FXII \cdot A) + K_{S1}} \quad (\text{Eq. A.8})$$

Previous work (Guo 2006) demonstrated that autohydrolysis is not a major enzyme generation pathway at biomaterial surfaces in plasma so that the two remaining pathways— autoactivation and reciprocal-activation— are the two significant mechanisms of FXII activation at material surfaces in plasma.

Since concentration of FXII for a given batch of plasma is a constant,  $k_2 \cdot [FXII]$  may be replaced with another constant  $K_I$  in Eq. A.6, and can be integrated to calculate the amount of enzyme generated (Eq. A.9).

$$[FXIIa] = \frac{K_I \cdot A}{K_S + A} t \quad (\text{Eq. A.9})$$

Using Eq. **A.9** to replace  $[FXIIa]$  in Eq. **A.3** yield Eq. **A.10**

$$CT = \frac{a \cdot \frac{K_1 \cdot A}{K_s + A} \cdot CT + b}{\frac{K_1 \cdot A}{K_s + A} \cdot CT + c} \quad (\text{Eq. A.10})$$

For a known CT, using parameters  $a$ ,  $b$  and  $c$  determined from FXIIa-titration (Eq. **A.3**), Eq. **A.10** may be solved to determine  $K_1$ , indicative of the “catalytic potential” of the added solid procoagulant. The amount of FXIIa generated for a given CT can then be calculated from Eq. **A.9**.

### **A.3 Literature citations**

Guo, Z., K. M. Bussard, K. Chatterjee, R. Miller, E. A. Vogler and C. A. Siedlecki (2006). "Mathematical modeling of material-induced blood plasma coagulation." Biomaterials **27**: 796-806.

## **Appendix B**

### **Plasma coagulation response to surfaces containing dual chemical groups**

#### **B.1 Objective**

The objective of this study was to characterize the plasma coagulation response to a series of test surfaces containing different proportions of two terminal chemical groups: carboxyl (-COOH) and methyl (-CH<sub>3</sub>). These surfaces were prepared using a series of two-component silane solutions yielding a series of test surfaces spanning a wide range of surface water-wettability (a measure of surface energy).

#### **B.2 Materials and methods**

##### **B.2.1 Preparation of test surfaces**

Test surfaces were prepared by silane treatment of glass particles of 425-600  $\mu\text{m}$  diameter (nominal diameter = 500  $\mu\text{m}$ , Sigma-Aldrich, St. Louis, MO) similar to previously-reported procedures (Chatterjee 2006; Guo 2006; Miller 2006; Zhuo 2005) (see also 2.2.2, 3.2.2). Glow-discharge-treated glass particles were incubated for 1 hr in solutions containing a total 1% v/v silane in chloroform where 2-carbomethylethoxytrichlorosilane (CMETS) and butyltrichlorosilane (BTS) were mixed in varying proportions. Both silanes were obtained commercially (Gelest Inc., Morrisville, PA). The particles were rinsed in fresh chloroform and air-dried. All

surfaces were treated with 0.1 M NaOH (Sigma-Aldrich) followed by 0.1 N H<sub>2</sub>SO<sub>4</sub> (VWR) for 10 min each, with a water rinse between the two steps.

Water-wettability for each surface was measured on 12 mm diameter glass coverslip witness samples (VWR). Contact angles on the resultant surfaces were measured by the horizontal sessile drop method using a Krüss goniometer with 18 MΩ water (Millipore simplicity unit) as the probe liquid.

### **B.2.2 Coagulation assay**

An in vitro coagulation assay used to measure the coagulation response of platelet poor plasma (PPP) to test surfaces has been reported previously (Chatterjee 2006; Guo 2006) (see also 2.3.2, 3.3.2).

### **B.2.3 Mathematical modeling of coagulation response**

A previously-published mathematical model was used to quantify the measured coagulation response to these surfaces (Guo 2006) (see A.1 and A.2 for summary).

## **B.3 Results**

A series of surfaces prepared using solutions containing mixtures of CMETS and BTS yielded a series of surfaces containing varying proportions of functional groups on the surface. The terminal ester groups on the CMETS molecules were converted to carboxyl acid groups by treatment with NaOH (for consistency all surfaces including

those prepared from single-component BTS solution were also treated in NaOH). This yielded a series of surfaces with mixtures of -COOH and -CH<sub>3</sub> groups. They are referred to as “x : y”, where x and y refer to the proportions of CMETS and BTS, respectively, in the mixed silane solutions. For example, “0.75 : 0.25” refers to surfaces prepared in solutions containing 0.75% CMETS and 0.25% BTS (v/v) in chloroform. Note that the total silane content for all treatments was fixed at 1%. These proportions do not indicate the actual ratios of the two functional groups on the prepared surfaces, which was not characterized. However, a gradient in surface water-wettability (Table **B-1**) with change in the ratio of contents of the silanes indicates that mixtures of two terminal groups were obtained on these surfaces.

Table **B-1**:  $K_I$  values for the solid procoagulants

Procoagulant Surface (CMETS : BTS)	Sessile Drop Contact Angle	$K_I$ ( $\mu\text{M}/\text{min}$ )
1.00 : 0.00	$10^\circ \pm 2^\circ$	$(3.5 \pm 0.9) \times 10^{-1}$
0.75 : 0.25	$28^\circ \pm 3^\circ$	$(2.6 \pm 0.3) \times 10^{-1}$
0.67 : 0.33	$37^\circ \pm 4^\circ$	$(1.6 \pm 0.4) \times 10^{-1}$
0.50 : 0.50	$47^\circ \pm 4^\circ$	$(2.2 \pm 1.2) \times 10^{-2}$
0.25 : 0.75	$74^\circ \pm 5^\circ$	$(4.2 \pm 2.7) \times 10^{-3}$
0.00 : 1.00	$92^\circ \pm 1^\circ$	$(3.0 \pm 1.9) \times 10^{-3}$

Values are displayed as mean  $\pm$  S.D. for  $n \geq 3$

Results in Figure **B-1** present coagulation time (CT) recorded for surface-area-titration for these different surfaces in PPP. Fitting of a mathematical model yielded a parameter  $K_I$  that scales with the catalytic efficiency of the surface (listed in Table **B-1**).

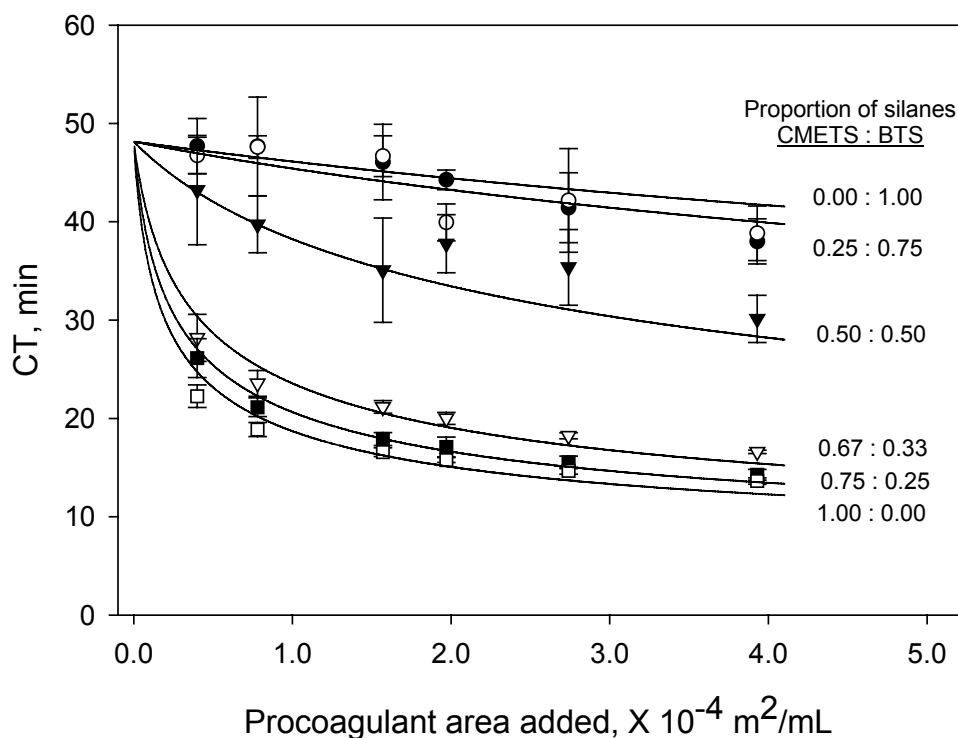


Figure **B-1**: Surface area titration (SAT) in PPP showing experimental CT vs. added surface area of six different procoagulant materials prepared from a dual component silane solution containing CMETS:BTS in varying proportions. Data for 0.00:1.00 (solid circles ●), 0.25:0.75 (open circles ○), 0.5:0.5 (closed triangles ▼), 0.67:0.33 (open triangles ▽), 0.75:0.25 (closed squares ■), and 1.00:0.00 (open squares □) are shown. (All data expressed as mean  $\pm$  S.D. for  $n \geq 3$ ).

Results in Table **B-1** indicate that  $K_I$  scales with the surface water-wettability of the surface, where hydrophilic surfaces exhibit highest catalytic efficiency whereas



hydrophobic surfaces that are weaker procoagulants have low catalytic efficiency. Figure B-2 plots  $K_I$  as a function of water-adhesion tension (scales with cosine of the water-contact angle). A similar trend is observed when surface are prepared using single-component silane solutions resulting in only one type of surface chemical groups; scaling of  $K_I$  with surface wettability for carboxyl, amine and methyl terminated self-assembled-monolayers is seen in 2.3.2.

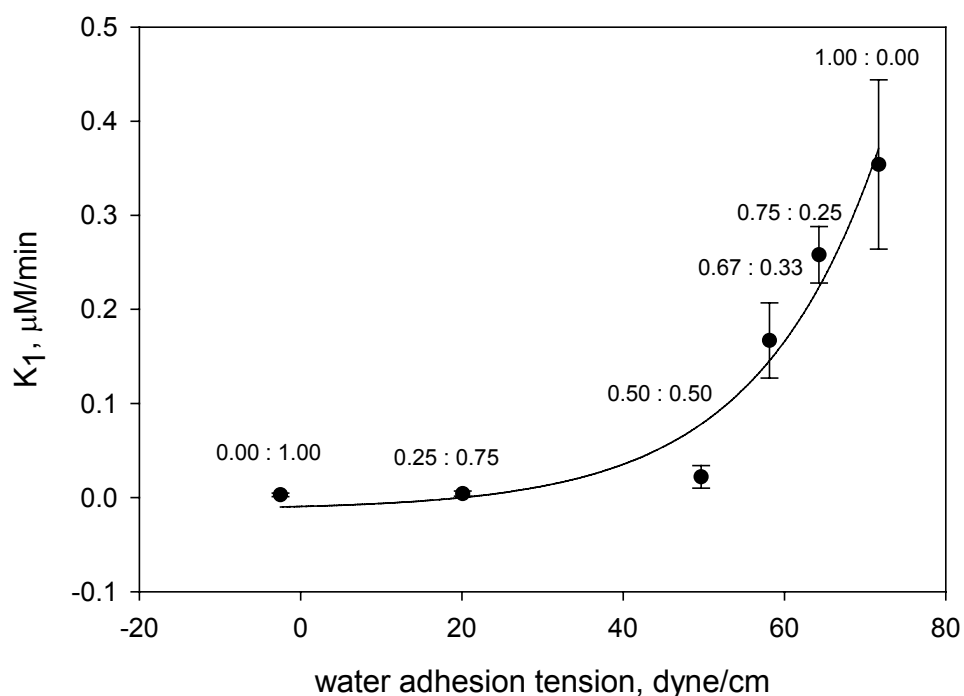


Figure B-2: Plot showing the relationship between  $K_I$  (a measure of catalytic efficiency) and the water adhesion tension (surface energy) of test surfaces from mixtures of CMETS and BTS in different proportions.

These results provide additional evidence demonstrating that plasma coagulation response to surfaces scales with surface water-wettability, and not due to a biochemical specificity arising out of anionic groups on the surface.

#### **B.4 Literature citations**

Chatterjee, K., E. A. Vogler and C. A. Siedlecki (2006). "Procoagulant activity of surface-immobilized Hageman factor." Biomaterials **27**: 5643-5650.

Guo, Z., K. M. Bussard, K. Chatterjee, R. Miller, E. A. Vogler and C. A. Siedlecki (2006). "Mathematical modeling of material-induced blood plasma coagulation." Biomaterials **27**: 796-806.

Miller, R., Z. Guo, E. A. Vogler and C. A. Siedlecki (2006). "Plasma coagulation response to surfaces with nanoscale chemical heterogeneity." Biomaterials **27**: 208-215.

Zhuo, R., R. Miller, K. M. Bussard, C. A. Siedlecki and E. A. Vogler (2005). "Procoagulant stimulus processing by the intrinsic pathway of blood plasma coagulation." Biomaterials **26**: 2965-2973.

## **Appendix C**

### **Material-induced whole-blood coagulation**

#### **C.1 Objective**

Thrombosis is known to result as combination of cellular (coagulation cascade) and humoral (platelet) pathways, as described in 1.2. While the coagulation assay used for our studies (2.2.4, 3.2.3, 4.2.3, 6.2.3) has served as a useful tool to measure coagulation response of PPP to test surfaces, the significance of these measurements to whole blood, a more physiologically relevant system is undetermined. Therefore, in this study the objective was to measure the coagulation response in whole blood to test surfaces and contrast to the coagulation response in platelet-poor-plasma (PPP) used for other studies.

#### **C.2 Materials and methods**

##### **C.2.1 Preparation of test surfaces**

Test surfaces spanning a wide spectrum of water-wettability (surface energy) were prepared by silanization of glass particles (425-600  $\mu\text{m}$  diameter, nominal diameter = 500  $\mu\text{m}$ , Sigma-Aldrich, St. Louis, MO) as previously described in 2.2.2 (Chatterjee 2006; Guo 2006; Miller 2006; Zhuo 2005). Glow-discharge-treated glass particles served as model hydrophilic surface, whereas particles treated with n-octadecyltrichlorosilane

(OTS) served as model hydrophilic surface. Particles treated with 3-aminopropyltriethoxysilane (APS) served as test surfaces of intermediate water-wettability.

### **C.2.2 Coagulation assay using whole bovine blood**

Fresh citrated bovine blood (100 mL blood containing 14 mL of CPDA as anticoagulant) was collected from healthy calves (following Institutional Review Board-approved procedures). The anticoagulation procedure is similar to that typically followed in a blood bank in the collection of human blood.

The coagulation response to test surfaces was assayed following previous procedure, where whole bovine blood supplanted human PPP prepared from salvaged plasma described in 2.2.4, 4.2.3 (Chatterjee 2006; Guo 2006; Miller 2006; Zhuo 2005).

### **C.3 Results and Discussion**

Surface area titration (SAT) plots for three test surfaces (spanning a wide range of water-wettability) in recalcified whole blood are presented in Figure C-1. The general trends in coagulation response indicating increased coagulation response with increasing surface area for any given surface is similar to that observed in SAT plots using PPP in 2.3.2 (Chatterjee 2006; Guo 2006; Miller 2006; Zhuo 2005). Further, results in Figure C-1 also indicate that for a given surface area of solid procoagulants, CT scales with the surface energy of the solid procoagulants, similar to trends for PPP seen in 2.3.2

(Chatterjee 2006; Guo 2006; Miller 2006; Zhuo 2005). For identical experimental conditions, CT measured in whole blood are shorter than corresponding values in human PPP seen 2.3.2 (Chatterjee 2006; Guo 2006; Miller 2006; Zhuo 2005). This is not surprising since whole blood contains platelets, which provide an additional pathway for faster clotting.

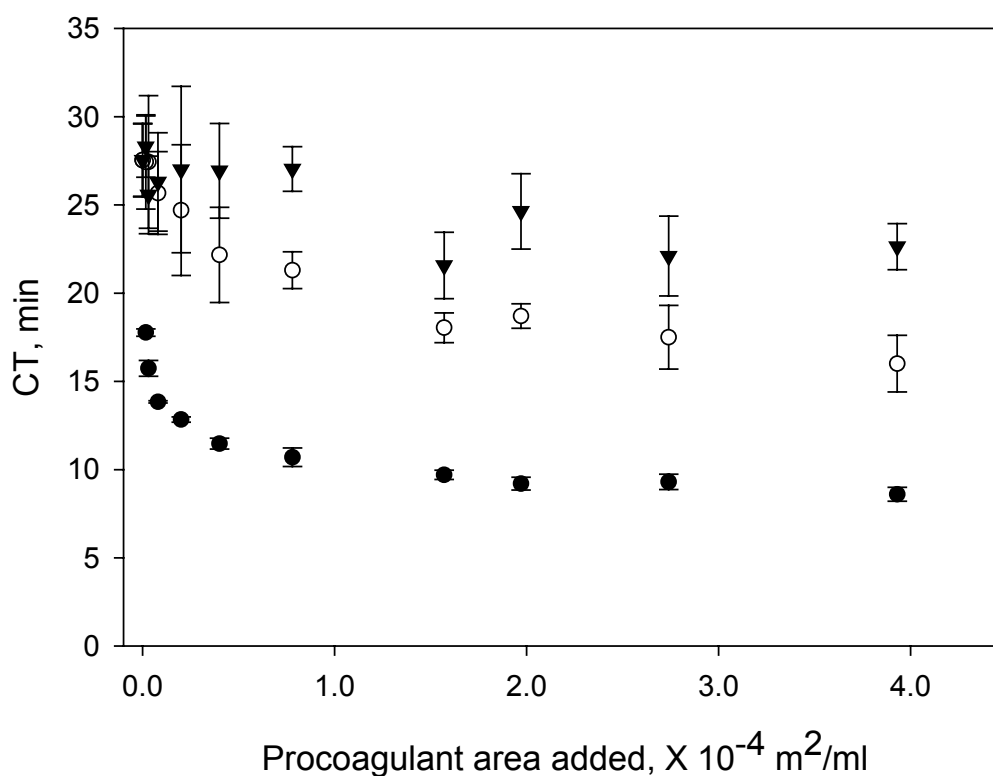


Figure C-1: Surface area titration (SAT) in whole bovine blood showing experimental CT vs. added surface area of three different procoagulant materials. Data for glass-particles (solid circles ●), APS particles (open circles ○) and OTS particles (closed triangles ▼) are shown. (All data expressed as mean  $\pm$  S.D. for  $n \geq 3$ ).

Results from this semi-quantitative study demonstrate that coagulation in whole blood may be justifiably reduced to a PPP system to study contact activation. In future, with increased understanding of the role of material surface in plasma coagulation the complexity of the system can be enhanced to incorporate the contribution of platelets.

#### **C.4 Literature citations**

Chatterjee, K., E. A. Vogler and C. A. Siedlecki (2006). "Procoagulant activity of surface-immobilized Hageman factor." Biomaterials **27**: 5643-5650.

Guo, Z., K. M. Bussard, K. Chatterjee, R. Miller, E. A. Vogler and C. A. Siedlecki (2006). "Mathematical modeling of material-induced blood plasma coagulation." Biomaterials **27**: 796-806.

Miller, R., Z. Guo, E. A. Vogler and C. A. Siedlecki (2006). "Plasma coagulation response to surfaces with nanoscale chemical heterogeneity." Biomaterials **27**: 208-215.

Zhuo, R., R. Miller, K. M. Bussard, C. A. Siedlecki and E. A. Vogler (2005). "Procoagulant stimulus processing by the intrinsic pathway of blood plasma coagulation." Biomaterials **26**: 2965-2973.

## VITA

### Kaushik Chatterjee

#### Education

- Ph.D. Candidate (Bioengineering)  
Pennsylvania State University, Hershey, PA.
- M.S. (Materials Science and Engineering) 2003  
University of Virginia, Charlottesville, VA
- B.E. (Metallurgical Engineering) 2001  
Bengal Engineering College, Calcutta, India

#### Awards

Penn State College of Medicine: Alumni Society Endowed Scholarship Award 2007  
American Society for Artificial Internal Organs (ASAIO): Student Fellowship 2007  
Society for Biomaterials: STAR Award (Student Travel Achievement Recognition) 2007  
Penn State Graduate School: Graham Graduate Student Fellowship 2003

#### Journal Publications

- K. Chatterjee, J.L. Thornton, E.A. Vogler, C.A. Siedlecki “Protein-adsorption competition moderates prekallikrein-factor XII interactions in surface activation of plasma coagulation” **submitted**
- K. Chatterjee, Z. Guo, E.A. Vogler, C.A. Siedlecki “Contributions of contact activation pathways of coagulation factor XII in plasma” **in revision**
- K. Chatterjee, E.A. Vogler, C.A. Siedlecki “Procoagulant activity of surface-immobilized Hageman factor” **Biomaterials** 2006, 27: 5643-5650
- Z. Guo, K.M. Bussard, K. Chatterjee, R. Miller, E.A. Vogler, C.A. Siedlecki “Mathematical modeling of material-induced blood plasma coagulation” **Biomaterials** 2006, 27: 796-806
- J.M. Howe, A.R.S. Gautam, K. Chatterjee, F. Phillipp “Atomic-level dynamic behavior of a diffuse interface in an Au-Cu alloy” **Acta Materialia** 2007, 55: 2159-2171
- K. Chatterjee, J.M. Howe, W.C. Johnson, M. Murayama “Static and in situ TEM investigation of phase relationships, phase dissolution, and interface motion in Ag-Au-Cu alloy nanoparticles” **Acta Materialia** 2004, 52: 2923-2935
- J.M. Howe, A.M. Mebed, K. Chatterjee, P. Li, M. Murayama, W.C. Johnson “Effect of phase fraction on the tri-junction in two-phase nanoparticle systems” **Acta Materialia** 2003, 51: 1359-1372